Development of Calibration Strategies for Gasoline Direct Injection Engines within the Scope of Sustainable Mobility

Department of Mechanics, Mathematics and Management

MECHANICAL AND MANAGEMENT ENGINEERING

Ph.D. Program

SSD: ING-IND/08 – FLUID MACHINERY

Final Dissertation

Development of Calibration Strategies for Gasoline Direct Injection Engines within the Scope of Sustainable Mobility

---

by

Eng. Emanuele Bottalico

Supervisors:

Prof. Eng. S.M. Camporeale

Dr. Eng. F. Fersini

Dr. Eng. S. Gabriele

Dr. Eng. V. Rosito

Coordinator of Ph.D Program:

Prof. Eng. Giuseppe Pompeo Demelio

Course n° 33, 11/01/2018 – 10/03/2021

LIBERATORIA PER L'ARCHIVIAZIONE DELLA TESI DI DOTTORATO

Politecnico di Bari

Al Magnifico Rettore
del Politecnico di Bari

Il sottoscritto EMANUELE BOTTALICO nato a BARI (BA) il 01/01/1982, residente a BARI (BA) in STRADA CEGLIE BITRITTO TERRA ROSSA N. 31, e-mail: ebottalico462@gmail.com, iscritto al 3° anno di Corso di Dottorato di Ricerca in INGEGNERIA MECCANICA E GESTIONALE ciclo XXXIII, ed essendo stato ammesso a sostenere l'esame finale con la prevista discussione della tesi dal titolo:

DEVELOPMENT OF CALIBRATION STRATEGIES FOR GASOLINE DIRECT INJECTION ENGINES WITHIN THE SCOPE OF SUSTAINABLE MOBILITY

DICHIARA

1) di essere consapevole che, ai sensi del D.P.R. n. 445 del 28.12.2000, le dichiarazioni mendaci, la falsità negli atti e l'uso di atti falsi sono puniti ai sensi del codice penale e delle Leggi speciali in materia, e che nel caso ricorressero dette ipotesi, decade fin dall'inizio e senza necessità di nessuna formalità dai benefici conseguenti al provvedimento emanato sulla base di tali dichiarazioni;
2) di essere iscritto al Corso di Dottorato di ricerca INGEGNERIA MECCANICA E GESTIONALE ciclo XXXIII, corso attivato ai sensi del "*Regolamento dei Corsi di Dottorato di ricerca del Politecnico di Bari"*, emanato con D.R. n.286 del 01.07.2013;
3) di essere pienamente a conoscenza delle disposizioni contenute nel predetto Regolamento in merito alla procedura di deposito, pubblicazione e autoarchiviazione della tesi di dottorato nell'Archivio Istituzionale ad accesso aperto alla letteratura scientifica;
4) di essere consapevole che attraverso l'autoarchiviazione delle tesi nell'Archivio Istituzionale ad accesso aperto alla letteratura scientifica del Politecnico di Bari (IRIS-POLIBA), l'Ateneo archivierà e renderà consultabile in rete (nel rispetto della Policy di Ateneo di cui al D.R. 642 del 13.11.2015) il testo completo della tesi di dottorato, fatta salva la possibilità di sottoscrizione di apposite licenze per le relative condizioni di utilizzo (di cui al sito http://www.creativecommons.it/Licenze), e fatte salve, altresì, le eventuali esigenze di "embargo", legate a strette considerazioni sulla tutelabilità e sfruttamento industriale/commerciale dei contenuti della tesi, da rappresentarsi mediante compilazione e sottoscrizione del modulo in calce (Richiesta di embargo);
5) che la tesi da depositare in IRIS-POLIBA, in formato digitale (PDF/A) sarà del tutto identica a quelle **consegnate**/inviate/da inviarsi ai componenti della commissione per l'esame finale e a qualsiasi altra copia depositata presso gli Uffici del Politecnico di Bari in forma cartacea o digitale, ovvero a quella da discutere in sede di esame finale, a quella da depositare, a cura dell'Ateneo, presso le Biblioteche Nazionali Centrali di Roma e Firenze e presso tutti gli Uffici competenti per legge al momento del deposito stesso, e che di conseguenza va esclusa qualsiasi responsabilità del Politecnico di Bari per quanto riguarda eventuali errori, imprecisioni o omissioni nei contenuti della tesi;
6) che il contenuto e l'organizzazione della tesi è opera originale realizzata dal sottoscritto e non compromette in alcun modo i diritti di terzi, ivi compresi quelli relativi alla sicurezza dei dati personali; che pertanto il Politecnico di Bari ed i suoi funzionari sono in ogni caso esenti da responsabilità di qualsivoglia natura: civile, amministrativa e penale e saranno dal sottoscritto tenuti indenni da qualsiasi richiesta o rivendicazione da parte di terzi;

7) che il contenuto della tesi non infrange in alcun modo il diritto d'Autore né gli obblighi connessi alla salvaguardia di diritti morali od economici di altri autori o di altri aventi diritto, sia per testi, immagini, foto, tabelle, o altre parti di cui la tesi è composta.

BARI, 06/04/2021 Firma _____

Il sottoscritto, con l'autoarchiviazione della propria tesi di dottorato nell'Archivio Istituzionale ad accesso aperto del Politecnico di Bari (POLIBA-IRIS), pur mantenendo su di essa tutti i diritti d'autore, morali ed economici, ai sensi della normativa vigente (Legge 633/1941 e ss.mm.ii.),

CONCEDE

- al Politecnico di Bari il permesso di trasferire l'opera su qualsiasi supporto e di convertirla in qualsiasi formato al fine di una corretta conservazione nel tempo. Il Politecnico di Bari garantisce che non verrà effettuata alcuna modifica al contenuto e alla struttura dell'opera.
- al Politecnico di Bari la possibilità di riprodurre l'opera in più di una copia per fini di sicurezza, back-up e conservazione.

BARI, 06/04/2021 Firma _____

Department of Mechanics, Mathematics and Management

MECHANICAL AND MANAGEMENT ENGINEERING
Ph.D. Program
SSD: ING-IND/08 – FLUID MACHINERY

Final Dissertation

Development of Calibration Strategies for Gasoline Direct Injection Engines within the Scope of Sustainable Mobility

by
Eng. Emanuele Bottalico

Referees:

Prof. Eng. A. Viggiano

Prof. Eng. M.C. Cameretti

Supervisors:

Prof. Eng. S.M. Camporeale

Dr. Eng. F. Fersini

Dr. Eng. S. Gabriele

Dr. Eng. V. Rosito

Coordinator of Ph.D Program:
Prof. Eng. Giuseppe Pompeo Demelio

Course n° 33, 11/01/2018 – 10/03/2021

Acknowledgements

This thesis would be impossible without the support of the following individuals in my PhD Course. First of all I'd like to give the sincerest gratitude to Eng. P. CICCARESE for giving me the opportunity to become part of a wonderful context like BOSCH.

Another deep and sincere thanksgiving goes to my Prof. Eng. S. M. CAMPOREALE for providing me an invaluable guidance in my PhD Course.

I also thank my GrL Eng. F. MICCOLIS, my internal tutors Eng. F. FERSINI, Eng. S. GABRIELE, Eng. V. ROSITO for the precious teachings transmitted, without their support these pages would've never existed.

Thanks go to ETW Team and to my colleagues Eng. D. D'ELIA, Eng. A. BALESTRA and Eng. C.M. GERVASIO for the initial support to my activities.

Finally, I would like to thank Centro Studi Componenti per Veicoli Company and Polytechnic of Bari for providing scholarship, supporting my PhD Course.

And last but not least a special thank to my wife and my daughter for the charge transmitted every day during this wonderful path.

Contents

Abbreviations / Definitions

ABDC – After Bottom Dead Center
AKI – Antiknock Index
ATDC – After Top Dead Center
BBDC – Before Bottom Dead Center
BMEP – Break Mean Effective Pressure [bar]
BSFC – Brake-specific fuel consumption [g/kWh]
BTDC – Before Top Dead Center
BTEX – Benzene, Toluene and Ethylbenzene-Xylenes
CFD – Computational Fluid Dynamics
CI – Compression Ignition
CO – Carbon Monoxide
CO_2 - Carbon Dioxide
COPD – Chronic Obstructive Pulmonary Disease
CPSI – Cells per square Inch
DBE – Double Bond Equivalent
DI – Direct Injection
DPF – Diesel Particulate Filter**EC –** Ethanol Content
ECU – Engine Control Unit
EGR – Exhaust Gas Recirculation
EPA – Environmental Protection Agency
EU6-RDE – Real-World Driving Emissions
FBP – Final Boiling Point
FTP – Federal Test Procedure
GDI – Gasoline Direct Injection
GPF – Gasoline Particulate Filter
HC – Hydrocarbons
HiL – Hardware in the Loop
HO – Homogeneous Injection
LDGV – Light Duty Gasoline Vehicle
LHV – Lower Heating Value
MHEV – Mild Hybrid Electric Engine
MON – Motor Octane Number [-]
MPI – Multi Point Injection
NEDC – New European drive cycle
NOx – Nitrogen Oxides
OC – Oxygen Content

OOC – Other Oxygenates Compounds
PFI – Port Fuel Injection
PICS – Products of Incomplete Combustion
PM – Particulate Matter
PN – Particulate Number
PN Indicator [-] – (PN Total [#/cm^3] / PN min [#/cm^3])
RON – Research Octane Number [-]
RON 95 E5 – Gasoline with a RON of 95 and Ethanol content of the 5%
RON 98 – Gasoline with a RON of 98
RPM – Revolutions Per Minute
SAT – Saturates
SG – Spray Guided
SI – Spark Ignition
SiL – Software in the Loop
SOI – Start Of Injection [°CAD]
T10 Temperature when 10% of a fuel by volume boils away during a distillation test [°C]
T50 Temperature when 50% of a fuel by volume boils away during a distillation test [°C]
T90 Temperature when 90% of a fuel by volume boils away during a distillation test [°C]
THC – Total Hydrocarbons
TWC – Three Way Catalyst
UFPs – Ultra-fine Particulates
VP – Vapour Pressure [kPa/PSI]
VCR – Variable Compression Ratio
WG – Wall Guided
WLTC – World Harmonized Light Vehicle Test Cycle

General Introduction

In order to limit the contributions to global warming due to burning of fossil fuels, major countries across the world have set new targets on reducing vehicular fuel consumption and tailpipe CO_2 emissions. As the CO_2 emission standards around the world become more stringent, the turbocharged downsized gasoline direct injection (GDI) engine provides a mature platform to achieve better fuel economy. For this reason, it is expected that the GDI engine will capture increasing shares of the market during the coming years. The in-cylinder liquid injection, though advantageous in most engine operation regimes, creates emissions during the cold crank-start and cold fast-idle phases. The engine cold-start is responsible for a disproportionate share of the hydrocarbons (HC), carbon monoxide (CO), nitrogen oxides (NO_x) and particulate matter (PM) emitted over the certification cycle. Understanding the sources of the pollutants during this stage is necessary for the further market penetration of GDI under the constraint of tighter emission standards. This thesis aims to examine the formation processes of the principal pollutants during various conditions in a GDI engine, and the sensitivity of the pollutant emissions to different calibration strategies. To this end, a detailed analysis was carried out with regard to the main engine combustion parameters. The results show that the pollutant formation processes are strongly dependent on the mixture formation and on the temperature and pressure history of the combustion process, so particular attention must be reserved to the engine calibration.

Targets

Within the research topics of the PhD course, the principal targets have been the following:

1. **Experimental investigation of impact of injection timing on particulate number emission of a modern gasoline direct injection engine using RON 98 and RON 95 E5 Fuels.**
   In this work, a wide injection timing sweep window was studied and this helps a better understanding of the impact of the mixture preparation on engine performance. Therefore, this work also examined the strong impact of injection timing on combustion process and particulate matter emissions under different loads and speed conditions of a GDI engine. In addition with regard to the studies in literature, it is still not conclusive as to whether the use of Ethanol may cause an increase or decrease in particulate emissions from current SI engines. In fact for GDI engines, results show both increases and decreases demonstrating that the details of combustion system design and engine operating points are very important. In this work a meticulous analysis was performed in order to understand the effects of Ethanol on PN emissions.

2. **Numerical study on emissions reduction using multiple injection strategies.**
   In order to meet the required performance and emission targets, focusing on the reduction of particulate emission, a multiple injection strategy can be considered as an option to control both the mixture stratification and the wall impingement.
   It's well known that, for the engine cold conditions, the use of multiple injection strategies is very common in order to avoid the PN increase emissions, these last linked to the piston impingement effects. In this work a numerical investigation is performed with the aim of understanding the potential benefits of multiple injections strategies also for engine warm conditions and for an upper middle operating point. The analysis makes use of an advanced simulation tool, which allows to select particular strategies to be validated on engine bench. As first step an accurate engine model and calibration setup were realized in order to have a better prediction in terms of performance, fuel consumption and pollutants emissions with regard to the measures obtained from the test bench. As second step an accurate analysis was realized with regard to the comparison between homogeneous and stratified operations, thus leading to important final considerations.

3. **Research and development of calibration strategies for catalyst heating.**
   For the engine in cold conditions, the Three way catalyst is not at operating temperature so its emission conversion capability is significant inhibited. As a consequence, the tailpipe emissions during the first phase of an engine cold start make up about 60 ÷ 80 % of the total emissions during a regulatory test procedure. In this work the target has been of finding a good calibration strategy in order to ensure an optimum compromise of catalyst heating potential, smooth running and low raw emission levels.

1. Why the Emphasis on Gasoline Direct Injection Engines ?

In order to limit the contributions to global warming due to burning of fossil fuels, major countries across the world have set new targets on reducing vehicular fuel consumption and tailpipe CO_2 emissions (see Figure 1.1). Achieving these targets would require CO_2 reductions of the order of 3% – 6% per year across major markets. In response, vehicle manufacturers are rapidly advancing and implementing various technologies aimed at reducing fuel consumption and tailpipe emissions [1]. One approach that has gained popularity is that of replacing traditional port fuel injected (PFI) or multi-port injected (MPI) gasoline engines by boosted, downsized gasoline direct injected (GDI) engines [2, 3, 4, 5].

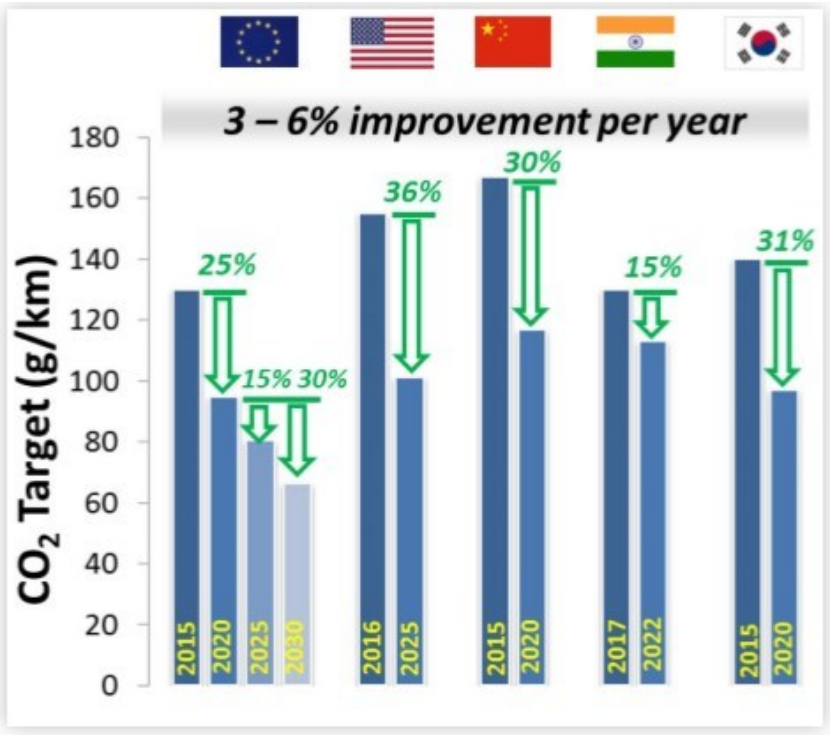

Figure 1.1 Vehicular tailpipe CO_2 targets in selected countries [1]

In 2016, GDI vehicles captured ~49% of the light-duty car and truck market share in the United States, within only 9 years from their introduction [6]. The key difference between GDI and PFI engines lies in the fuel-air mixture preparation before combustion. In PFI engines, the fuel is injected upstream of the intake valve or in the intake manifold for mixing with air before entering the cylinder. In GDI engines, fuel is injected directly into the combustion chamber, and the associated charge cooling mitigates engine knock and enables operations at higher compression ratios. Furthermore, the amount and timing of fuel injected into the chamber can be more precisely controlled, leading to improved combustion and fuel economy gains.

However, the improved fuel economy of GDI engines is accompanied with an undesirable increase in the formation of particulate emissions. The direct injection of fuel in the combustion chamber leads to insufficient time for mixture formation and fuel impingement on the relatively cooler combustion chamber surfaces, leading to fuel-rich regions, incomplete combustion, and particulate formation. On the vehicle side, practically all diesel engines are equipped with a diesel particulate filter (DPF) to capture these particulates.

1.1. GDI Vs PFI

PFI is a pressurized indirect injection system, in which the injection of fuel takes place in the inlet port, before the air enters in the combustion chamber. The electronic control unit (ECU) commands the amount of fuel per injection event by adjusting the length of time a fixed orifice in the injector is open. Fuel is injected as a fine spray in the air inlet port, where homogenous mixing of fuel and air takes place. The homogenized combustible mixture, also known as 'charge', enters the cylinder via the cylinder intake valve. The fuel is injected at a pressure slightly higher than the intake manifold pressure, so that the amount of fuel injected per injection event is determined only by the length of time the orifice in the injector is opened by the ECU. The length of time is known as the 'pulse width' of the injector. The engine fuel requirements change according to engine speed, load and temperature. The ECU tailors the amount of fuel injected based on these factors by modulating the pulse width of the injector, and the frequency of injection events. However, since the injection point is upstream of the intake valve, a liquid fuel film can form on the intake port walls and intake valve in PFI engines. Accumulation of liquid film on the walls alters in an uncontrolled manner the air-fuel ratio of the charge delivered to the cylinders, and causes lags and overshoots in the fuel flow with respect to the airflow delivered [7, 8, 9, 10]. In comparison, GDI is a high-pressure direct injection system. Similar to PFI, the ECU controls the amount of fuel injected per injection event by adjusting the length of time a fixed orifice in the injector is open. Unlike PFI, the fuel is injected directly into the cylinder at a much higher pressure with the intent of creating heterogeneous variation in the fuel and air mixture, also known as a 'stratified charge'. Stratified charge in GDI can be used to ignite mixtures which are, on average, leaner than PFI, but are richer closer to the spark plug. GDI reduces fuel transport delay, which enables very precise control of injection timing and air fuel ratio. The amount and timing of fuel injected in GDI can be better tailored to match variation in engine load than in PFI due to in-cylinder injection. Direct injection reduces errors in maintaining proper combustion stoichiometry, which are also known as fuel-metering errors. GDI also eliminates the formation of a liquid fuel film found on intake port walls and intake valves in PFI engines. However, fuel impingement can occur on cylinder walls and piston surface in the GDI. In GDI, the timing of fuel injection event can be varied, and there can be multiple injection events during intake stroke and/or compression stroke within the same combustion cycle. More than one injection pulse enables variation in the level of stratification in the combustion chamber.

Injection events during the intake stroke result in homogenous charge and during the compression stroke result in heterogeneous charge. Thus, more than one injection events enable staged combustion in GDI. Staged combustion helps prevent knock, which enables an increase in compression ratio for improved engine efficiency [7, 8, 11, 12, 13, 14, 15, 16, 17]. Directly injected fuel vaporizes utilizing heat within combustion chamber, thereby producing a cooling effect. This results in a higher compression ratio and volumetric efficiency than a PFI engine [8, 11]. Compression ratio, which is the ratio of the maximum to minimum volume in the cylinder, is limited by the temperature inside the combustion chamber at the end of the compression stroke. If the temperature at the end of the compression stroke is higher than the flash point of the fuel, the charge will auto-ignite, producing a 'knock'. The cooling effect of the injection spray results in lower temperature at the end of the compression stroke, and allows GDI engines to have higher compression ratio than PFI engines by 1 to 2 ratios [7, 8, 11, 12, 17]. Volumetric efficiency is the ratio of the mass of air and fuel mixture drawn into the cylinder during the intake stroke to the mass that would occupy the displaced volume of the cylinder if the air density in the cylinder were equal to the air density in the air intake manifold. Volumetric efficiency is, thus, a mass ratio and not a volume ratio. When the volume of final mixture decreases, the density of the mixture increases, which results in higher volumetric efficiency [18]. The cooling effect of the spray increases volumetric efficiency of GDI engines over PFI engines. The cooling effect of the spray increases volumetric efficiency of GDI engines over PFI engines. In a PFI engine, droplets of liquid fuel sprayed into the intake port wet the intake port wall and intake valve, and evaporate mainly by absorbing thermal energy from these surfaces. In contrast, in a GDI engine, fuel droplets are vaporized mainly by absorbing thermal energy from the air. This results in cooling of the mixture, which in turn leads to a decrease in the volume and increase in the density of the mixture [8, 11, 12]. Calculations and experiments to quantify the potential volumetric efficiency benefits and reduction in temperature of charge have been done by [8, 11]. Anderson *et al.* [11] calculated the change in final mixture volume compared to the volume of intake air for two extreme cases. Both cases consider typical conditions where initial intake air temperature is 100°C and fuel temperature is 50°C. A decrease of 5% in final mixture volume was estimated for a case in which fuel was completely evaporated by air, and an increase of 2% in final mixture volume was estimated for a case in which fuel was evaporated completely due to the intake port wall and intake valve surface. These extreme cases are unrealistic, as the fuel also absorbs heat from the air in a PFI engine, and from the cylinder walls in a GDI engine, but they serve to illustrate the potential differences. Anderson *et al.* [11] postulated that the actual volumetric efficiency advantage of GDI engines over PFI engines lies in between these two ideal cases. If the intake air and fuel temperatures are varied, the estimated difference at constant pressure in charge temperatures for these extreme cases can be as large as 30°C. In experiments performed by Wyszynski *et al.* [8], they found that changing from PFI to GDI in the same engine led to a 9% increase in volumetric efficiency. Wyszynski *et al.* [8] found that the improvement is between 50 and 70% of the theoretical maximum possible, which they have calculated separately under varying intake air and fuel temperatures. The improvement is limited by the finite time available for evaporation of the fuel droplets, and by direct impingement of the injection spray onto surfaces in the combustion chamber in a GDI engine.

Higher compression ratio and volumetric efficiency, coupled with better control of fuel and air staging, lead to higher specific power output, higher torque and increased engine efficiency [7, 8, 11]. For achieving higher injection pressure and more precisely timed fuel injection events, GDI engines require more sophisticated fuel injection hardware, a high-pressure fuel pump and a more complex engine control system compared to PFI engines [7, 11]. GDI engines are, therefore, more difficult to build, require better materials and higher precision in manufacturing. This increases the cost to design and manufacture GDI engines by $213 to $321, depending on the engine size [19]. A high-pressure fuel pump also requires more electrical power to operate, which affects the fuel consumption [7].

1.2. Types of GDI Systems

In GDI engines, fuel is injected into the cylinder from a single point orifice, which can be located either on the side wall, or at the top of the cylinder. GDI engines in which fuel injector is mounted in the side wall are known as wall-guided (WG), whereas, GDI engines in which the injector is mounted at the top of the cylinder are known as spray-guided (SG). In WG systems, the fuel injector is located on the side of the cylinder near the corner of the cylinder head and the cylinder wall, and fuel-air mixing primarily relies on piston head geometry. The fuel spray is injected towards the piston head where it is redirected towards the spark plug for ignition. WG systems were employed in the first generation GDI engines. The major disadvantage of WG systems is fuel impingement on piston surface and cylinder walls, which results high particulate emissions. SG systems are an improvement over WG systems, due to their potential to reduce particulate emissions. In SG systems, the location of injector relative to the spark plug is such that some of the fuel is directed towards the spark plug for ignition, while the remaining fuel is dispersed into the remainder of the cylinder. The injected fuel-vapor cloud assumes a hollow conical shape inside the chamber. SG systems are designed to reduce fuel impingement on piston surface and cylinder walls. There has been a movement towards SG systems in lieu of WG systems. SG systems are being employed in the second generation GDI engines [7, 20, 21, 22].

1.3. Operation of GDI under Low and High Loads

The operation of GDI engines differs for low and high engine load conditions. For low engine loads, there is typically a single injection event in which fuel is injected near the end of the compression stroke. High injection pressure and heat from the intake air help atomize the fuel in the cylinder. Due to shorter mixing time, the charge is not well-mixed, and becomes stratified, resulting in pockets of fuel-rich and fuel-lean mixtures. Thus, the air-fuel ratio inside the cylinder varies depending on location within the cylinder. The fuel is injected such that the fuel-air mixture is richer close to the spark plug and leaner towards the wall of the cylinder.

The overall average air-fuel ratio in the chamber can be as lean as 50:1, but close to the spark plug it is still rich enough to ignite easily [7, 8, 11, 14, 17, 23]. At higher engine load, fuel is injected in multiple events. A portion of fuel is injected during the intake stroke so that the air flowing into the chamber can aid air-fuel mixing. This creates a homogenous charge, in which fuel is evenly distributed throughout the cylinder, similar to a PFI engine. However, the mixture is too lean to ignite. A second shot of fuel is injected as the piston comes up during the compression stroke, forming a fuel-rich mixture region near the spark plug surrounded by the fuel-lean mixture throughout the rest of the cylinder. This rich-lean stratification within the cylinder helps prevent uncontrolled combustion, or knocking and, along with the cooling effect of the spray mentioned earlier, enables a higher the compression ratio. Higher compression ratio increases engine torque and efficiency and, in turn, improves fuel economy. GDI engines are more fuel efficient to a large extent because of their higher compression ratios [7, 8, 11, 20, 14, 17, 23].

1.4. Fuel Economy of GDI versus PFI

There are varied reports of the fuel economy advantage of GDI vehicles when compared to conventional PFI vehicles. Early studies, such as [7] have theoretically estimated the fuel economy advantage to be close to 25% depending on the test cycle. Another study [23] theoretically estimate the advantage at 20%. The study [24] reported the measured advantage to be 20 to 30%, while another study estimated only a 1.5% decrease in fuel consumption (National Research Council, 2015). The study [15] measured a 2% to 4% fuel economy advantage. Thus, there seems to be a lack of consensus regarding the fuel economy advantage of GDI engines over PFI engines. Recent studies focusing on particulate matter (PM) emissions from GDI engines, such as [7, 8, 11, 20, 14, 17, 23]. Other studies [21, 25, 26] cited the earlier studies, and EPA rated fuel economy data regarding the fuel economy advantage, but have not reported any new data. Moreover, the existing reports are based on either theory or lab-based dynamometer tests, and do not account for real world fuel economy.

1.5. Emission Rates of GDI versus PFI

Due to differences in fuel entry and combustion dynamics, GDI engines are expected to have different emission characteristics than PFI engines. GDI engines emit higher rates of 15 ultrafine particles (UFPs) compared to PFI engines, both in terms of mass and particle number [7, 14, 17, 20, 21, 25, 26, 27, 28, 29, 30, 31, 32, 33, 34, 35]. In GDI engines, when the fuel is injected late during compression stroke, the process of fuel vaporization and gas phase mixing remains essentially incomplete, which leads to both fuel-rich and fuel-lean mixture pockets. Direct injection can also lead to impingement of fuel on the cylinder walls and the piston head.

While impingement on piston surface is a part of WG systems design, uneven fuel flow due to carbon build-up and regular wear in the injectors in both WG and SG systems can result in fuel impingement on cylinder walls and piston surface. These surfaces create a "wall effect" because they tend to be much "cooler" than the flame temperature reached in the central part of the cylinder. Colder temperatures slow down combustion kinetics. Pockets of fuel rich mixtures, coupled with slower reaction kinetics, can lead to products of incomplete combustion (PIC). Fuel-rich combustion can produce UFP and unburned hydrocarbons (HCs). UFP formation is also attributed to incompletely volatilized fuel droplets in the unburnt gas [7, 14, 20, 25, 27, 28, 30, 31, 32, 36, 37]. The total soot particle number emitted by GDI engines is generally higher compared to PFI engines, and to diesel engines equipped with a Diesel Particulate Filter (DPF) [22, 31] reported that a GDI LDGV had black carbon (BC) emissions an order of magnitude higher than for PFI engine vehicles based on chassis dynamometer measurements. Automobile manufacturers have been trying to reduce PM emissions by improving engine designs and calibrations. First-generation WG GDI engines are known to have higher PM emissions than the second-generation SG GDI engines [30, 39]. BC emissions from vehicles measured on the Federal Test Procedure (FTP) and US06 for WG GDI were highest compared to SG GDI and PFI. In contrast, SG GDI BC emissions were lower on the aggressive US06 driving cycle, compared to PFI [38] Higher particulate emissions from WG systems are largely because fuel spray in WG systems impinges on piston and cylinder surfaces more so than for SG systems, which leads to cooling of the fuel spray and more particle formation [40]. Reduction in PM emissions from GDI engines can be achieved through improving variables such as air-fuel ratio, fuel injection timing, number of injections, injection pressure, coolant and engine temperatures [33]. Another solution to reduce PM emissions from GDI engines are Gasoline Particulate Filters (GPFs). GPFs have the same general operating principle as DPFs [41]. GPFs are shown to control both PM mass and particle number emissions from GDI engines [33, 42]. A prototype GPF, based on a design similar to a DPF, reduced BC emissions by 73 percent to 88 percent on the FTP and by 59 percent to 80 percent on the US06, depending on temperature [33]. As an added advantage, catalyzed GPFs could reduce emissions of other regulated pollutants [42]. However, there are concerns related to the implementation of GPFs. GPFs are estimated to add approximately $100 to the cost of a vehicle [43]. GPFs have an influence on the system back pressure. Increase in system back pressure may cause an increase in fuel consumption [33]. Due to the concerns regarding implementation of GPFs, they are more likely to be required in markets that use the Euro 6 or similar particle number standards, than in in markets such as the U.S. where there are only PM mass emission standards (DieselNet, 2017). GPFs are now being used in Europe to meet the Euro 6 particle number standard of 6.0×10^{11} particles per kilometer for direct injection engines that went into effect in 2017 (DieselNet, 2018). For a PFI engine, as the air-fuel mixture becomes leaner from stoichiometric, NO_x formation increases at first, due to availability of oxygen coupled with sufficiently high flame temperature. However, NO_x levels drop as the mixture is leaned beyond 16:1 or 17:1 [9, 11]. This is due to decrease in temperature in the reaction zone, which results in a decrease in NO_x formation and engine-out NO_x emission concentrations. For a GDI engine, there are several competing factors that dictate the overall rate of NO_x formation. Fuel-rich zone at the core of stratified charge reduces initial NO_x formation. Fuel-rich zone followed by a fuel-lean secondary zone enables burn-out of PICs without forming additional NO_x.

Thus, the rate of NO_x formation is reduced due to staged combustion in GDI engines. However, rate of NO_x formation tends to increase with pressure inside the combustion chamber. High compression ratio increases NO_x formation in GDI engines. Cooling effect of fuel vaporization in the cylinder lowers the peak flame temperature in GDI engines, which tends to lower NO_x formation. These competing phenomena tend to compensate each other [7, 27]. The study [11] found that when the fuel is injected early during the intake stroke in a GDI engine, NO_x emissions of GDI nearly match PFI operation in the same cylinder head. This is due to creation of a homogenous charge inside the combustion chamber and similar residence time in both cases. In case of homogenous charge, NO_x levels increase as the mixture is leaned from stoichiometric, and then decrease if leaned beyond 16:1 or 17:1, both for GDI and PFI engines. In contrast, if the fuel is injected during the compression stroke in GDI, the NO_x levels for a stoichiometric overall air-fuel ratio are lower for late injection GDI than either case of homogenous mixing, i.e., early injection GDI and PFI. This indicates that a greater fraction of fuel combusts at an air-fuel ratio that is locally richer than stoichiometric. Leaning the charge further from stoichiometric overall air-fuel ratio results in monotonically increasing NO_x emissions in the case of late injection GDI, which indicates that a substantial fraction of the fuel is combusting at local air-fuel ratios which produce higher levels of NO_x than the overall air-fuel ratio would suggest. The study [21] conducted field measurements using remote sensing for a total of seven GDI vehicles in Toronto, Canada, and compared their results with the Toronto vehicle fleet emission factors reported by [44]. The emission factors reported by [44] are based remote sensing measurements of 100,000 vehicle-related plumes of the Toronto vehicle fleet, which is comprised of 94% gasoline-powered vehicles. The study [45] reported that for NO_x, the average fuel-based emission factors from GDI vehicles were 52nd percentile of the total vehicle fleet, indicating that NO_x emissions from GDI were in line with Toronto vehicle fleet. Saliba et al. (2017) found no statistically significant differences in NO_x emissions from laboratory-based tests for GDI and PFI vehicles. Another study [24] reported that cycle average NO_x emission rates for GDI vehicles tested in laboratory-based chassis dynamometer test were on average lower by 30% than PFI vehicles that were tested. CO is formed due to incomplete oxidation of fuel. In PFI engines, CO formation is high for homogenous fuel-rich mixtures, and decreases steeply at first as the homogenous mixture leans towards stoichiometric ratio. CO formation for stoichiometric charge, which is 14.6:1 air to fuel ratio, is considerably lower than if the ratio were 13:1 or 12:1. CO formation decreases further as the charge leans from stoichiometric ratio, however, the decrease is not as steep as between 13:1 and 14.6:1 [9]. In GDI engines, pockets of fuel-rich mixture in the stratified charge generate CO emissions, even if the overall combustion is relatively lean [7]. However, while CO formation is higher in the fuel-rich pockets, it is possible for the CO produced from fuel-rich pockets to oxidize as it mixes with burnt fuel-lean charge, which will still be rich in oxygen. This is known as post-flame oxidation. [21] report that CO was not detected in significant concentrations in the GDI exhaust, since the vehicles they tested were new. Low CO emissions can be attributed to the high effectiveness of three-way catalyst (TWC) in newer vehicles. The effectiveness of TWC decreases with age. [21] reported that CO concentrations in 65% to 90% of vehicle plumes from GDI vehicles they measured using remote sensing were below detectable limits, depending on the distance of the monitor from the roadside.

Due to small sample size of plumes where CO emissions were detected, [21] concluded that the GDI CO emissions from the vehicles tested relative to the fleet are uncertain. [24] found that CO cycle average emissions were on average 40% lower for GDI vehicles than PFI vehicles. [26] found no statistically significant differences in CO emissions between GDI vehicles and PFI vehicles. HC is formed either due to incomplete oxidation of fuel in fuel-rich mixtures, or when fuel-lean mixtures are not completely burned inside the combustion chamber, which results in emission of unburned HCs in vaporized fuel. For PFI engines, HC formation is high when the charge is fuel-rich, decreases as the mixture leans towards stoichiometric air-fuel ratio of 14.6:1, is nearly constant between an air-fuel mixture of 14:1 and 18:1, and increases after the mixture leans beyond air-fuel ratio of about 18:1 [9]. In GDI engines, production of HCs is more complex than PFI engines due to stratification of charge. HC emissions are produced both due to fuel-rich pockets and fuel-lean pockets. Unburned HC emissions resulting from fuel-lean pockets depend on how far the flame propagates through the cylinder [27]. In addition, HC emissions are also produced in a GDI engine due to wetting of cylinder wall and piston head, which depend on design of the combustion chamber, timing of injection and location of the injector. Wetting of cylinder wall and piston head is typically more prevalent in WG GDI systems than SG GDI systems. Thus, HC formation is inherently higher in WG systems due to their design, compared to SG systems. Cooling effect of fuel spray, which lowers the charge temperatures by up to 21 30°C in the combustion chamber, reduces the degree of post-flame oxidation of HCs, leading to engine-out HC emissions [11]. For the case of multiple injection events, GDI and PFI are reported to have similar HC emissions for all overall air-fuel ratios. For the case of late injection during the compression stroke, HC emissions are reported to be similar for GDI and PFI at richer overall air-fuel ratios. However, combustion becomes unstable at overall ratios leaner than about 18:1, resulting in high engine-out HC emissions from GDI engines [11]. The study [45] reported benzene, toluene and ethylbenzene-xylenes (BTEX) instead of total HCs. It reported that BTEX emissions from seven GDI vehicles they measured were substantially higher compared to the Toronto fleet (range: 80^{th} – 90^{th} percentile), and suggested that GDI vehicles may increase ambient BTEX levels. [45] inferred that BTEX, which are soot precursors, may be elevated due to incomplete or fuel-rich combustion in the GDI engines. In contrast, [26], with results based on a larger fleet of 15 GDI vehicles tested, found no statistically significant differences in BTEX emission rates of GDI and PFI vehicles. GDI vehicles tested by [26] consisted of 11 WG and 2 SG GDI vehicles. 2 GDI vehicles were unclassified. Further, [26] also reported that for the GDI vehicles they tested, BTEX emissions mirrored total HC emissions. [26] also found no statistically significant difference in HC emission factors between GDI and PFI vehicles. However, [24] found that 3 GDI vehicles they tested had 45% less HC emissions than a fleet of PFI vehicles they tested.

2. Mechanisms for the formation of the Pollutant Emissions

2.1. Carbon Monoxide Pollution – CO

Carbon monoxide is the result of a partial oxidation of carbon caused by an oxygen defect that does not allow the transformation into carbon dioxide. CO is also produced under conditions of a sufficient quantity of air, but its formation also depends on chemical kinetics. The sequence of reactions is:

$$RH \rightarrow R \rightarrow RO_2 \rightarrow RCHO \rightarrow RCO \rightarrow CO$$

and is characterized by being a succession of very rapid reactions that leads to an almost complete oxidation of carbon to CO. Next we have:

$$CO + OH \rightarrow CO_2 + H$$

and since at high temperatures there are high concentrations of CO and OH with the consequent equilibrium of the chemical system of C, O-H. These form the CO_2 only if sufficient residence times are ensured for adequate training temperatures; the speed, as a function of temperature, however, becomes practically zero below 700 °C and can lead to stopping the reaction. Carbon monoxide is produced during incomplete combustion. Anything that leads to incomplete combustion increases CO production. Two major causes are a rich fuel mixture (more fuel than is needed), or restricted air supply (dirty or plugged air filter). A gasoline engine producing 10,000 ppm CO at the ideal air-fuel ratio will produce over 60,000 ppm when the fuel is increased. Other causes of high CO production include a cold engine, misfiring, incorrect engine timing, defective or worn parts, exhaust system leaks, and defective catalytic converters.

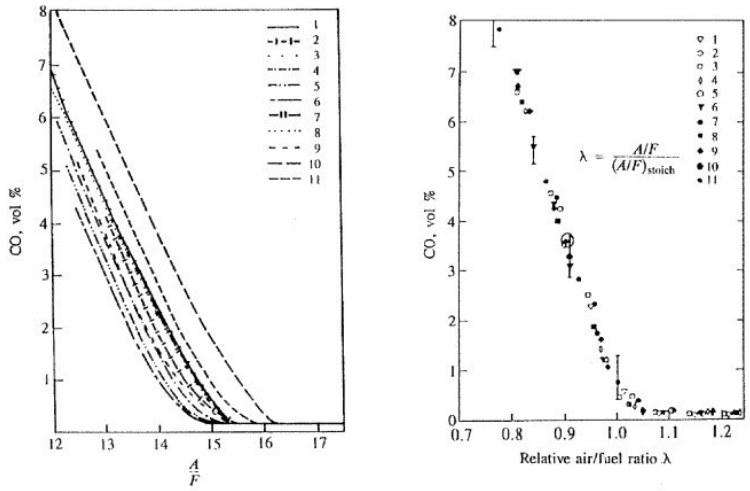

Figure 2.1: Effects of Air-Fuel Ratio on CO emissions [46]

2.2. Hydrocarbons Pollution – HC

Index of combustion efficiency, but not pollution, is the amount of unburnt hydrocarbons, those products given by incomplete oxidation of the fuel, the composition of the fuel determines which type of waste. The gases of exhaust contain many types of unburnt hydrocarbons and the composition of the fuel can greatly influence the composition and extent of HC, however most of HC is not formed in combustion, but by pyrolysis, or by decomposition of organic compounds by temperature reached in the cylinder. Others to mention are the carbonyls, characteristic especially in Diesel while the phenols that are divided into aldehydes and ketones are typical of those engines that use alcohol as fuel. The principal sources of unburned HC in SI engines are the following:

- Crevices
- Absorption and desorption in oil layers
- Absorption and desorption in deposit
- Quenching (bulk and wall layer)
- Liquid fuel effects
- Exhaust valve leakage

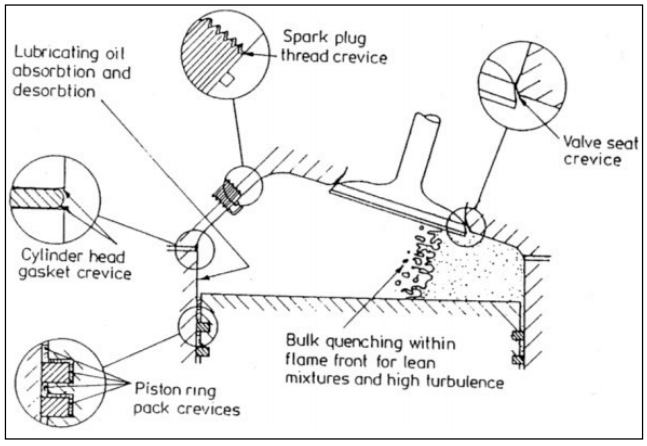

Figure 2.2: Crevice HC mechanisms [47]

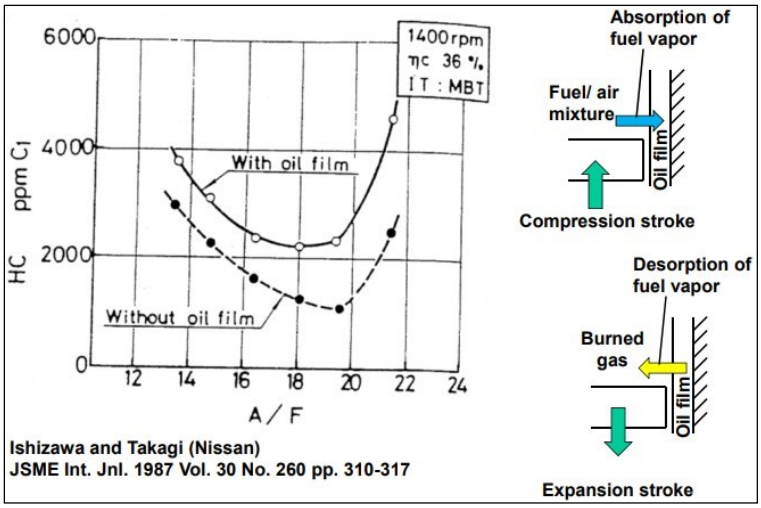

Figure 2.3: Absorption and desorption of fuel vapor [47]

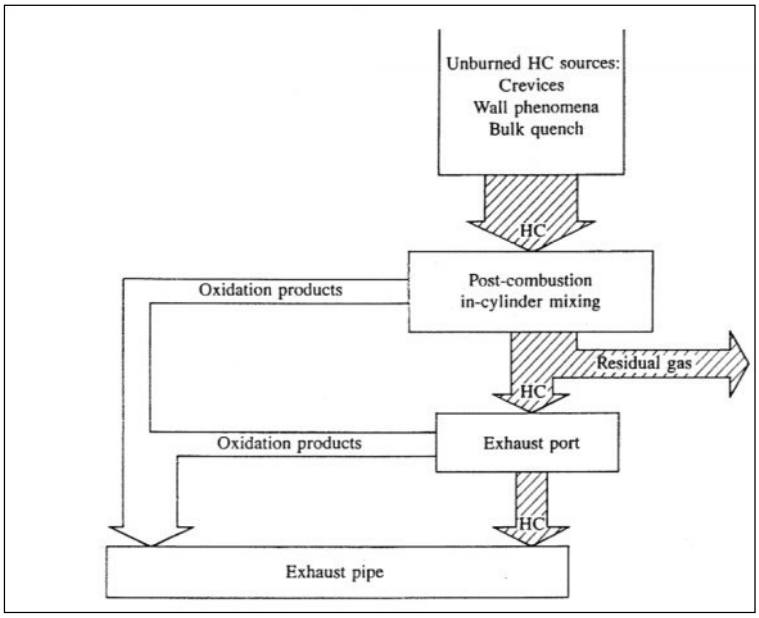

Figure 2.4: HC Pathway [47]

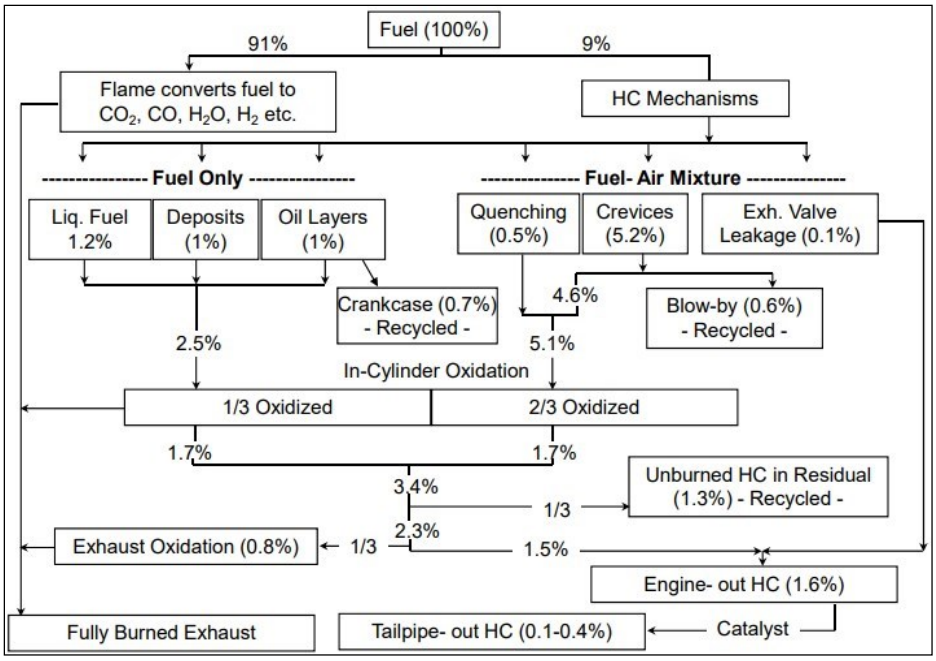

Figure 2.5: HC Pathway – Steady State [47]

Source	% Fuel Escaping Normal Combustion	Fraction Emitted as EOHC	% Fuel as HC Emissions	% of Total EOHC Emissions
Crevices	5.2	0.15*	0.682*	42.6
Quench	0.5	0.15	0.074	4.6
Oil Layers	1.0	0.09**	0.090**	5.6
Deposits	1.0	0.30	0.300	18.7
Liquid Fuel	1.2	0.30	0.356	22.2
Valve Leakage	0.1	1.00	0.100	6.3
Total	9.0		1.60	100

* Blowby (0.6%) subtracted
** Amount to crank case (0.7%) subtracted

*steady state cruise condition (1500 rpm, 2.8 bar NIMEP)

Table 2.1: HC Sources: magnitudes and percent of total engine-out emissions* [47]

In order to control the HC emissions the principal strategies are the following:

- Reduce crevice volume
- Keep liner hot
- Comprehensive cold start strategy
  - Retarded timing, fuel rich followed by exhaust air injection.
- Spark retard
  - Higher burned gas temperature in the later part of expansion stroke and higher exhaust temperature.

2.3. Nitrogen Oxide Pollution – NO_x

Nitrogen oxide (NO_x) emissions consist of nitric oxides (NO) and nitrogen dioxides (NO_2). At high temperatures, characteristic of the combustion chamber of engines, nitrogen molecules in air react with oxygen to form NO gas. NO_2 is predominantly formed from the reaction of NO and peroxy radicals, but is rapidly converted back to NO at high-temperature environments containing an abundance of H and O radicals. The nitrogen atoms in the formation of NO_x primarily come from the nitrogen in air, which is composed of 78% N_2.
The nitrogen atoms in some fuels (e.g. coal) can also contribute to NO_x emissions, but this is not relevant for most transportation fuels. NO can be formed via a number of reaction mechanisms, the two most significant being thermal and prompt NO formation:

- Thermal NO : This mechanism for NO formation is considered relevant at temperatures above 1,800K where the strong N_2 bond can be broken to initiate the following series of reactions:

$$N_2 + O \rightarrow NO + N$$

$$O_2 + N \rightarrow NO + O$$

$$N + OH \rightarrow NO + H$$

  This mechanism is the dominant source of NO in fuel-lean and stoichiometric conditions (Section 3.2) [49].

- Prompt NO : This mechanism is responsible for the formation of NO in the colder part of the flame and becomes significant under fuel-rich conditions, since it requires a high concentrations of the hydrocarbon radical species to initiate the sequence of reactions. These reactions first produce Cyanonitrene (NCN) and hydrogen cyanide (HCN), which undergo further reactions to form NO [50]**:**

$$CH + N_2 \rightarrow HCN + N$$

$$CH_2 + N_2 \rightarrow HCN + NH$$

$$N + O_2 \rightarrow NO + O$$

$$HCN + OH \rightarrow CN + H_2O$$

$$CN + O_2 \rightarrow NO + CO$$

An important operating condition of an engine is the air-fuel ratio, λ. For any combustion process, both fuel and oxidizer are required for a chemical reaction. If the exact right amount of air is supplied to burn off all of the fuel, this proportion of air to fuel is referred to as stoichiometric ($\lambda = 1$). If there is not enough air to burn all of the fuel, the mixture is called fuel-rich ($\lambda < 1$). Lastly, if there is excess air, the mixture is called fuel-lean ($\lambda > 1$). For gasoline, the stoichiometric air-fuel ratio is 14.7. Figure 2.6 shows the emissions associated with each combustion regime.

At higher loads, engines often operate at rich conditions for maximum power. The higher flame speed of ethanol helps in achieving complete combustion for rich mixtures. Most SI engines are designed to operate at stoichiometric or lean conditions and to minimize fuel enrichment, except during short periods of high-load (e.g. acceleration). The various operating conditions of the engine have respective NO_x emissions. However, these values of NO_x are all well within the capacity of three-way catalytic converters, which convert NO to N_2 in order to meet regulatory standards.

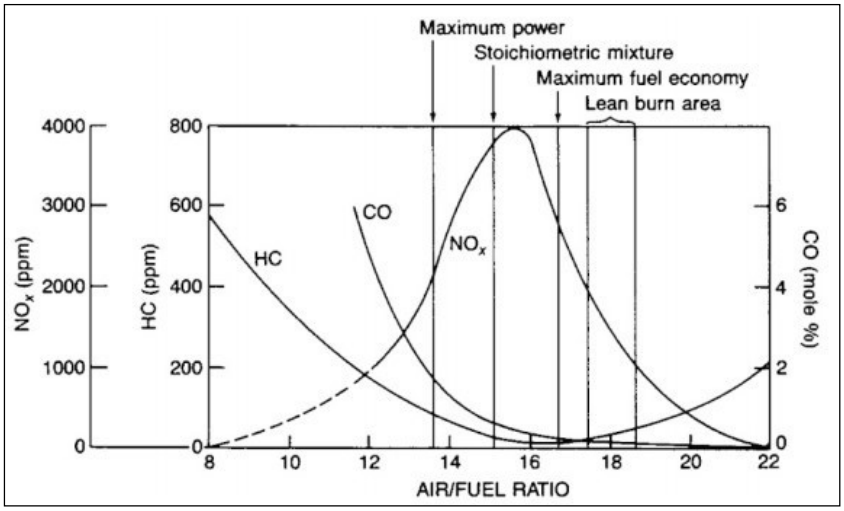

Figure 2.6: Concentration of HC, CO, and NO_x emissions as a function of air-fuel ratio in a typical gasoline engine. Stoichiometric mixture (λ=1) corresponds to an air-fuel ratio of 14.7 [51].

2.4. Particulate Matter Pollution – PM/PN

For many years, gasoline particulates were seldom-discussed, due to the rationale that "if you can't see it, it doesn't exist." Diesel engines have long been implicated as particle producers, producing visible smoke due to high particulates. The Euro 4 regulations in Europe (EU) required a particle mass (PM) reduction. The Euro 5b regulation required further PM reduction and introduced a particle number (PN) standard. Subsequent regulations in the United States required particulate filters on all diesel vehicles using PM standards. Now, one seldom sees visible smoke from a diesel engine in the western world, unless the owner has tampered with the system (sometimes referred to as rolling coal) or the system has a defect.

Diesel vehicles equipped with particulate filters are now cleaner than gasoline vehicles, from both a PN and PM standpoint. While gasoline engines seldom emit visible smoke, they can and do produce a lot of particles. Gasoline engine technology has improved power and fuel economy, such as in the case of gasoline direct injection (GDI) technology, but can also produce additional unseen particles. A typical gasoline engine emits many trillions of particles every km (about a billion particles every meter).

This makes car-starting locations, like curbsides, home garages, and parking garages, potentially high-concentration zones. Other potential high-risk zones include areas near stoplights and traffic throughways. European entities appear to be the first to recognize the importance of limiting the number of particles emitted from both diesel and gasoline engines, in addition to the mass of the particles. Europe began to regulate gasoline direct injection engines in 2014, with a PN limit of 6×10^{11} particles/km (that's 600 billion particles/km) on the new European drive cycle (NEDC) certification test cycle. For the first 3 years, manufacturers were allowed to exceed this PN value by a factor of 10. Since September 2017, the 6×10^{11} particles/km limit value has to be met for all new type approvals, tested now over the new certification cycle, the world harmonized light vehicle test cycle (WLTC). In addition to the new test cycle, the European regulators also added a second condition for real-world driving emissions (EU6-RDE), to assure that the PN won't exceed the regulatory limit (plus a measurement error, currently set at 0.5 times), on the EU6-RDE or during normal driving. The EU regulations will be fully phased in by 2020. Particulates are most often the result of incompletely combusted fuel, with many potential mechanisms occurring simultaneously under a wide variety of engine conditions to produce particles. Particulate output and composition change as the result of a number of varied factors including, but not limited to, temperature, altitude, fuel quality, vehicle power-to-weight ratio, drive cycle, as well as engine hardware and software. In addition, high exhaust temperatures during high-speed and high load operation can lead to PM storage and release of material from sampling system surfaces [52] and exhaust systems [53], increasing uncertainty for OEMs.

2.4.1.1. Regulations on Vehicular Exhaust Particulate Emissions

In Europe, PN limits have been in place for diesels since 2013. Starting in 2014, new GDI platforms have had to also effectively meet a PN-based limit of 6×10^{12} #/km, for solid particles larger than 23 nm in diameter. This limit tightened to 6×10^{11} #/km in September 2017 for new type approvals, and all new vehicles have to meet the limit starting September 2018. Other than the PN limits, the Euro 6 regulations also further limit tailpipe gas emissions and set PM limit at 4.5 mg/km (7.2 mg/mi). Durability is specified at 160,000 km. The emission limits and introduction timings are summarized in Figure 2.7, and details on the test methods are provided in the following section. Other than the regulated limits mentioned above, the increased emphasis on public disclosure is worth highlighting. Information on real-world driving emissions (EU6-RDE) testing must be provided via free website and include maximum test values for NO_x and PN [54]. Also, an "extended documentation package" is to be provided by OEMs on Auxiliary Emission Strategies.

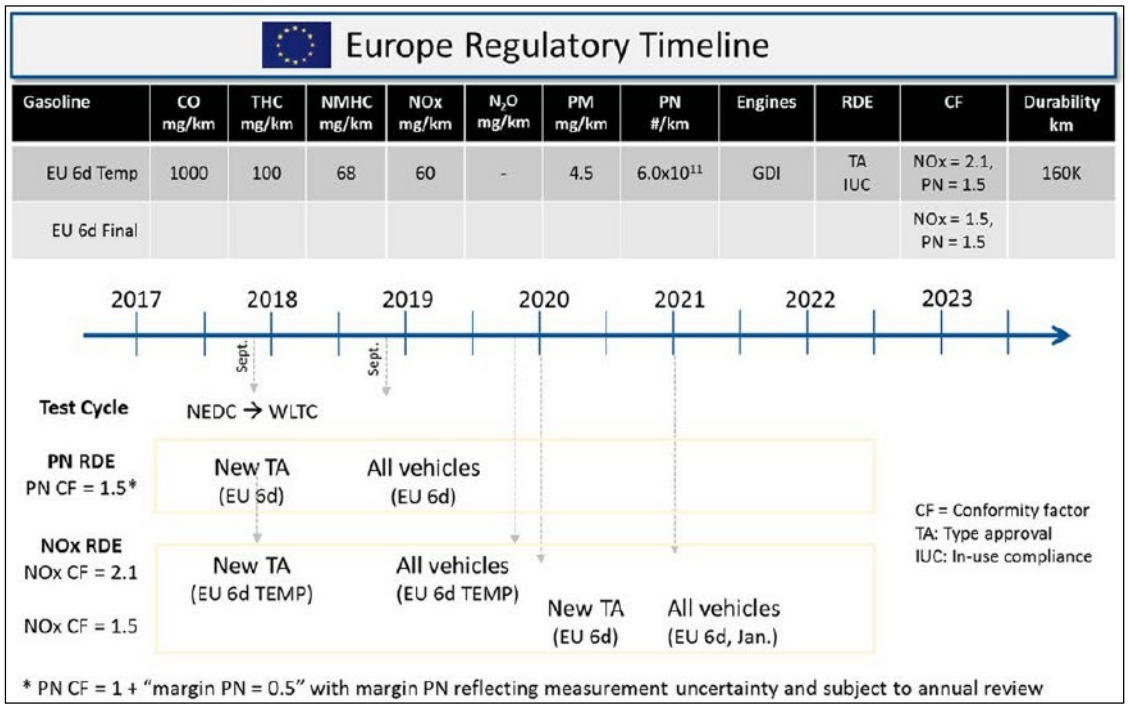

Fig. 2.7 Overview of Euro 6d regulations and implementation timeline [260].

2.4.1.2. Test Procedures

The Joint Research Centre (JRC) reported [55] the issue of on-road emissions far exceeding the certification values obtained under controlled lab testing. The study demonstrated the accuracy and reliability of portable emissions measurement systems (PEMS) for measurements of tailpipe emissions from on-road vehicles. Accordingly, several important changes have been recently introduced in the legislation to ensure compliance with emission norms under real-world driving conditions. Starting September 2017, the chassis-dynamometer-based certification test cycle is changed from the New European Drive Cycle (NEDC) to the World Harmonized Light Vehicle Test Procedure (WLTP) [56]. A complementary EU6-RDE test procedure is introduced and not-to-exceed (NTE) limits have been expressed as Euro 6 emission limits multiplied by the "conformity factors (CF)". The development of the EU6-RDE legislation was split in four packages. The first two outlined the basic test procedures: boundary conditions for a valid EU6-RDE test, data evaluation tools, requirement of the PEMS equipment, and specification of CFs. The third package included the evaluation of cold-start emissions, regeneration events, and test provisions for hybrids, while a fourth and final package covers in-service compliance, surveillance tests, and provisions for light commercial vehicles. At the time of this printing, the fourth package had not been published. The conditions for a valid EU6-RDE test have been designed to be representative of normal driving conditions on European roads. The vehicle is to be driven for 90-120 min on a mix of urban, rural, and motorway (highway) routes, starting with the urban segment. The segments are identified by the vehicle speeds, and these are noted in Table 2.2 summarizing some of the EU6-RDE trip specifications. The EU6-RDE emission limits along with the associated CFs must be met over the entire EU6-RDE trip and the urban part separately as well. For new type approvals, the CF is set at 1.5 for PN and temporarily at 2.1 for NO_x starting September 2017, while the latter is also reduced to 1.5 in January 2020 (the timing is extended by 1 year for all vehicles in both cases). The conformity factors are expressed as "1+margin error" with the equipment margin of error being set at 0.5 for the final factors for both NO_x and PN.

	Urban	Rural	Motorway
Distance	>16 km	>16 km	>16 km
Relative fraction	29%–44%	23%–43%	23%–43%
Driving speeds	15–40 km/h	60–90 km/h	>90 km/h >100 km/h for at least 5 min V_{max} < 145 km/h

Table 2.2: EU6-RDE trip specifications [260].

Other boundary conditions have to be complied with for a test to be valid:

- The altitude difference between the start and end points of the test should be less than 100 m, and the cumulative altitude gain should be limited to 1200 m/100 km.

- Moderate and extended temperature and altitude ranges are specified-emissions associated with any data points which fall in the extended category are divided by 1.6:
    - The moderate conditions are 0 to 700 m altitude and 0°C to 30°C ambient temperature.
    - The extended conditions cover 700 – 1300 m altitude and between −7°C to 0°C and 30°C to 35°C ambient temperatures.
    - If any data point falls outside these boundary conditions, the entire trip is considered invalid.
- For valid tests, the data has to be further processed using at least one of two methods: the moving-average window method (with associated EMROAD software) and the power-binning method (with associated software called CLEAR).

Vehicle preconditioning is described: the vehicle has to be driven for at least 30 min and parked with engine turned off for 6 – 56 h before starting the EU6-RDE test. In the first two packages of EU6-RDE, cold-start emissions, as defined by emissions occurring in first 5 minutes or until engine coolant reaches 70°C, were excluded. Recognizing that a significant fraction of emissions occur during cold start, the 3rd package [57] specifies that these emissions are now included in the analyses. Also included are emissions associated with regeneration events, corrected through the use of Ki-factors. If regeneration occurs during the first test, it can be voided at the request of the manufacturer, but the 2nd test is considered valid even if regeneration occurs, and the associated emissions during regeneration are included in the overall evaluation. The 3rd EU6-RDE package also describes the calculation of emissions from hybrid vehicles. The internal combustion engine has to be working for at least 12 km under urban driving conditions, and it is recommended that the trip be started in charge sustaining mode. The emissions are weighted according to the CO_2 emissions under charge-sustaining mode as described below.

Emissions of any species (*M*) are calculated according to the following equation:

$$M\left(\frac{\text{mg}}{\text{km}},\frac{\#}{\text{km}}\right)=\frac{\text{Total emissions}\left(\text{mg or}\,\#\right)}{\text{Total}\,\text{CO}_2\left(\text{mg}\right)}\times \text{CO}_{2,\text{WLTC}}\left(\frac{\text{mg}}{\text{km}}\right)$$

where $CO_{2,WLTC}$ is measured in charge-sustaining mode. Looking ahead, the accuracy of PEMS equipment is expected to improve, and with the availability and review of EU6-RDE data, a downward revision of CFs to 1 may be expected. Furthermore, there are also considerations to include ultra-fine particles below 23 nm in the regulated limits, and the emission profiles and measurement capabilities are being reviewed [58].

2.4.2. Technology Pathways

Various strategies are being pursued to minimize particulates [59, 60]. This section provides a brief overview of technical considerations and pathways for reduced particulate formation and tailpipe emissions.

2.4.2.1. In-Cylinder Methods

A lot of work is being done to minimize the in-cylinder formation of particulates and thereby reduce the emissions at the source. Primary consideration is given to achieving mixture preparation and avoiding fuel-rich regions. Piston bowl, engine, and injection system design is aimed at reducing impingement of fuel on the cool piston and cylinder surfaces, known sources for increased particulates. The combustion system is broadly classified into spray-guided and wall-guided systems, which differ primarily in terms of the strategy used for charge stratification. In spray-guided systems, the injector and spark plug are in close proximity and some of the fuel is directed towards the spark plug. Wall-guided systems rely on the fuel impingement on piston bowl surfaces and the subsequent transport of fuel towards the spark plug by the charge motion and flow field. Both systems have their challenges relevant to particulate formation: in spray-guided systems, the close proximity of injector and spark results in shorter time for fuel evaporation, whereas in wall-guided systems, fuel impingement with cold cylinder and piston surfaces leads to higher particle emissions.

2.4.2.1.1. Injection System

Proper design of the injection system is critical to achieve the desired mixture preparation within a short time between the opening of inlet valves and spark timing. The rapid, fine atomization of fuel requires the use of higher injection pressures as compared to PFI engines. Injectors are probably the most important element in the system. These have to be designed for accurate, rapid metering of fuel, at correct timing and small droplet size to ensure quick evaporation. Several factors of injector design and calibration are considered for achieving high fuel economy, low emissions, and low particulates [61, 62], including (a) the number of injection holes, spray pattern, duration and number of injections, fuel rail pressure, etc., and (b) higher fuel rail pressures (>250 bar), to help with better atomization and penetration of fuel spray and lower particulates. In one study [63], optimization of injection timing, and increased injection pressure from 200 to 500 bar was shown to reduce the particulate emissions by half. Coking of injectors should be minimized, as this is a key contributor to increased particulate emissions over the lifetime of a vehicle [64, 65, 66, 67, 68].

Coking of injectors leads to increased spray penetration and risk of fuel impingement on walls, reduced fuel atomization quality, increased fuel leakage during injector closing, and diffusion flame due to fuel absorbed by porous deposits. Injector prototypes developed recently [69] show that a significant reduction in PN emissions can be realized through the use of injectors which protrude into the combustion chamber, thus exposing them to higher temperatures which minimize deposit formation. Particulate formation is sensitive not only to the hardware but to the injection timing as well [70]. High emissions occur with early injection at intake stroke, due to impingement of fuel on piston surfaces. On the other hand, high emissions can also occur with highly retarded injection into the compression stroke, as this leads to insufficient time for mixture formation before onset of combustion. A split injection strategy is commonly used where the first injection introduces a fraction of the fuel early in the cycle to form a well-mixed lean charge, followed by a second injection done late in the compression stroke for increased heat release and early catalyst light-off. A combination of port fuel injection and direct injection can be used to reduce particulates [71]. Also multiple (double or triple) injections are carried out at low temperatures during warm-up or under high loads for improved fuel economy, knock mitigation, and lower emissions.

2.4.2.1.2. Variable Compression Ratio (VCR)

VCR has been developed over several years and primarily offers improved fuel economy through the optimal selection of compression ratio (CR) per the load requirement. During cold start, low CR results in increased distance between piston and injector, and therefore reducing propensity of particulate formation due to fuel impingement. Also, the improved combustion overall is expected to lower emissions in general. Despite its increased complexity, the benefits have led to commercialization of this system [72].

2.4.2.1.3. Exhaust Gas Recirculation (EGR)

EGR is increasingly being used to reduce NO_x emissions and also offer improved fuel economy. A benchmarking study done by EPA [73] showed a 7.5% improvement in fuel economy possible with the use of cooled EGR, starting with an Atkinson engine with a 14:1 compression ratio engine. Cooled EGR is also effective in reducing particulate emissions. In one study [74], EGR ratios (fraction of exhaust gas reintroduced in the engine) of up to 25% were studied. At part loads, brake-specific soot mass and solid particle number were reduced by more than 50% and 38%, respectively. At high speed, high-load conditions, fuel enrichment can be used to mitigate engine knock and to limit the high temperatures, which are detrimental to downstream components, such as turbochargers. Fuel enrichment, however, leads to high particulate and HC emissions and also leads to a fuel penalty, so it is generally avoided.

EGR is also effective in reducing the gas temperatures and therefore eliminate the need for fuel enrichment. Thus, particulate emissions reduction was observed even for the high-load conditions. In a more recent study [75], up to 75% reduction in PN was observed through the use of 15% EGR when fuel enrichment at high loads was avoided. The use of a GPF to clean the recirculated exhaust before entering the engine was found to yield a further reduction in particulates.

2.4.2.1.4. Lean and Low-Temperature Combustion

GDI engines can be operated in both stoichiometric and lean-burn combustion modes. Lean-burn operation is attractive due to its potential to reduce fuel consumption by 5%-15% compared to stoichiometric GDI engines. By definition, lean combustion avoids the fuel-rich combustion regime and is inherently suited for low particulate emissions. In practice though, particulate emissions were found to be high, in both the lean stratified and lean homogenous combustion modes. The modulated rich periods required to make ammonia for non-urea-based NO_x control for lean-burn operation are associated with transient particulate emissions [76], and the use of GPFs was shown to be effective in capturing particulates with >95% filtration efficiency. Much progress is also being made on achieving low-temperature combustion via compression ignition engines. Oak Ridge National Laboratory has provided an excellent summary on the various strategies being pursued [77], differing in the level of fuel stratification. The overall goal is to achieve (a) sufficient premixing of fuel/air to avoid soot formation associated with fuel-rich combustion and (b) reduce peak combustion temperatures via dilution with air or EGR to avoid NO_x formation. The key challenge for this technology is that by definition, exhaust temperatures are low, and this poses a challenge to keep the catalyst above light-off temperatures. An example is the development of the gasoline direct injection compression ignition (GDCI) engine targeted to meet Tier3-Bin30 limits [78].
A BSFC (brake-specific fuel consumption) of 211-214 g/kWh was demonstrated over a wide load range, utilizing a high CR of 16:1 and injection pressure of 350 bar.
The difficulty of achieving the very high conversion efficiencies (>99%) needed for HC has translated into a rather complex aftertreatment system, which at the latest stage includes a pre-turbo catalyst, HC trap, SCR, and a passive GPF for off-cycle particulates. An announcement of the commercialization of a spark-assisted HCCI engine was recently made [79] and promises to cut fuel consumption and likely emissions as well.

2.4.2.1.5. Electrification

Electrification of the powertrain is an attractive approach for reducing tailpipe emissions. Increasing on-board power on hybrid architectures—ranging from 48 V mild hybrids to full and plug-in hybrid electric vehicles (PHEVs)—can be used for propulsion of the vehicle and thereby reducing fuel consumption and associated emissions. However, there is increasing evidence that particulate emissions for hybrids can be equivalent or even higher than vehicles without any electrification. In a study in Japan [80], particulate emissions were measured on the JC08 test cycle from several gasoline and diesel vehicles, including one GDI and one MPI hybrid. Most of the particulate emissions for GDI and MPI engines were associated with cold start, with almost no emissions after the engine warmed up. However, in the case of hybrids, emissions were found to occur even after engine warm-up, most likely due to transient engine turn-on events. Overall, emissions from hybrid MPI vehicles were found to exceed those from diesels fitted with DPFs. In another study, a GDI engine was used to simulate HEV start-stop operation on an NEDC test [81]. Although the engine only operated 28% of the time during the cycle, the PN emissions were 4.5X higher than when the engine was run in conventional mode. In the case of PHEVs, attention is being given to particulate emissions associated with "high-powered cold starts" [82]. This is the scenario when the engine turns on for the first time when the vehicle is already moving at a high speed or under high load and results in cold-start emissions which are larger than would be under normal cold starts. A recent study focused on this issue and measured real-world emissions from a 1.5L GDI PHEV certified to Euro 6b standards and driven with various levels of charge on the battery [83]. As expected, the PN emissions in urban conditions were eliminated when the vehicle was propelled by battery alone. When the battery was depleted though, the demand on the IC engine was high and PN emissions were the highest. A peak in particulate emissions was observed when the engine turn-on was coupled with a high power demand. Hybrids and their power management strategies are evolving, and clearly there is room to improve on some of the above shortcomings. In the meantime, robust aftertreatment solutions are seen to be necessary to cover the operation of hybrids under widely varying real-world conditions.

2.4.2.2. Fuel Consideration

Concurrent with engine improvements, high fuel quality is a prerequisite when moving to the next level of regulations, both for its impact on combustion and aftertreatment systems. Major markets noted above have committed to low-S (<10 ppm) fuel. The chemical composition and physical properties of the fuel affect the injection quality and combustion characteristics, and there are several studies which link these properties with particulate formation [84, 85, 86, 87, 88, 89, 90]. Unfortunately, in many markets, fuel quality varies widely, even when fuels are within the legal specifications. The topic of fuel and its influence on particle formation is also a topic covered in more detail in another chapter of this book. A PM index (PMI) model has been proposed [91], which quantifies the relationship between fuel composition and the particulate emissions.

The model accounts for the double bond equivalents, vapor pressure, and weight fraction of each component in the fuel. A strong correlation has been confirmed between the PMI index and particulate emissions. Aromatics are clearly linked with increased particulates, both through their role in the formation of PAHs and through their lower volatility which leads to slower mixture formation. One study [89] found that compared with a domestic Korean fuel with high oxygen content, the use of Euro 5 fuel with higher aromatics led to a 77% increase in PN emissions over the NEDC test cycle. In a study of the emissions from various GDI and PFI engines on the LA92 test cycle [92], Tier2-Bin2 and SULEV vehicles showed an increase in cumulative PM by 148% when the aromatics content was increased from 15% to 25%, and further increase by 73% when the aromatics content was increased to 35%. In light of these studies, the availability of fuel with low aromatics content will be an important consideration to achieving low in-use emissions. The aromatics content in gasoline has been lowered over the years. In the United States, the Tier 3 gasoline fuel specifications cap the aromatics content at 25%. Other components such as oxygenates which improve combustion or volatility can be expected to lower particulates. One such oxygenate which is already added mandated in some regions is ethanol. In the United States, the Renewable Fuel Standard requires the use of renewable fuel to be blended with gasoline, and ethanol is primarily used. Ethanol is considered potentially beneficial for lowering particulates due to the increased oxygen content and the displacement of aromatics. There are conflicting reports, which also found an increase in emissions when using ethanol [93], and the differences in findings likely stem from the sensitivity of particulate formation to other properties such as its impact on physical properties and the engine operating conditions. Other studies confirm the benefit of using ethanol-blended fuels during the cold-start phase of the FTP test cycle [94] and on the WLTC [95]. Other oxygenates have also been studied. The impact of M15 methanol/gasoline blends [96] on spray behavior and particulate emissions showed that the blend did not consistently lead to low particulate emissions. Higher oxygenates, such as butanol, also show promise. In one study [97] testing a GDI vehicle on FTP75 and US06 cycles, both PN and PM emissions were found to reduce, compared to reference E0 fuel when it was splash blended with 10% ethanol (E10) and 16% isobutanol (iB16). The blend with butanol gave higher reductions. On the US06 test cycle, PM emissions reduced from 2 mg/mi for E0 to 1.9 mg/mi for E10 and to 0.4 mg/mi for iB16.
In another study, addition of 33% butanol to E5 gasoline (5% ethanol) was shown to reduce particulates while keeping a similar particle size distribution [98].
In order to meet the CO_2 targets, a wide variety of advanced gasoline engine technologies are being pursued which have implications for tailpipe emissions [99]. Some of these engine improvements have an added benefit in terms of reduced particulates. Since the advent of modern automobiles, the spotlight has been mostly focused on one key feature of its operating fuel - the octane rating. This number quantifies a fuel's capacity to resist autoignition when compressed. Vehicles with spark-ignition (SI) internal combustion engines, which run on gasoline, comprise over 90% of the U.S. fleet. SI engines operate by first compressing the fuel-air mixture in the combustion chamber and then, at a carefully determined time, igniting that compressed mixture to transfer chemical energy to mechanical energy. If the fuel auto-ignites before the ignition is initiated by the spark plug, the engine experiences knocking, which can have negative performance effects or even damage the engine (Fig. 2.15). Proper functioning of an SI engine relies on high-octane gasoline fuels, since they have higher anti-knock properties.

Automakers design the extent of piston compression of their engines to be compatible with current fuel octane standards. An engine's compression ratio (CR) is the proportion of the cylinder volume at the bottom of the piston stroke to the top of the stroke. CR directly correlates to engine efficiency therefore, extending octane ratings beyond the current minimums can enable automakers to produces engines with better performance and fuel economy.

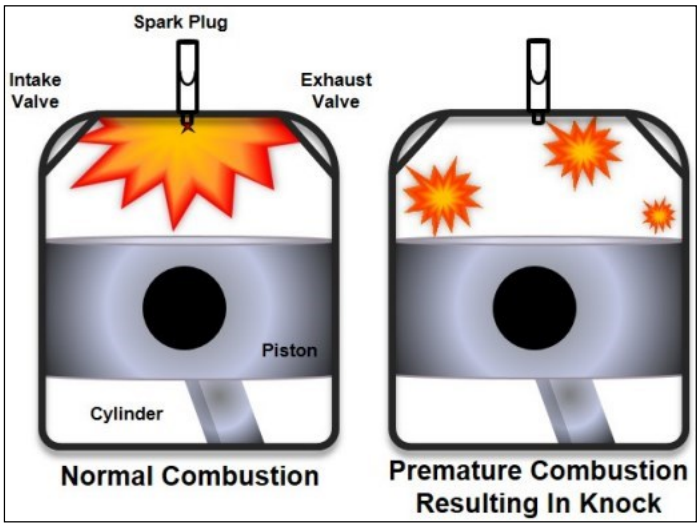

Fig. 2.8 Cartoon of internal combustion engine. Under normal operation, the spark plug initiates the propagation of a premixed flame in the combustion chamber. Premature combustion caused by low-octane fuel results in uneven burning, which reduces the power output and can damage valves, pistons, and other engine components [260].

2.4.2.2.1. History of Octane

Two pure compounds with opposite knocking behavior, n-heptane and isooctane (2,2,4-trimethylpentane), were used to establish the octane scale in 1927. As the name implies, isooctane has superior antiknock properties and was assigned an octane rating of 100, while n-heptane was assigned a 0 rating. Gasoline and other fuel blends are tested for knock and compared to various mixtures of n-heptane and isooctane. A sample is assigned an octane rating corresponding to the ratio of n-heptane and isooctane required to match its knocking properties. The composition of the mixture that matches the observed knocking of the sample is assigned as the octane rating of that fuel [100]. The Research Octane Number (RON) tests the fuel performance under standard conditions, whereas the Motor Octane Number (MON) simulates more severe operation representative of conditions at high-load or speed. The average of a fuel's RON and MON is referred to as its Anti-Knock Index (AKI). Figure 2.9 shows the trend in fuel AKI, and illustrates the correlation between the rating and engine CR. Today, the AKI federal standard for regular grade gasoline is 87.

Anti-knock agents, also called octane enhancers, are added to gasoline to help meet these federal standards. One of the most widely used octane enhancer for many years was tetra-ethyl-lead (TEL), which at approximately 3g/gal gives a 10- to 15-point increase in AKI. As observed in Figure 2.9, lead compounds were phased out of gasoline beginning in 1975. Lead deposits damage the vehicle's catalytic converter, motivating the transition to unleaded gasoline, which increases engine life by as much as 150 % [101]. Octane enhancers, such as methyl t-butyl ether (MTBE), were first developed to replace lead. MTBE has both a high AKI rating and causes minimal corrosion to the engine and other parts. However, when gasoline containing MTBE leaks from underground storage tanks, it contaminates the groundwater, resulting in an unpleasant taste and odor in drinking water. This led to limitations on MTBE blending in gasoline, and in certain areas of the country, a total ban on its use.

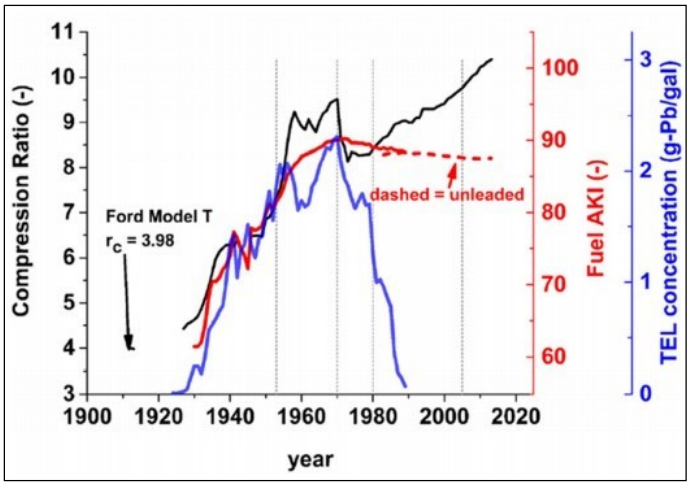

Fig. 2.9 Averaged trends in compression ratio (black), fuel AKI (red), and fuel TEL concentration (blue) for the U.S. as a function of year. Plot adapted from Splitter et al. [101].

2.4.2.2.2. Gasoline Composition

The crude oil that is pumped out of the ground is a complex mixture of several thousand organic compounds. These compounds include:

- straight-chain alkanes (paraffins),
- cycloalkanes (naphtenes),
- aromatic hydrocarbons (aromatics),
- alkenes (olefins).

These are natural constituents of crude oil, but can also be produced in various refining operations.

Techniques such as catalytic cracking and reforming are used to convert lower-demand components to high-demand products or to high-octane streams. By molecular rearrangement or dehydrogenation, catalytic reforming converts low-octane, heavy naphthas into aromatic hydrocarbons, which are added to gasoline components known as reformates. Alkylation and isomerization are also used to convert low-octane straight-chain paraffins to higher-octane branched paraffins, called alkylate, used in premium gasoline blending stocks for its exceptional anti-knock quality. Furthermore, aromatics are known to form polycyclic aromatic hydrocarbons (PAHs), which are precursors to soot and contribute to secondary organic aerosol (SOA) formation. These health factors, along with an effort to lower the cost of refining, have increased interest in the use of alternative, low-cost, octane boosting oxygenates such as ethanol with RON = 109 [102].

2.4.2.3. Aftertreatment System

It is clear that there are various pathways to mitigate particulate emissions via engine design and fuel improvements. Nevertheless, there is potential for deterioration of emissions with vehicle mileage. As mentioned previously, coking of injectors is known to increase emissions and could potentially lead to an increase in particulates over the lifetime of the vehicle [103, 104, 105]. Coking of injectors leads to increased spray penetration and increased risk of fuel impingement on walls, reduced fuel atomization quality leading to modified droplet size and velocity, increased fuel leakage during injector closing and diffusion flame due to fuel absorbed by porous deposits. There is limited data on changes in emissions with vehicle mileage. A study [106] on two 2010 GDI vehicles found that particulate emissions on the FTP test cycle improved from 3–4 mg/mi for a relatively new vehicle to ~1.5 mg/mi at 30–60K mileage, and then followed by an increase again to 2–3 mg/mi for 90–150K miles. The final option for eliminating particles before leaving tailpipe is via aftertreatment systems. Existing aftertreatment of gasoline vehicles consists of three-way catalysts (TWCs), which primarily convert gaseous emissions. Studies have shown that TWCs can help eliminate some of the smaller particles (<20 nm) especially during cold start, when the catalyst is below light-off temperature [107, 108]. This is likely due to condensation of nucleation mode particles formed from heavy HC on the catalyst, which are either oxidized or released later, when the temperature is above light-off. The use of a GPF is seen as a reliable way to ensure that the emissions are controlled well below the regulated limits, over a broad range of driving conditions.

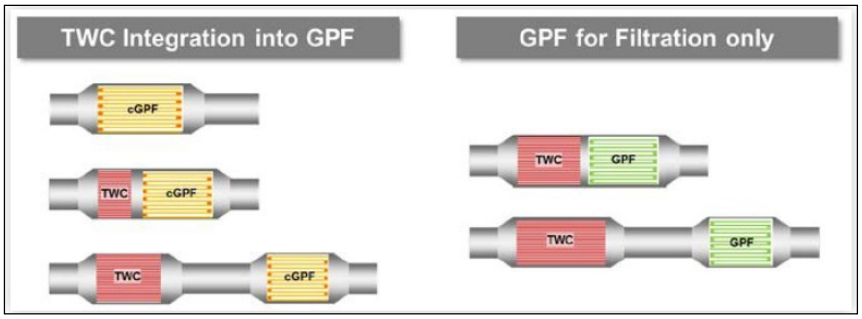

Fig. 2.10 Potential product choices and gasoline aftertreatment system layouts including GPFs [260].

Particulate filter technology is not new. All modern diesel vehicles in advanced markets are equipped with DPFs, and these have shown robust performance over millions of miles in accumulated driving history. There are some key differences in the design of the filters for GPFs due to the higher operating temperatures for gasoline (up to 900°C compared to <400°C for diesel), lower PM (1–3 mg/km compared to 10 mg/km for diesel), lower PNs (~10^{12} #/km compared to ~10^{13} #/km for diesel), and lower O_2 concentrations. Potential aftertreatment system layouts include use of either bare (uncoated) or TWC-coated GPFs (see Figure 2.10). In the former, the main functionality is filtration only, while the latter provides efficient space utilization via adding functionality of gas emissions conversion. The filters can be added in the close-coupled (CC) or in the under-floor (UF) position, as dictated by the emissions and space constraints. The key requirements are high filtration efficiency and also low pressure drop, the latter to minimize the impact on fuel economy and driving characteristics. In addition, the filters must have adequate porosity to host the catalyst, sufficient channel volume for soot and ash accumulation, and thermomechanical robustness to withstand the stresses during canning and exotherms associated with soot regeneration. These often conflicting requirements are met through selection of the appropriate material, optimizing the overall size and cell design, and engineering the pore structure. Subsequent chapters will delve into details of the design and performance aspects. It is only noted here that several studies now confirm that the replacement of a TWC with a coated GPF can be done without impacting the fuel economy.

The performance of GPFs–filtration, pressure drop, and gas conversion–has been studied extensively in the past few years, and there is ample evidence that this is a robust technology which helps meet the current regulations over diverse, real-world driving conditions. For the future, as was mentioned in the previous section, particles below 23 nm may be regulated. Studies are emerging which show that GPFs are very effective at capturing very fine, sub-23 nm particles. This is probably not surprising, given that the increased Brownian motion of smaller particles lends to increased filtration efficiency. In a study [109] involving 5 GDI vehicles, high PN emissions (~6×10^{12} #/km) were recorded when sub-23 nm particles were included. GPFs were found to be effective in near total capture of these small particles. In another study [110] of a 1.4 liter Euro 6b GDI vehicle under real-world driving conditions, an increase in engine-out PN by >50% was recorded when particles below 23 nm were included, while the tailpipe emissions after the GPF increased only by ~20%. The GPF filtration efficiency increased by ~10% when filtration of the smaller particles was included, and all tailpipe emissions comfortably met the regulated PN limit of 6×10^{11} #/km.

2.4.2.3.1. Gasoline Particulate Filter Design, Fundamentals and Function

The basic design of all GPFs in use today is the same as for diesel particulate filters, shown schematically in Figure 2.11.

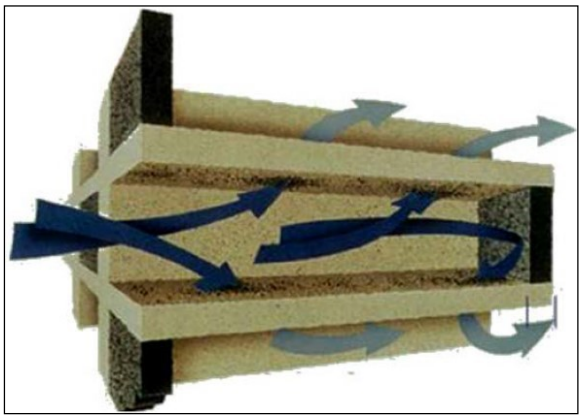

Fig. 2.11 Wall-flow particulate filter design [260].

The filters are based on a refractory, porous ceramic honeycomb structure. The channels are plugged in a checkerboard pattern at alternate ends. This results in a structure that forces the exhaust gas to flow from the inlet channels, through the porous wall, and back out into the outlet channels. Within the porous wall structure, particles are removed by filtration resulting in a significant reduction in particulate matter emissions. This type of filter is commonly referenced as a wall-flow filter. The main design parameters for these filter technologies, aside from material selection, are those describing the macroscopic structure of the honeycomb and those that describe the microstructure of the porous filter wall.
The honeycomb structure is usually characterized by its cell density, that is, the number of cells or channels per unit area, and the thickness of the walls or webs. The unit commonly used to describe the cell density is cells per square inch, cpsi, or in some cases as cells per cm^2. The web thickness, *tw*, is usually provided in 1/1000 of an inch (a customary U.S. unit called “mil”), or in metric units in mm or µm. Two key characteristics of the honeycomb structure, which can be derived from the aforementioned values, are the open frontal area (OFA) and the hydraulic diameter, d_h. For square channels, these values can be calculated by (1) and (2):

$$d_h = (CPSI)^{-1/2} - t_w\,, \quad (1)$$

$$OFA = d_h^2 \,/\, (d_h + t_w)^2\,. \quad (2)$$

The microporous wall material is typically described by its porosity and its median pore size (D50) as determined by mercury porosimetry. Common values used for GPF designs and materials are summarized in Table 2.3.

Property	Uncoated GPF	Coated GPF
Porosity	45%–55%	55%–65%
Median pore size	10 µm–15 µm	15 µm–25 µm
Cell density	200 cpsi–360 cpsi	300 cpsi
Web thickness*	6 mil–12 mil	8 mil–12 mil

Table 2.3: Range of typical gasoline particulate filter properties [260].

The selection of the optimal filter design and filter material is determined by a number of application requirements:

- Filtration performance: The absolute value of filtration efficiency required is determined by the engine-out raw emissions and the regulatory standards to be met.

- Pressure drop: The pressure drop, or resistance to flow, has impact on the fuel efficiency as well as the peak power of an engine and typically has to be as low as possible.

- Catalyst activity and utilization: Applicable only for coated GPFs, with the main parameter from the filter substrate being the washcoat capacity and catalyst efficiency.

- Mechanical and thermomechanical robustness: The filter has to withstand the mechanical stress applied during canning as well as the thermomechanical stress from temperature gradients in operation.

- Passive soot oxidation and soot mass limit: The filter has to be robust enough to withstand potentially severe soot regenerations, but also enable a maximum of passive soot regeneration.

The requirements for GPF performance are new, particularly as it relates to (a) thermal shock resistance, which are for GPFs similar to those for flow-through TWC substrates, (b) the need for monolithic structures to maximize the accessible filter volume and frontal area due to a sometimes very compact packaging space, as well as (c) the desire to have a low thermal mass and low thermal conductivity material that quickly responds to temperature changes to take advantage of passive soot regeneration potential. The key characteristics of the advanced cordierite ceramics are their low thermal expansion (~10−6 m/mK), their high temperature capability (>1300°C), their low intrinsic material density (2500 kg/m^3), and their high intrinsic strength. The particles found in gasoline exhaust are typically in the range of roughly 10–400 nm (described by their electrical mobility diameter), several orders of magnitude smaller than the typical pore sizes (10–25 µm) used in GPFs (see Table 2.3). Hence, filtration is not the result of a sieving effect but is rather primarily based on deposition due to Brownian motion and interception. Inertia effects can also play a role, but usually to a lesser extent. These mechanisms are summarized schematically in Figure 2.12. The filtration based on Brownian motion is related to the random movement or diffusion of small particles relative to the fluid stream lines.

Once a particle gets close enough to a solid surface, it can deposit and is removed from the fluid stream. This mechanism is dominant for small particles, for example, those <100 nm, and its contribution decreases as the particles become larger, since the Brownian motion decreases with particle size. Interception occurs when a particle's trajectory passes within one particle radius of the collecting body. In such a case, the particle traveling along that stream line makes contact with the body and may be collected there. As one would expect, this collection mechanism decreases in relevance as particles become smaller. It is therefore most effective for particles of intermediate sizes. Deposition as a result of inertia is relevant for large, heavy particles only, which do not follow the fluid steam lines. In the following paragraphs, only a brief description of the physics describing the two most relevant mechanisms for GPF applications will be provided to enable a basic understanding of the relevant parameters. Most models represent the porous filter wall as an assemblage of unit collectors, onto which the soot particles are deposited. The size and number of the unit collectors can be derived from the mean pore size and porosity, for example, by assuming spherical shape:

$$d_c = \frac{3}{2} \cdot \frac{1-\varepsilon}{\varepsilon} \cdot d_{pore} \quad .(3)$$

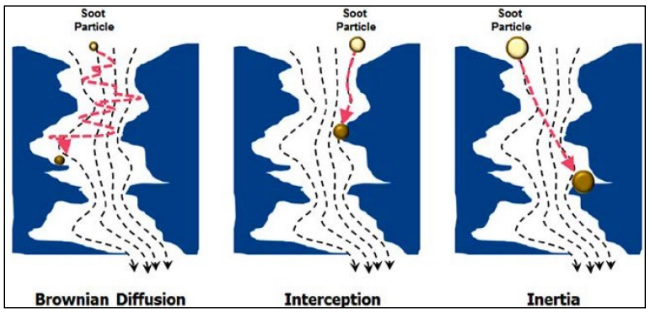

Fig. 2.12 Relevant filtration mechanisms [260].

For these unit collectors, the efficiency can be determined using established correlations, as given,

$$\eta_{int} = 1.5 \cdot N_r^2 \frac{[g(\varepsilon)]^3}{(1+N_r)^s} \quad .(4)$$

Where $g(\varepsilon)$ and the power s are functions of the porosity. The dependence on soot particle and collector size is considered by $N_r = ds/dc$. From the correlation, it can be observed that η_{Int} is independent of the flow rate and temperature. For Brownian motion, the unit collector efficiency η_{BM} can be described by:

$$\eta_{BM} = 4 \cdot \frac{A_s^{\frac{1}{3}}}{Pe_i^{\frac{2}{3}}} \cdot (1-\varepsilon)^{\frac{2}{3}} \quad .(5)$$

with A_s being a parameter, primarily dependent on the porosity ε, and Pe_i being the Peclet number. The Peclet number is proportional to the fluid velocity inside the pore space u_w/ε and the ratio between collector diameter dc and diffusion coefficient for Brownian motion D_{BM}:

$$Pe_i = \frac{u_w}{\varepsilon} \cdot \frac{d_c}{D_{BM,i}} \quad .(6)$$

The particle size ds and temperature T dependence of this collection mechanism are introduced via the Brownian diffusion coefficient, $D_{BM} \sim (T/d_s^2)$. To better understand the effect of the different design and operating parameters, examples are shown in Figure 2.13 for the filtration efficiency, as function of the particle size. First of all, one can observe that the filtration efficiency is generally very high for small particles and for large particles. In the intermediate range, a minimum can be observed.

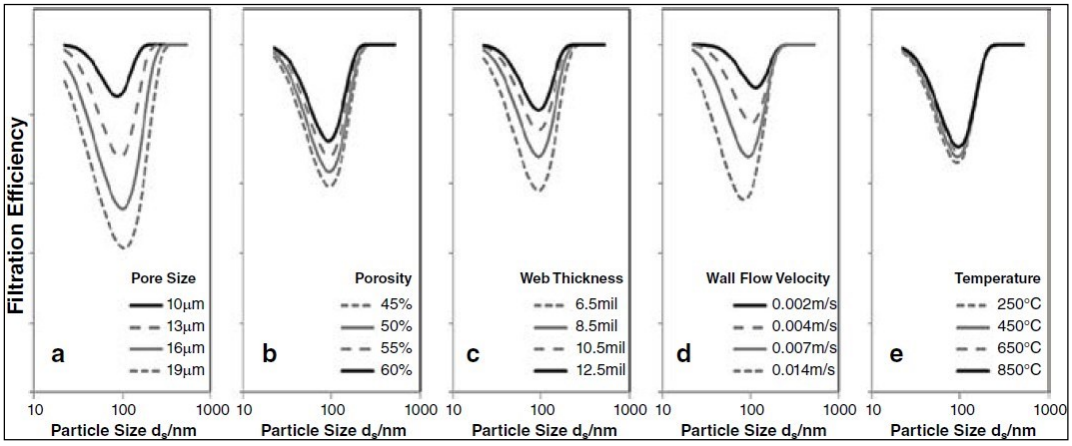

Fig. 2.13 Examples for the influence of different parameters on the filtration efficiency: (a) pore size, (b) porosity, (c) web thickness, (d) wall flow velocity, and (e) temperature [260].

This "V" shape behavior is due to the overlapping effect, with deposition due to Brownian motion dominating in the small particle range and decreasing as particle size gets larger, and interception (and inertia) dominating for large particles but decreasing as particles become smaller. The minimum is due to both mechanisms having lower efficiency. From Figure 2.13 (a) and (c), one can see the expected trend with small pores or thick walls enabling higher filtration efficiency over the entire size range. The porosity dependence is at first counterintuitive, with higher efficiencies for higher porosities. The reason for this is that as porosity is increased, the residence time within the pore space increases, providing more time for particles to be collected. This trend breaks down as we approach porosities of $\varepsilon \rightarrow 1$. For the flow velocity and temperature effect, one can observe that only the Brownian motion collection is impacted, as described above. Figure 2.13 shows that for GPFs, where the particles in the exhaust are expected to be primarily in the range of 10–100 nm, the collection based on Brownian motion is dominant.

A simplified model based on Brownian motion only, which is useful as a practical engineering tool, is based on a number of mathematical simplifications, which enable establishment of a simple correlation for the filtration efficiency based on a filtration characteristic parameter, A_{Filt}:

$$A_{Filt} \sim \frac{\varepsilon^{0.43} \cdot t_w \cdot (CPSI)^{1/3}}{d_{50,pore}^{5/3} \cdot SV^{2/3}} \quad .(7)$$

This parameter covers all basic filter design variables. The correlation was validated and calibrated using data from a large number of laboratory experiments with filters of very different properties and test conditions. In Figure 2.14, the correlation is shown using experimental data as well as a large number of additional data. The experimental data include filters covering porosities between 45% and 67%, median pore sizes between 9.8 µm and 28 µm, cell densities between 180 cpsi and 350 cpsi, and web thicknesses between 7 mil and 19 mil. In addition, a wide range of part sizes and space velocities were used. With the help of the definition of A_{Filt}, one can understand the sensitivity of filtration to changes in any of the design and process variables. Just considering the different powers in the correlation, one can observe the following order: pore size > web thickness > space velocity > porosity > cell density. Catalyst coating on the particulate filter also changes its filtration characteristics. Catalyst particles, which are coated into the porosity of the filter wall, usually called in-wall coating, consume some of the pore space and change the effective porosity, as well as the effective pore size. The reduction in effective pore volume always reduces the amount of soot required to reach the saturation in filtration efficiency. The change in effective pore size can result in enhanced filtration, as well as decreased filtration efficiency, depending on the coating technology as well as the substrate microstructure properties. In some cases, coatings may also be applied onto the filter walls, usually referenced as on-wall coating. In this case, the coating acts like a membrane with effective properties that can be derived from its particle size and typical packing densities for random particles.

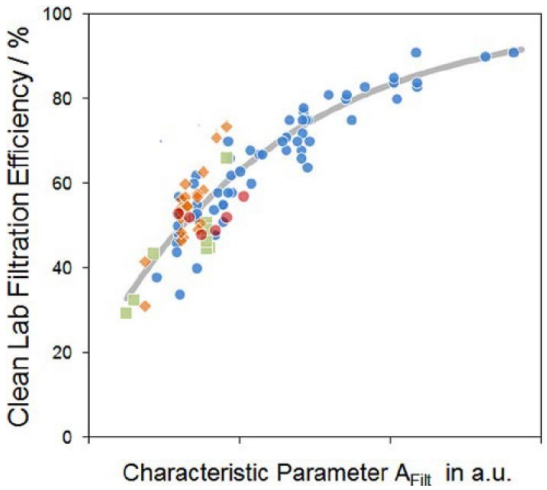

Fig. 2.14 Correlation of the filtration efficiency measured on laboratory equipment of clean research filter samples with the filtration characteristic parameter A_{Filt} [260].

The pressure drop of a filter is an application critical parameter of significant practical relevance, it impacts engine power as well as fuel consumption. The pressure drop of particulate filters is composed of five primary contributions, shown schematically in Figure 2.15. The inlet and outlet effects, shown as (1) and (5) in Figure 2.15, are due to the contraction and acceleration as the gas enters the inlet channels and the expansion and deceleration of the gas as it exits the channels, respectively.

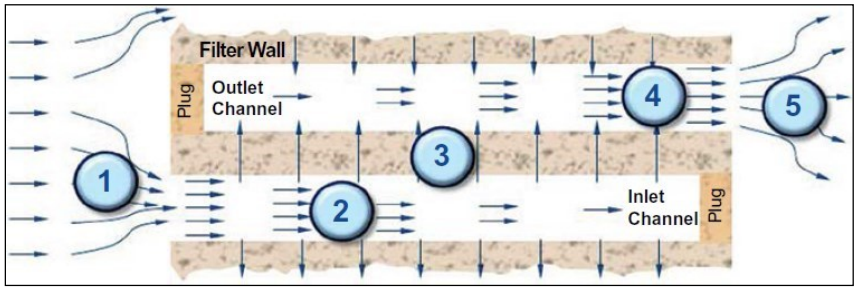

Fig. 2.15 Schematic of individual pressure drop contributions of wall flow filters [260].

The turbulent entrance effects that occur as a result of flow development inside the channels are typically lumped into these contributions. The inlet and outlet contributions are described by terms proportional to the kinetic energy, with the proportionality constant ζ_i:

$$\Delta p_j^{i/o} = \zeta_i \cdot \rho_j \cdot (\bar{u}_j^{\frac{i}{o}})^2 \quad .(8)$$

The index *j* represents filter inlet or outlet, and *i/o* indicates the condition at the inlet or outlet of the filter. Correlations for ζ are empirical and typically include the OFA as variable. For the frictional losses along the inlet and outlet channels (Figure 2.15, index 2 and 4), existence of a laminar flow profile is generally assumed within the channels. The pressure drop along the channels can therefore be described analogous to flow through substrates:

$$\Delta p_j^{ch} = 2 \cdot f_0 \cdot \eta \cdot \frac{L_{ch}}{d_h^2} \cdot u_j^{ch,eff} \quad .(9)$$

The index *j* again represents the inlet and outlet channel. η, *Lch*, and *dh* represent the viscosity, effective channel length, and hydraulic diameter, respectively. With respect to the velocity to be used, it has to be considered that at the inlet side (region of inlet plugs), all the flow is in the inlet channels, whereas the opposite is true on the outlet side (region of outlet plugs), with all the gas flow exiting via the outlet channels. Hence, the local flow rate in the inlet and outlet channels varies along the length, which has to be considered in the choice for $u_j^{ch,eff}$. The last contribution to pressure drop comes from the resistance to flow across the filter wall (index 3 in Figure 2.15), from the inlet to the outlet channels. It is worth noting that this is the only contribution determined by the porous microstructure of the filter.

In general, the pressure drop across the wall can be described by Darcy's law:

$$\Delta p^w = \eta \cdot \left(\frac{\Delta L_w}{k}\right)_{eff} \cdot u^w \quad .(10)$$

with ΔLw as effective thickness, κ as permeability, and uw as wall-flow velocity. The permeability of a clean wall is in general a function of the porosity, the pore size distribution, and the general morphology of the porous wall, considering, for example, the connectivity of the pore network. The simplest approaches to estimate the permeability are based on correlations utilizing the porosity and mean pore size only, as follows:

$$k_w = \frac{3}{200} \cdot \varepsilon \cdot d_{pore}^2 \quad .(11)$$

Here κ_w is the wall permeability, ε the porosity, and d_{pore} the median pore diameter. These correlations can provide reasonable estimates for the permeability of clean, uncoated filter walls. A comparison with some experimental values is shown in Figure 2.16. Typical permeabilities for uncoated filter technologies are in the range of $\kappa_w \approx 0.8 - 4 \times 10^{-12}$ m^2. Coating changes and decreases the permeability of the filter wall. For in-wall coatings, the catalyst particles consume some of the pore volume, reducing the effective porosity as well as pore size. In general, higher washcoat loading results in lower permeability. The impact in absolute terms depends significantly on the coating technology. The use of pore size and porosity data from mercury porosimetry measurements and the correlation provided above usually does not provide for sufficient results. The most effective way to describe the impact of in-wall coatings on the permeability is to use semi-empirical correlations, calibrated to experimental data from coated filters. The impact of on-wall coatings can be described reasonably well if a resistance in series approach of the coating layer and the porous wall is applied. The permeability of the coating layer itself is described by its particle size, porosity, and thickness.

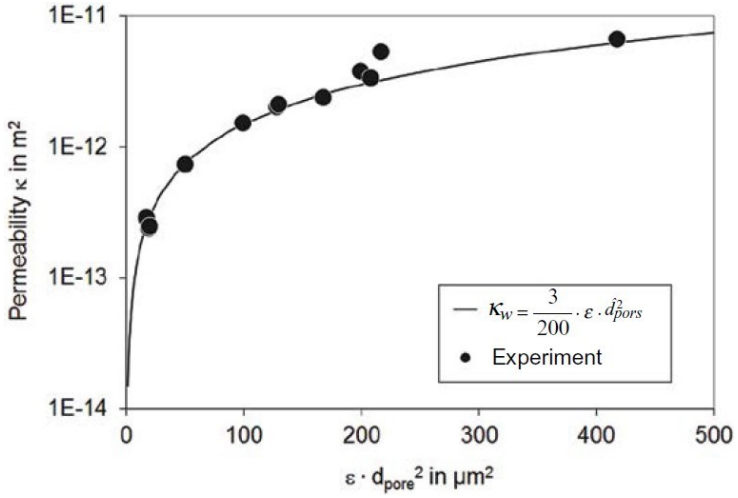

Figure 2.16 Permeability of filters. Experimental data and simple correlation [260].

The contribution of each of the individual pressure losses described above depends on the flow conditions, as well as the filter technology. In Figure 2.17, examples are shown for an uncoated as well as a coated GPF under different operating conditions. For the uncoated filter example, it can be observed that while the share of the resistance of the flow across the wall remains moderate and roughly constant, the contribution of the inlet and outlet effects increases significantly as the flow rate increases. For coated filters, the contribution of the wall is under all conditions higher compared to the uncoated filter technology due to the lower wall permeability. With respect to the distribution between the two other areas of pressure loss, the same holds as for uncoated filters. As for filtration, the accumulation of soot and ash also changes the permeability of the filter wall, resulting in an increase in pressure drop. Figure 2.18 shows laboratory measurements of pressure drop as function of the soot load, measured for a number of different GPF examples. The different data sets represent samples of a high-porosity GPF technology, all in the same size, two without coating and five with different coating technologies. For all cases, one can observe a steep initial increase at low soot loadings, then leveling off to a more moderate slope of pressure drop vs. soot load. The moderate slope is similar for all examples. It is driven by the increase in soot cake thickness, which is primarily related to the cell design of the filter (e.g., filtration surface area), which was 300/8, and the same for all samples tested.

The initial steep increase is the result of some soot accumulating in the pore structure, decreasing the local permeability. Since the local velocities inside the pores can be high due to the local porosity, this effect is very pronounced. As the examples show, this effect is a strong function of the coating applied to the filter. The different coatings shown vary in washcoat level as well as coating technology. The washcoat load of coatings A, B, and C is the same and at a medium level, but different technologies were applied. The washcoat loading for coating D is higher compared to A–C and very high for coating E. The effect of the washcoat loading level is to some extent driven by the fact that more coating results in greater reduction of open pore volume. The absolute effect, however, depends also on the selected coating technology, as can be seen by comparing coatings A–C.

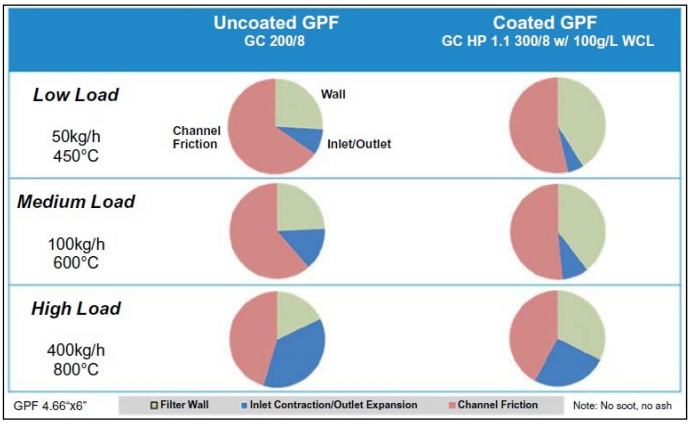

Figure 2.17 Share of the different pressure drop contributions for uncoated and coated GPFs at different operating conditions [260].

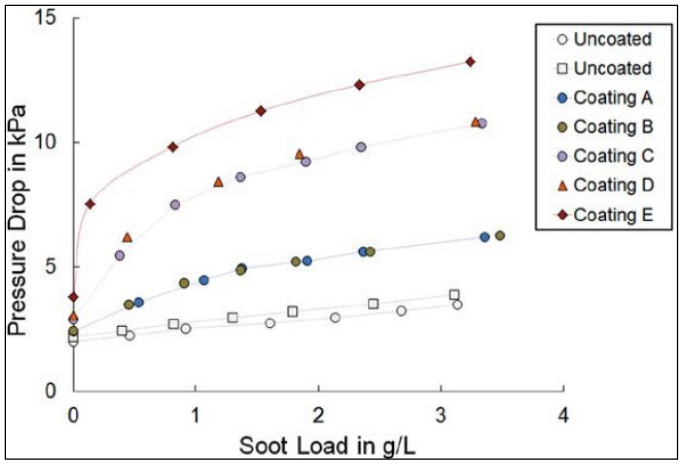

Figure 2.18 Pressure drop as function of soot load for different GPFs with different coating technologies. All filters with same technology and 300 cpsi/8 mil design [260].

2.4.3. Soot Formation in Combustion

The particles emitted by combustion engines typically consist of three distinct types, labeled "Nucleation Mode," "Accumulation Mode," and "Course Mode." Coarse mode particles are of varying nature, such as rust from the exhaust system. They are not emitted directly but formed from the other two modes. The predecessors stored within the exhaust system become attached to each other and re-enter the exhaust flow as larger particles. Because of these storage and release processes, the coarse mode is an inconsistent emission. However, it is suggested that they consist of a solid core and an outer layer of volatile material. As the coarse mode is of unsettled state, artificial nature, and comparative rarity, these particles have been little studied [111]. Historically, nucleation mode particles have been less studied, because they are at the limit of detection for many instruments. The consistency of these particles is still a topic of research. A literature survey by Giechaskiel, Manfredi, and Martini gives an overview about the current state of research on nucleation mode particles [112, 113]. They state:

> *The structure of primary particles is sometimes different (more amorphous) and unburned hydrocarbons or volatile organics can be found. This means that differences in the thermal pre-treatment (temperature, residence time of PN systems) might lead to different results. A lot of studies have found a solid core mode with older and modern diesel engines, both at low and high loads. Solid core mode is often observed at gasoline engines with port fuel injection (G-PFI) and it is assumed to originate from the metals of the lube oil or from fuel additives. At GDIs a shoulder at 10-20 nm appears quite often. For mopeds very often the size distribution after thermal pre-treatment peaks at or below 20 nm. It should be mentioned that in many studies it was recognized that the 'solid' core mode was re-nucleation artifact of the PMP (Particle Measurement Programme) method and the dilution factors employed.*

Accumulation mode particles consist of a collection of much smaller “primary” particles. The size of the primary particles ranges from about 20 to 50 nm. It should be mentioned that accumulation mode particles vary in size because they contain both greater or fewer numbers of primary particles, not because the primary particles vary in size. The number of primary particles to form an agglomerate is not a fixed number and varies from tens through hundreds to thousands. The morphology of agglomerates is also of a diverse nature, as the surface is coated by a layer of volatile or semi-volatile material. The chemical composition of particles can be defined according to the four layered conceptual model by Eastwood [111], depicted in Figure 2.19. The five main components of the particles are subsequently presented according to the discussion by Eastwood [111]. As the sulfate bound in the fuel mainly contributes to the sulfate fraction, it is important to mention that this model was based upon diesel particles.

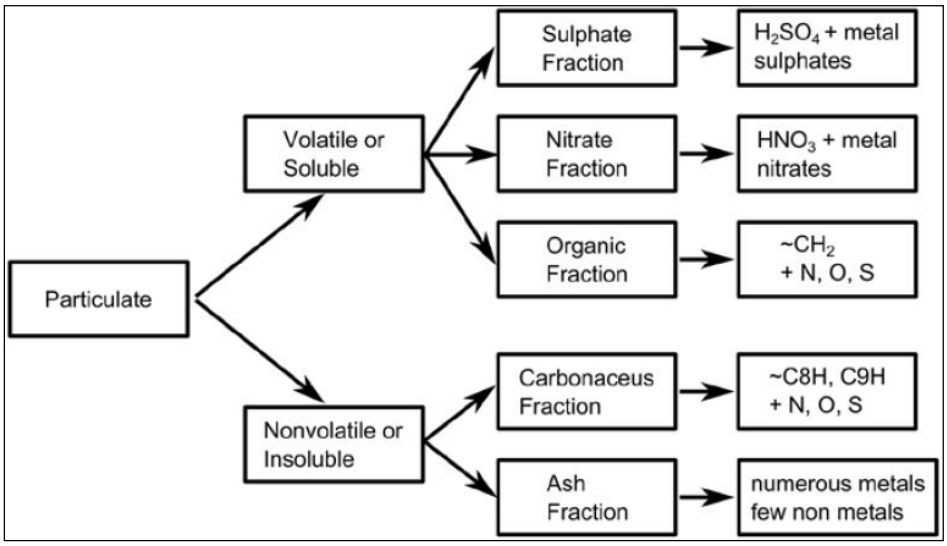

Fig. 2.19 Conceptual composition of particle composition according to Eastwood [111].

2.4.3.1. Organic Fraction

Based on the assay method, the organic fraction is also known as soluble organic fraction, or volatile organic fraction. However, the mass of soluble organic fraction is usually quite close to the mass of volatile organic fraction, even though the separation processes are based on different properties that do not necessarily generate the same end result. The organic fraction consists of several hundred compounds, such as alkenes, alkanes, alcohols, esters, ketones, acids, and aromatics. Even lighter C_4 to C_8 compounds were detected, which should be in the gaseous state, thus supporting the assumption that surface interactions are strong.

2.4.3.2. Sulfate Fraction

The sulfate fraction mainly consists of water-soluble sulfates, or the SO_4^{2-} ion, with the chief component sulfuric acid, H_2SO_4. There is a connection between the amount of sulfuric acid and the amount of water on the filter, thus dependent on the humidity in the filter's immediate environment. Therefore, prior to gravimetric measurements, the filters must be conditioned for a certain period of time in a closely defined environment.

2.4.3.3. Nitrate Fraction

The nitrate fraction consists of water-soluble nitrates, like the NO_3^- ion, with the chief compound nitric acid, HNO_3. Compared to the sulfate fraction, the amount of the nitrate fraction is usually lower. Additionally, nitric acid has a lower boiling point as compared to sulfuric acid, thus showing a greater volatility.

2.4.3.4. Carbonaceus Fraction

The title "carbonaceous" implies that this fraction is predominantly but not exclusively carbon. In the research community, this fraction is also titled as "Soot," "Graphite Carbon," "Elemental Carbon," or "Black Carbon."

2.4.3.5. Ash Fraction

The ash fraction covers inorganic compounds or elements, such as metals and a few nonmetals, and is a mixture of highly variable composition. A method to characterize the ash fraction is to burn all the particles and thereafter analyzing the remains, which is the "Incombustible Ash." The ash fraction is mostly caused by fuel additives and oil as well as the elemental composition of the working fluid itself. The ratio for each of these fractions on the total particle emissions depends upon the composition of the working fluids, the engine operating parameters, the wear performance of the engine, as well as influences of the exhaust gas aftertreatment devices. Besides the chemical composition, particles are classified according to their diameters. As smaller particles do not contribute strongly to the particle mass, the legislative authority saw it necessary to limit the particle number and thus the emission of fine particles. A typical distribution of the particle emissions of a diesel engine can be found in works by Kittelson et al. [114] and Dageforde [115].

Thereby, particle size distributions are plotted in three ways: according to number, area, and mass. Fundamentally this is the domination of different ranges by number and mass. Concerning particle numbers, most of the particles reside in the nucleation mode, while for the particle mass, the maximum is found in the accumulation mode. Generally, the particles are classified by their diameter as follows:

- PM10 for particles with a diameter not exceeding 10 µm.
- PM2.5 for particles with a diameter not exceeding 2.5 µm ("fine particles").
- PM0.1 for particles with a diameter not exceeding 100 nm ("ultra-fine particles").
- Particles with a diameter not exceeding 50 nm are known as "nanoparticles."

Even though the term "diameter" implicates particles to be of spherical shape, particles are more likely to show branched or reticular structures. Therefore, the measured diameter of particles by the actual measurement system is a comparative value and gives the reference diameter of an ideal round particle, which would behave comparatively to the measured particle. According to Hinds, different definitions for the reference diameter are common [116]:

- *Hydrodynamic Diameter*—diameter of a reference particle showing equal diffusion properties

- *Aerodynamic Diameter*—diameter of a reference particle with the density of 1 g/cm^3 and equal descent rate

- *Electrical Mobility Diameter*—diameter of a reference particle with a well-defined charge that shows equal mobility in an electrical field

The different diameters can be converted to each other as exemplarily shown by Jimenez et al. [117] and McMurray et al. [118]. However, the existence of different definitions with different values for the diameter supports the assumption that shape, mass, and surface of particles with equal diameters can show significant differences. Furthermore, the nucleation mode particles, in particular, can consist of a large number of volatile particles. As the nucleation mode particles are mostly dominated by volatile particles, the sampling position and the thermal pretreatment of the exhaust gas can influence the measured size distributions.

2.4.4. Soot Formation

From the above-mentioned particle fractions, ash and soot are generated within the engine's combustion process, while the other components form later in the exhaust system or even not before entering the surrounding air [111]. Even though today the formation process of soot is not determined in every detail, it is known that polycyclic aromatic hydrocarbons (PAH) play a major role in the process. This mechanism proposed by Bockhorn et al. [119] is schematically shown on the left-hand side of Figure 2.20. The formation process of PAH is dominated by acetylene (C_2H_2), which is present in a greater amount in fuel-rich flames. By reactions with CH and CH_2, C_3H_3 is created, which tends to build up a benzene ring (aromatic ring formation) by recombination and rearrangement. By abstraction of hydrogen and acetylene addition (HACA mechanism) [120], spatial structures with a graphite-like structure are formed from the plain PAH molecules which are soot precursor molecules. The three-dimensional structures resulting from the initial nucleus formation are known as primary soot particles. Due to surface growth and coagulation, which means a conglomeration of particles, the soot formation continues and extends. The growth of singular particles is limited, even though the reasons are not yet fully understood. This process is followed by the agglomeration of colliding particles, creating loosely structured agglomerates. A maximum output of soot is thereby visible for rich air-fuel equivalence ratios and temperatures from 1600 to 1700 K. For lower temperatures, the formation of radical precursors like C_3H_3 is inhibited. For higher temperatures, these precursors are pyrolyzed and oxidized. Therefore, the soot formation is limited to temperatures from about 1000 to 2000 K. Soot oxidation can occur at the precursor, nuclei, and particle stages of the soot formation process. Heywood states that in general, the rate of heterogeneous reactions such as the oxidation of soot depends on the diffusion of reactants to and products from the surface as well as the kinetics of the reaction [121]. There are many species in or near the flame that could oxidize soot, such as O_2, O, OH, CO_2, and H_2O. For the homogeneous, stoichiometric combustion in gasoline engines, the soot oxidation process is assumed to be dominated by OH, as the concentration of O and O_2 is at a low level [121]. However, in compression ignition engines, a large fraction of the soot formed is oxidized within the cylinder due to the excess of oxygen [122]. There are a number of models available which describe the dependency of the soot oxidation process on oxygen partial pressure and temperature [111, 123]. As it has been proven difficult to follow the oxidation of soot aerosols in flames, studies of bulk samples of pyrographite can be used to understand the soot oxidation process. The semi-empirical formula of Nagle and Strickland-Constable [124] has shown to correlate pyrographite oxidation with oxygen partial pressures below 0.1 MPa and temperatures in the range of 1100 to 2500 K and is therefore often used to describe soot oxidation mechanisms [121].

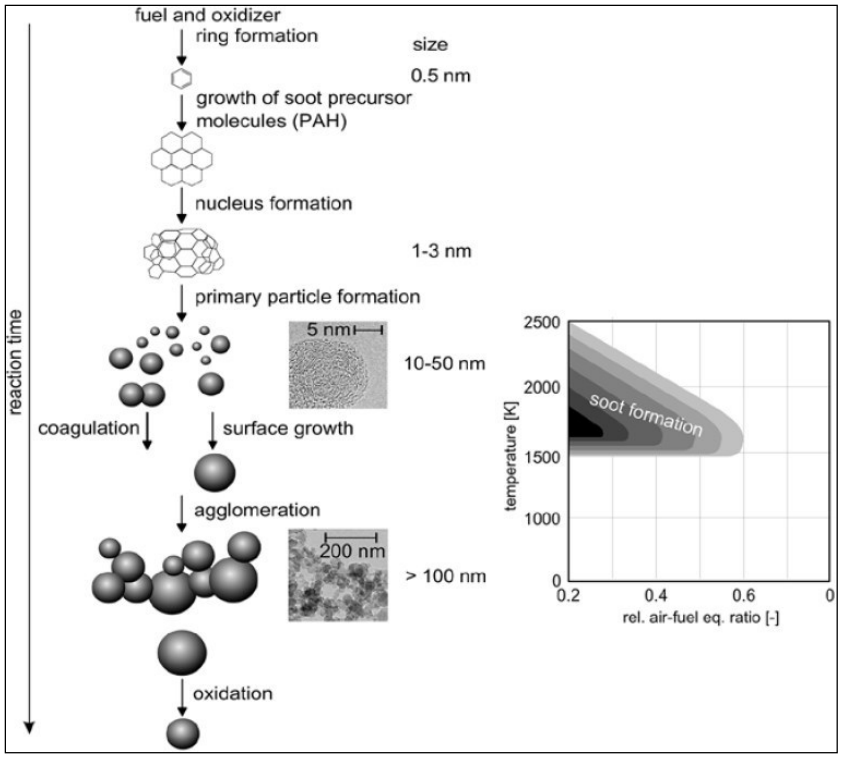

Fig. 2.20 Soot formation process according to Bockhorn [119] with pictures of soot structure created with HRTEM (left figure) and soot output dependency of temperature and air-fuel ratio by Böhm et al. (right figure).

2.4.5. Influencing Factors on Soot Formation in Gasoline Engines

The influencing factors on soot formations in gasoline direct injection (GDI) engines are shown in Figure 2.21. Spray-wall interactions and the resulting impingements of liquid fuel on piston and liner result in insufficient mixture preparation. If the time for evaporation of the liquid fuel films is too short, a diffusive combustion with increased soot emissions is the consequence. However, at steady-state operation, these emissions can be prevented by a proper dimensioning of spray targeting, injection pressure, and injection timing. Concerning multi-hole injectors, the deposit formation at the injector tip is a major source of particle number emissions. At the end of the injection process, the impulse of the injection is low and the liquid fuel of the nozzle sac and the nozzle hole volumes can wet the injector tip. Due to insufficient evaporation of this liquid fuel, deposits are formed in a diffusive combustion at the injector tip. Furthermore, the built-up deposits further on act as a reservoir for liquid fuel in a self-enforcing process. Due to this effect, the particle number emissions can be increased by more than one order of magnitude without influencing any other emission characteristic, such as THC or NO_x. Also, a dominant reason for particle emissions is inhomogeneities caused by insufficient mixture preparation.

Possible sources for inhomogeneities are, for instance, spray-wall interactions, spray-valve interactions, or late injection timings and thus not enough time for mixture preparation.

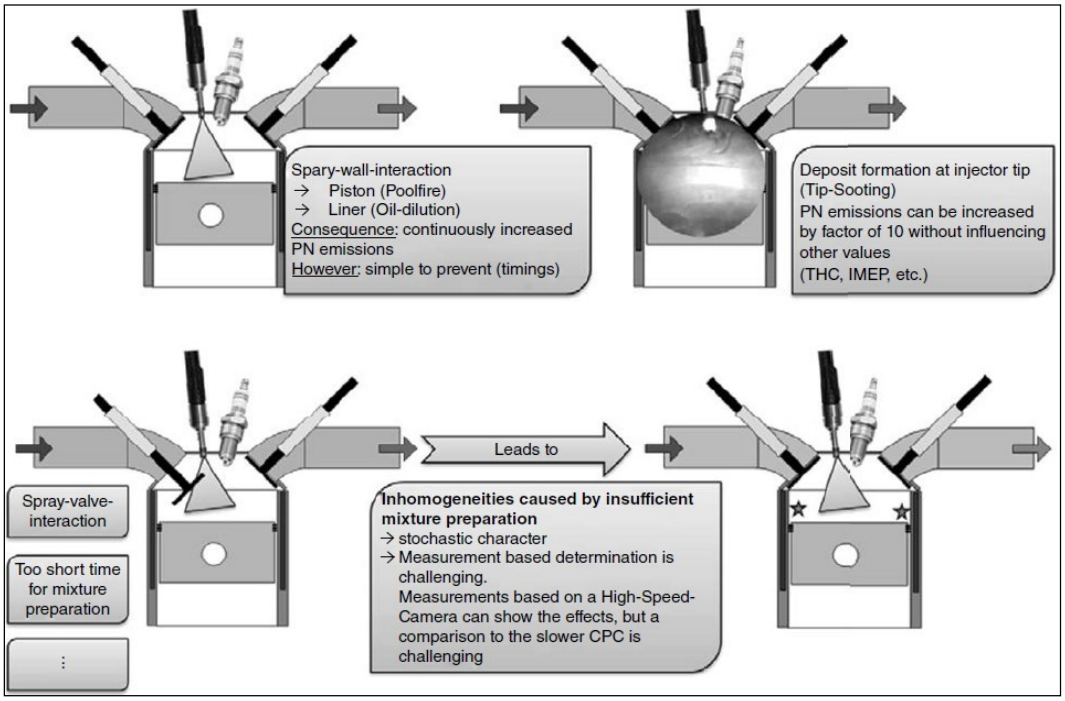

Fig. 2.21 Influences on particle formation according to Bertsch et al. [125].

2.4.5.1. Inhomogeneity

Soot formation generally depends on the local temperature and on the local air-fuel ratio [126]. Theoretically, fuel-rich zones should not exist for a homogeneous, stoichiometric operation of a GDI engine. Investigations show that spray-wall interaction is one of the main causes for soot formation in GDI engines [127, 128, 129, 130]. Concerning soot formation, this spray-wall interaction becomes critical, only if the time before ignition is too short to evaporate and sufficiently homogenize the liquid fuel. During the following combustion process, most of the injected fuel is oxidized. After regular combustion, the temperature in the combustion chamber is at a high level. In combination with the low oxygen content, due to the stoichiometric operation, ideal conditions for soot formation are present. Thus, even small amounts of fuel stored in the wall films can significantly lead to increased particle number emissions. Contrary to diesel engines, soot cannot be oxidized after the combustion because of the low oxygen content [131]. Schulz et al. have shown that in addition to the initial temperature, the injection pressure, and the distance from injector to the hot plate, the angle of the injector to the plate plays an important role, regarding the wall film area and the wall film mass [132].

Bertsch [133] shows that with the correct injection timings, piston film can be prevented even if high amounts of fuel have to be injected. They also show that hydraulic flow and large-scale motion have a significant effect on the wall impingement. In the studies of Dageforde et al. [134] and Notheis et al. [135], the influence of large-scale motion on the spray targeting could be shown and explain the different effects on the particle number concentration resulting from a poor interaction of the in-cylinder charge motion and the spray. This is also one reason for inhomogeneities caused by an insufficient mixture preparation. Fuel-rich zones with oxygen deficiency are formed, which are a potential source of soot emissions. In contrast to global fuel-rich conditions, a post-oxidation of the soot built up in the fuel-rich zones is possible. An insufficient mixture preparation caused by valve impingement or cold engine conditions can also lead to remaining droplets in the gas phase and therefore to diffusive flames. Steimle et al. used high-speed imaging to locate different forms of inhomogeneity in the combustion chamber [136]. The different effects are shown in Figure 2.22. Largely, impingement on different locations leads to an increase in particle formation. Under cold engine conditions, inhomogeneities in the mixture formation can lead to diffusive combustion in large areas of the combustion chamber and the occurrence of remaining fuel droplets as an additional soot source.

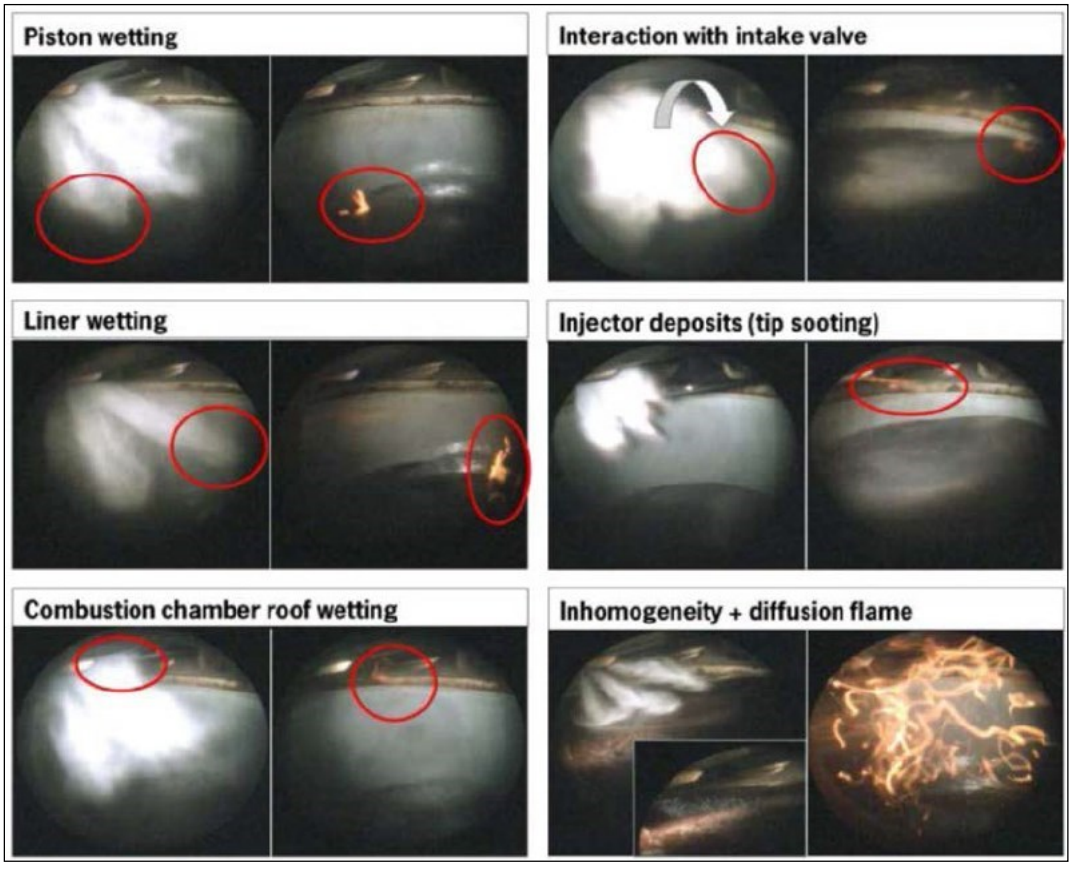

Fig. 2.22 Some of the most important sources of soot emissions in GDI engines according to Steimle et al. [136].

2.4.5.2. Tip Sooting

Using multi-hole injectors, another possible reason for soot emissions is a deposit formation at the tip of the injector, known as “Tip Sooting.” These deposits are formed as a result of a liquid fuel film on the tip. Using a clean injector, the fuel evaporates almost completely before the flame front reaches the injector. However, if deposits are formed at the tip, fuel is stored within the porous structure of the deposits. The evaporation process is delayed and leads to an insufficient mixture preparation of the stored fuel. The fuel is oxidized after the initial combustion under oxygen deficiency and leads to increased soot formation. Measurements by Berndorfer et al. [137] and Wiese et al. [138] have shown that this effect can increase the emitted particle number concentrations at steady-state operation by more than one order of magnitude, while neither the hydraulic flow nor the spray pattern are influenced by the deposits. Piock et al. have shown that an increased injection pressure is capable to reduce the deposit formation [139]. And even when deposits are built up at the injector tip, increased injection pressure of up to 40 MPa showed a reduction in particle number emissions. Figure 2.23 shows the result of tests on deposit formation using a multi-hole injector by Dageforde [140]. The picture on the left shows the injector tip before the start of the test. After running the engine about 500 minutes at 10 MPa injection pressure, the particle number emissions increased by about 360%, while the particle mass emissions increased by about 510%. After this test, the injector had deposits formed on the injector tip, as shown in the picture on the right.

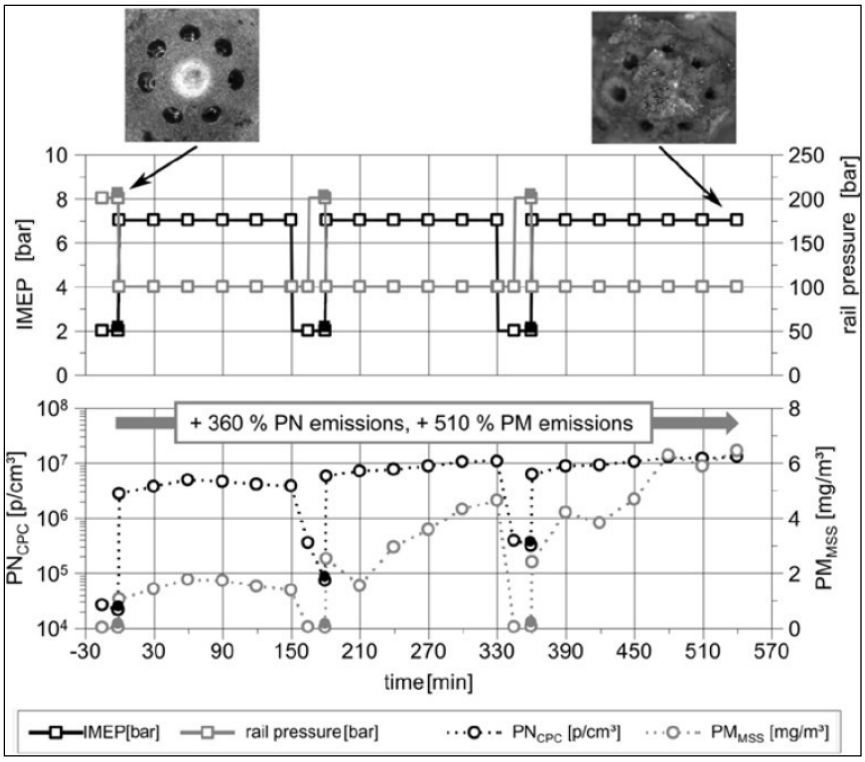

Fig. 2.23 Deposit formation on the injector tip measured by Dageförde [140].

2.4.6. Soot Formation in Different Operating Points

2.4.6.1. Higher Specific Loads and Low Engine Speeds

As downsizing and downspeeding are the most promising solutions to reduce the fuel consumption of modern engines, the engines operate more frequently at high engine loads and low engine speeds compared to engines with a larger displacement. For the higher engine load, a larger amount of fuel needs to be injected. In combination with the low in-cylinder charge motion caused by the low engine speeds, the mixture preparation is new. Bertsch and Notheis investigated different engine strategies and their influence on particle number emissions experimentally [141] and in comparison to CFD simulations [142]. The investigations using a single-cylinder research engine were used to classify the different influencing factors according to their particle number reduction potential. The three groups "Strong Influence," "Measurable Influence," and "Low Influence" are illustrated in Figure 2.24.

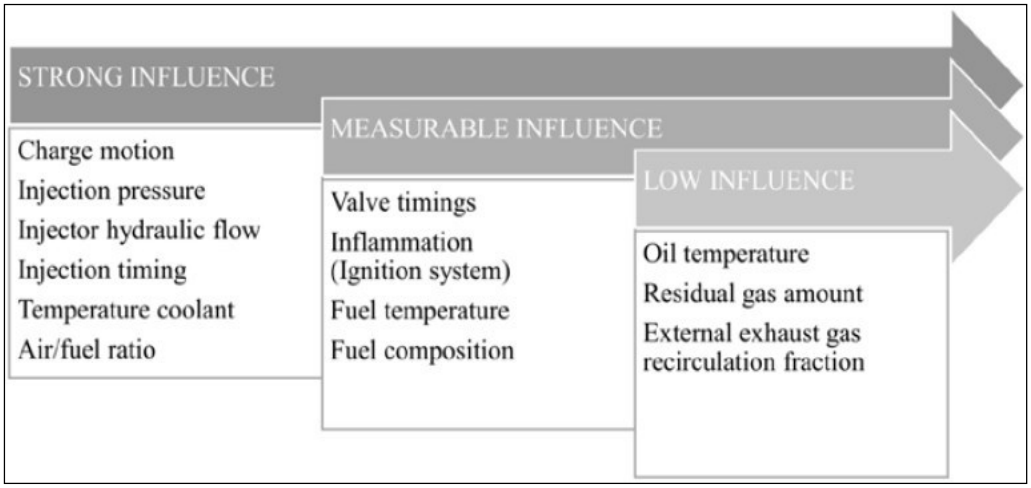

Fig. 2.24 Influencing factors on PN formation in GDI engines at high specific loads according to Bertsch [133].

One of the parameters with the strongest influence on particle number formation investigated in this project was the in-cylinder charge motion. Increased in-cylinder charge motion (tumble or swirl) leads to enhanced mixture formation and thus to reduced particle number formation, if the level of in-cylinder charge motion is matched to the engine. If not adjusted correctly, negative effects of the implemented charge motion are possible. Numerical studies on the same engine have shown that different charge motion strategies change the spray targeting. This could lead to a higher amount of cylinder wall impingement which increases the particle number emissions. With the relative cold temperatures of the cylinder walls, the evaporation of the liquid film is reduced. The fuel on the cylinder wall can get in the top land and burn diffusively as soon as the piston moves downwards.

Another promising solution to reduce particle number emissions is a combination of a reduced hydraulic flow of the injector with increased injection pressure.
The average droplet size is reduced and the evaporation process is enhanced due to the increased surface-to-volume ratio. By using an increased injection pressure, the necessary amount of fuel can be injected within a shorter time with lower average droplet sizes. It's likely that the different parameters leading to particle number emissions reduction potential are not additive and most of the effects interact with each other. It can also be stated that a cleaner combustion process, emitting particle number emissions slightly above the level of ambient air, can be realized in a gasoline direct injection engine at high engine load under steady-state, hot engine conditions.

Also, it could be recommended to operate gasoline direct injection engines with low particle number emissions at high engine load [133]:

- A short time for engine heat-up is required for low particle number emission engine concepts.

- The spray targeting, injection pressure, and injection timing need to be optimized synchronously and adjusted to the engine operation point.

- Operation with air/fuel ratio below $\lambda = 0.9$ should be prevented.

- Large-scale charge motion enhances the mixture formation process but needs to be applied to the engine geometry and operation settings.

- The ignition system can stabilize the ignition process and thus reduce particle number emissions.

- The fuel composition influences the evaporation process, soot formation, and soot oxidation. Therefore, future gasoline fuel for low particle number emissions should contain low amounts of aromatics and a high vapor pressure.

2.4.6.2. Engine in Transient Operation Points

Understanding the emission behavior of engines in transient operation points is one of the great challenges in order to optimize engine application for Real-Driving-Emission (EU6-RDE) standards regarding particle emissions. Transient conditions refer to changing engine conditions, which can be characterized in four major classifications as shown in Figure 2.25 proposed by Disch et al. [143]. The first-order transient is the reciprocating engine process itself. The cylinder pressure changes in a short timescale and processes have a high impact on engine and emission performance. Even in stationary engine operation, these processes are highly transient. Second-order transient describes cycle to- cycle variations. These are governed by driver requests such as changes in engine load and speed. The engine control unit (ECU) control strategies have a great effect on these timescales as well. Third-order transients describe changes in engine temperatures such as oil, coolant, and combustion chamber surface temperatures.

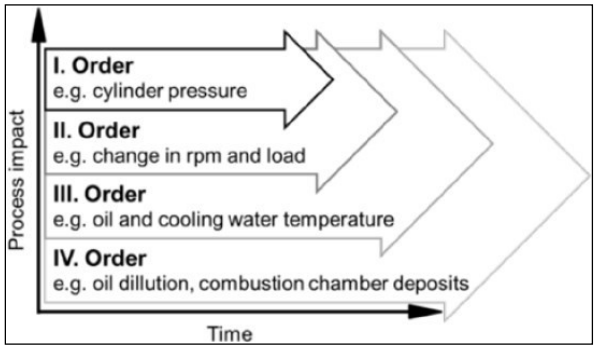

Fig. 2.25 Criteria for interpretation and evaluation of transient Engine operation [143].

These processes are slower and the impact on the emissions is high, but not as significant as first-and second-order processes. Cold start emissions in particular are influenced by the engine heat-up behavior. The fourth order describes engine processes over a longer timeframe such as wear, combustion chamber deposit build-up, and oil dilution [143].

2.4.6.2.1. Effects in Transient Operation during Load Step

The ECU calibration during load step conditions has a significant influence on mixture formation and especially the lambda value. Studies by Disch et al. have shown that during load steps, especially after coasting conditions, the lambda value control during the first combustion cycles is emission critical [144, 145]. To ensure a reliable engine torque build-up, the calibration of the initial combustion cycles, before the lambda control becomes active, has to be adjusted so that lean misfire is prevented. For this reason, a precise stoichiometric mixture with a high degree of homogenization is indispensable.

An under-stoichiometric ECU calibration and/or poor mixture formation, for the initial combustion cycles, causes peak values for particle number concentrations. In addition, the injection strategy during engine load changes has a superimposed impact. The in-cylinder conditions at start of injection (SOI) change significantly during the first few combustion cycles. Pool flames, as a result of piston wetting caused by early SOI applications can be detected. The cooling of the piston and wall surface during coasting requires a temporary SOI shift to later SOI timings. The temporary shift is an effective opportunity to reduce peak values of particle number concentrations. However, at later SOI timings, higher fluctuations of local lambda values close to the spark plug were observed. This leads to increased particle number emissions due to inhomogeneity and higher cycle-to-cycle variations. Figure 2.26 shows an example of pool flame occurrence during a fast tip-in and the corresponding particle number concentration and size distribution. Pool flames can be observed in early phases of the tip-in. In later phases, only a few droplets can be identified as sources of particle emissions, even with constant SOI timings. This is due to the heat-up of the piston surface during the firing operation. Tan et al. also showed a significant influence of spark timing and lambda value development during load changes. They state that in order to improve the transient behavior, extra development effort has to be invested in order to control the lambda value and its influence on transient emission behavior [146].

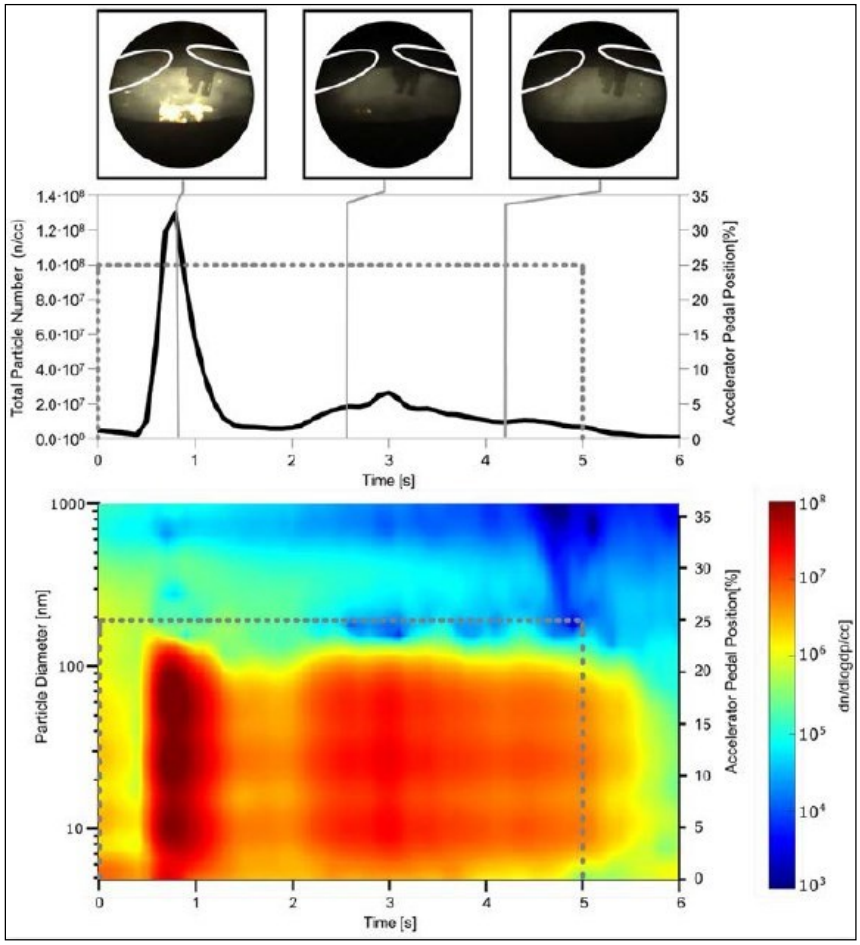

Fig. 2.26 Comparison of particle emission and high-speed imaging during tip-in [260].

2.4.6.2.2. Catalyst Heating Operation

The catalyst heating operation is a special case of transient engine operation. To effectively reduce exhaust gas emissions after engine start-up, the catalyst needs to be heated up above the light-off temperature. To facilitate a quick heat-up of the catalyst, a high exhaust enthalpy flow is needed in combination with low gaseous emissions and low cycle-to-cycle variations. During this operation mode with cold engine conditions, more than 50% of the cumulative particle number emissions are produced in the first 100 seconds of the NEDC test cycle [147, 148]. Therefore, the quality of the mixture formation process mainly influences the particle number emissions. For GDI engines with a centrally mounted injector, a multi-pulse injection strategy with a short injection pulse just before ignition timing can lead to low particle number emissions [149]. The split-up of the injection process reduces the penetration and thus can help avoid wall wetting. Additionally, the short injection pulse just before ignition timing leads to a local fuel enrichment and increased turbulence within the spark plug area [150]. While the turbulence supports the stabilization of the inflammation and combustion process, the local fuel enrichment and the very short duration between the last injection pulse and ignition timing can lead to a substantial increase of the particle number emissions [151].
Therefore, the timing and injected fuel mass must be carefully and precisely chosen. Besides the optimization of the injector and the spray targeting by new laser drilling methods [152, 153], a further increase in the injection pressure is a promising solution to reduce particle number emissions. Schumann demonstrated with a single-cylinder research engine that an injection pressure of up to 80 MPa enables stratified operation in the catalyst heating mode with low particle number and NOx and HC emissions [154]. Besides the optimization of the fuel supply system, increased in-cylinder charge motion supports the mixture formation process. Dageforde therefore reduced the maximum intake valve lift of a single-cylinder research engine and combined the increased in-cylinder charge motion with a split injection strategy and the use of different fuels [155]. Results showed that the increased in-cylinder charge motion and the short injection pulse, right before ignition timing, leads to a stabilization of the combustion process and lower particle number emissions. De Francqueville and Pilla performed detailed investigations on particle formation in catalyst heating operation, using an optical accessible engine with a transparent sapphire ring [156]. They used Laser-Induced Incandescence (LII) to localize soot in the combustion chamber and Laser-Induced Fluorescence (LIF) to measure the fuel distribution. It was possible to determine five mechanisms as causes for the soot formation: ballistic impacts on the piston or on the lower part of the liner, non-direct impacts on the upper part of the liner due to fuel transportation in the combustion chamber or rebounds, and the last mechanism identified was mixture heterogeneities in the bulk gases. In summary, they state that fuel impacts on the piston, and to a lesser extent on the liner, were identified as the main mechanisms for the soot formation in GDI engines.

2.4.7. PN Formation Mechanisms

Particulates can form by a number of mechanisms, often with multiple mechanisms being present simultaneously at a given engine condition. Engine-out particulate emission is the result of particulate inception, growth, and oxidation mechanisms. The physics and chemistry that drive these mechanisms can be complex, nonlinear, interdependent, and engine-specific; thus, what is presented here is a general outline and not a prescriptive guide meant to apply to every engine, injector, and mode of operation. This also means that as a given engine parameter changes (e.g., engine speed), particulate emissions may go up or down, depending on a number of other factors. In general, particulates are formed in regions with an over-abundance of fuel in the fuel/air mixture. This happens through either high-temperature thermochemical decomposition of the fuel by pyrolysis during the combustion or as a result of low temperature chemistry pathways of radicals after the time of combustion. These rich zones are typically found either in the gas phase, where under-mixed regions of fuel lead to locally rich zones, or due to liquid films on the surfaces of the combustion chamber (e.g., piston, fuel injector tip, walls) [157, 158, 159]. The sources for particulates can also be independent of the engine fueling and instead related to engine oil, examples being oil introduction through the crankcase ventilation system (PCV), oil suction past loose piston rings, or oil leakage from the turbocharger. These oil-related mechanisms are generally indicative of engine malfunctions or poor engine design.

2.4.7.1. Gas Phase

With regards to particulate formation, the ideal mixture is homogenous and contains no gas-phase rich zones capable of producing particulates. However, in direct-injection (DI) engines, liquid fuel is injected directly into the combustion chamber, requiring all the injected fuel to both vaporize and fully mix with the charge (air and EGR) present in the cylinder during the time available in the intake and compression strokes prior to combustion. If any locally rich zones persist until the time of combustion, they are likely to turn to soot. Sufficient mixing to prevent soot is driven by a combination of fuel injection characteristics (drop size, air entrainment in spray, penetration) and mixing characteristics (sufficient time and turbulence). High-speed imaging of the combustion chamber provides in situ spatial and temporal diagnostics of the combustion process. The incandescence of the soot particles are observed by imaging the combustion chamber through an endoscope. The still images of a DI combustion chamber with increasing gas-phase incandescence soot are presented in Figure 2.27. The images are taken at ~90° aTDC in an engine that is operating at room temperature to simulate an engine start. From left to right, the injection timing is retarded such that there is less time for mixing and evaporation. The result is that some liquid fuel is still present, and suspended in the charge, at the time of combustion. These rich pockets then burn as a result of pyrolysis and present themselves to varying degrees as incandescent light.

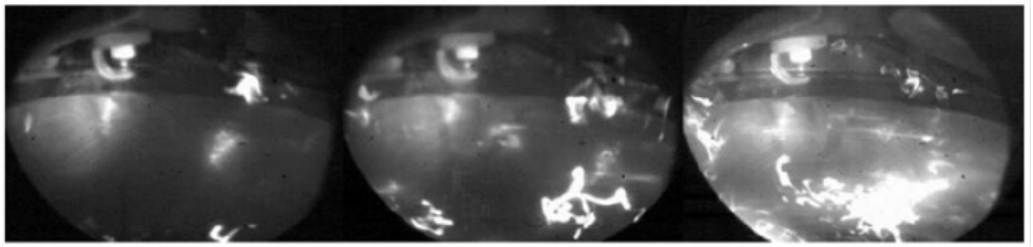

Fig. 2.27 In situ high-speed imaging via endoscope can visualize the origin of particle formation in the combustion chamber. In these images, the piston is at ~90° aTDC and the injection timing is retarded from left to right. Additionally the engine is at room temperature to simulate an engine start. The result is varying levels of gas-phase soot incandescence as a result of insufficient time for mixing and evaporation [260].

2.4.7.2. Liquid Films

Liquid films can form on any surface inside the combustion chamber and are a consequence of spray characteristics in DI engines. Frequent locations for liquid films are on the piston, combustion chamber walls, or intake valves. In these locations, a liquid film is formed due to improper spray targeting or injection timing. Liquid films can also form on the injector tip or within the nozzle holes and sac volume of the injector. These films are related to the injector needle movement characteristics and the internal geometry of the injector. These fuel films can lead to diffusion flames with rich combustion zones, which can significantly contribute to particulate emissions. Examples of diffusion flames initiated on the top of the piston (left panel) and tip of the injector (right panel) are presented in Figure 2.28. In this case, an engine with side-mounted injector was used and the injector is located at the top left corner of the viewing area. The engine was operated at part load condition during the imaging and the start of injection (SOI) was varied from advanced (left panel) to retarded (right panel) timing. The still images used in the left and right panels are taken at 35 °aTDC and 85 °aTDC, respectively, during the expansion stroke, at which time the main combustion event has ended.

Fig. 2.28 Left: Pool fire on the piston surface due to spray impingement and incomplete evaporation can be a significant source of particle emissions. Right: Soot incandescence from a diffusion flame due to liquid wall film on the injector tip [260].

2.4.8. Operating Conditions

An engine must operate under a wide range of conditions, and the particular speed/load profile that an engine experiences can vary drastically based on the vehicle application, drive cycle, transmission selection, and other calibration parameters. For a given accelerator pedal position and external environment (wind, road condition, temperature, elevation), the engine will need to produce a given amount of power, which dictates a choice of speeds and loads for the engine operation. The physics happening inside the engine are intrinsically related to the operating conditions, and an overview of the relationship between some of the most important operating condition parameters and soot mechanisms is presented here. Changing one engine parameter often changes multiple physical parameters simultaneously. For example, increasing RPM changes the component temperatures, air flow, and volumetric efficiency. Throughout the engine calibration process, the best control response for a given operating point is optimized, given the constraints in emissions, fuel economy, and engine responsiveness.

2.4.8.1. Engine Speed

Engine speed affects fundamental properties that influence the charge induction, fuel spray development, combustion, and engine-out emissions. Higher engine speeds reduce the time available for mixing and evaporation, which can have a negative effect on charge homogeneity. However, turbulence and mean air velocity increase as the engine speed increases, which improves mixing and enhances the charge homogeneity, thus mitigating the locally rich zones in the gas phase and reducing the particulate production. The resulting effect on mixing is engine and condition specific. Regarding fuel impingement on the piston, because piston speed increases at higher RPM, the piston moves away from the spray more quickly and reduces the piston impingement for a given SOI. Increased engine speed generally leads to higher component temperatures due to more friction and a shorter time for heat transfer. Higher temperatures accelerate the evaporation of the liquid fuel films on the components but can also promote low temperature soot formation reactions. Depending on the temperature range and the location of the fuel film, higher temperatures can exhibit non-monotonic emission behavior. For example, while non-monotonic particulate behavior can be observed for injector tip temperature [160], pistons generally benefit from being hotter with regards to particulate emissions, although the relationship is complex [161, 162]. The cumulative effect of all these changes indicates that PN (particle number) could go up or down as a function of engine speed, which is shown in Figure 2.29.

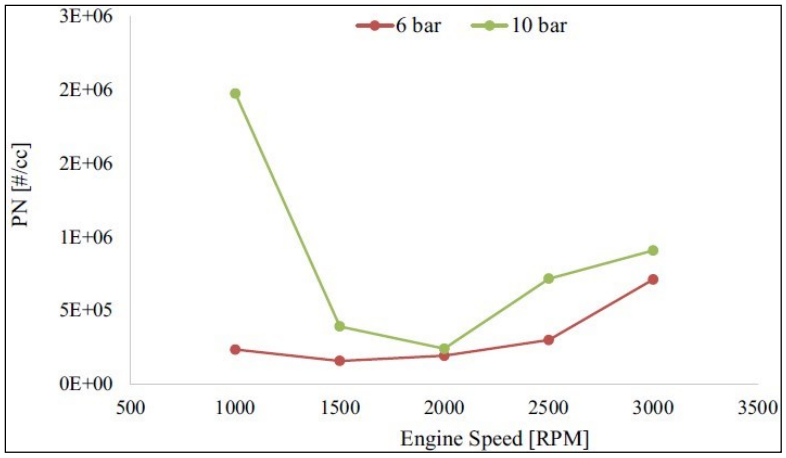

Fig. 2.29 Effects of engine speed/load on PN emission [161-162].

Sweeps of engine speed at two loads are presented for a turbocharged engine with a side-mounted injector. The tests were performed under warm engine conditions with a single injection per cycle at SOI = 280 °bTDC. While the engine showed insensitivity to engine speed in terms of PN emission for the load point of 6 bar BMEP between 1000 and 2500 RPM, at higher load (10 bar BMEP) significant sensitivity to engine speed is observed.

2.4.8.2. Engine Loads

As the engine load increases, the amount of injected fuel mass increases proportionally and PN typically increases. Keeping all other factors constant, as injected fuel mass increases, the amount of fuel which requires mixing increases, exacerbating under-mixing mechanisms. Impingement mechanisms also get worse since more fuel mass impacts surfaces like pistons or valves. At higher engine loads, the liquid film on the injector tip can also increase. In general, the engine component temperatures increase at elevated engine loads. As more fuel is burned per cycle, a greater heat flux through the combustion chamber leads to increased internal surface temperatures, such as in the piston, walls, and valves. For surface impingement—related PN mechanisms, the increase in temperature is generally helpful in promoting evaporation. A possible exception to this is the Leidenfrost effect. The Leidenfrost effect refers to the cases when the temperature of a surface is significantly higher than the boiling point of the fuel, which prevents the evaporation of the liquid film due to the instant creation of a thin vapor film below the liquid surface. This phenomenon alters the rebound and splash characteristics of the impinged fuel as well as the time for evaporation [161-162]. Engine-out PN emission as a function of the engine load is presented in Figure 2.30. The data represent a load sweep at 2000 RPM during warm engine operation. Optimized injection timing in terms of lowest PN emission was selected for each load point. The non-monotonic trends have been observed at different engine speeds and other engine tests.

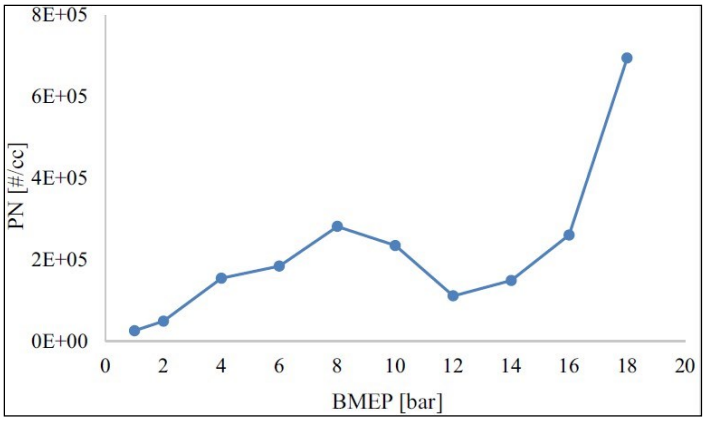

Fig. 2.30 The effect of engine load on PN can be non-monotonic but generally increases at high engine loads [161-162].

2.4.8.3. Oil and Coolant Temperature

The temperature of the oil and coolant of the engine also affects the fuel and component temperatures. Fuel temperature is initially at ambient (in the fuel tank), but while traveling through the fuel rail, it is heated to near coolant temperature. Because gasoline is a multi-component mixture of varying composition, the fuel temperature has a significant influence over the portion of the volatile components of the fuel. Colder fuel temperatures inhibit vaporization of the fuel and increase spray penetration and typically lead to an increase in PN. Colder component and temperatures also inhibit the evaporation of fuel films on internal engine surfaces. Emissions during cold start are a major issue, with often 50% or more of emissions being produced in the first few minutes of a drive cycle while the engine is still cold. The PN emissions during a steady-state engine warm-up process can be seen in Figure 2.31. The engine was operated at a constant load of 10 bar BMEP and 2000 RPM, starting from the ambient temperature condition until reaching the warm operation temperature.

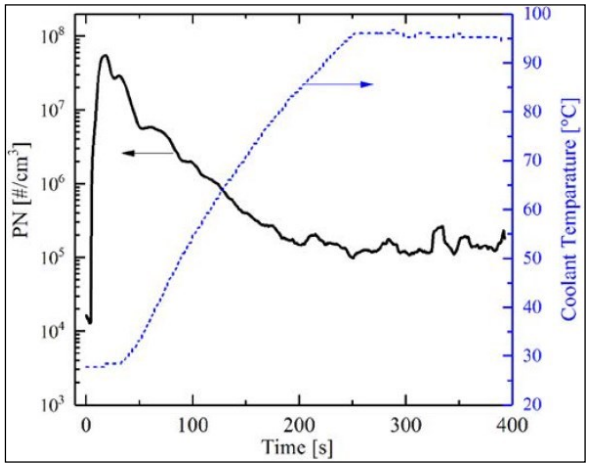

Fig. 2.31 PN emissions typically reduce with increasing engine temperature [161-162].

2.4.8.4. Engine Speed and Load Transient

During real world driving, the engine is frequently changing both speed and load due to vehicle acceleration and deceleration. In particular, increases in engine load are associated with increased PN. The increase in engine load is accompanied by an increase in injected fuel mass per pulse, and the added fuel mass penetrates further, possibly impacting the piston. Because the piston surface is colder from running at a lower load, evaporation is inhibited and soot production due to the surface diffusion flames is increased. This often results in a spike in particulate production during transient increases in engine load, which typically levels out to a steady-state level after tens of seconds.

These tip-in events can be simulated at the engine dyno tests by load jumps. The PN emission results of a load jump from idle to mid-load (1 bar to 6 bar BMEP) at 1500 RPM during warm engine operation is shown in Figure 2.32. The two panels presented in the figure are indicating the same load jump at two different injection timings. The retardation of the injection timing resulted in a significant decrease of steady-state PN emission during the high load portion of the load jump.

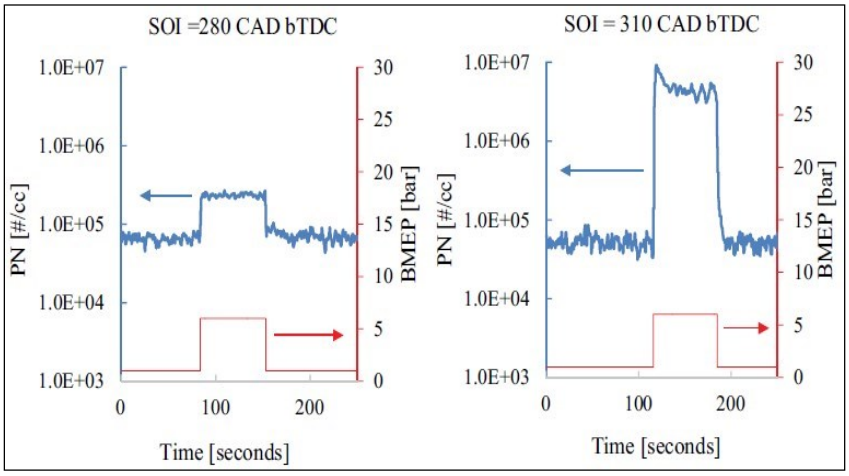

Fig. 2.32 Engine load transients are typically accompanied by a temporary spike in PN emission. The transient calibration refinement during the transients have potential of order of magnitude reduction [161-162].

2.4.9. Engine Calibration

While the operating conditions of the engine are mostly dictated by outside influences, such as the driver and road conditions, the calibration parameters are optimized to pick the best engine operation for a given demand. While many parameters are considered for the calibration parameters, such as gaseous emissions, fuel economy, and engine responsiveness, the calibration parameters influencing the PN emissions are discussed in greater detail below.

2.4.9.1. Injection Timing

Injection timing is a key parameter for influencing PN mechanisms. For homogeneous-charge engine operation (which is the norm for most of the speed/load operating points of most production DI engines), injection happens during the intake stroke. Injection timing is often a compromise between fuel consumption and PN.
Fuel consumption is generally improved as injection timing is moved earlier (presumably due to better mixing), but the likelihood of spraying fuel on the piston and causing PN due to piston wetting also increases with earlier injection timing, so injection timing should be chosen to be sufficiently late to avoid the piston. The injection timing also determines how much time is available for the charge to mix and for any liquid films to dry. Injection timing is often chosen to be as early as possible while still avoiding piston impingement, with an additional safety factor. This trade-off timing is significantly different depending on the engine geometry (i.e., side- vs. centrally mounted injectors) and the injector spray targeting.

2.4.9.2. Fuel Pressure

Increased fuel pressure is a valuable tool for PN mitigation. Increasing fuel pressure shortens the time needed to inject a given amount of fuel, increasing the time available for mixing and drying. Higher fuel pressure also increases the ratio of the inertial to viscous forces, thus enhancing the spray turbulence and improving the break-up and atomization of the spray, speeding vaporization and mixing, and increasing in-cylinder turbulence. Spray penetration often stays roughly constant with increased fuel pressure. Despite the higher spray momentum at higher injection pressure, the fuel droplets are smaller and thus have a smaller momentum-to-drag ratio and entrain more air into the spray plume, decreasing penetration. Therefore, for in-cylinder combustion characteristics, increased fuel pressure is beneficial. The primary drawbacks to increasing fuel pressure are the need for a more robust valve train to drive the fuel pump, the associated increase in the parasitic losses, and the need for advanced control strategies to control fuel mass during short injection events.

The effects of injection timing and the fuel injection pressure are shown in Figure 2.33 for a mid-load steady-state operating point at 2000 RPM. The sharp increase in the PN emissions by advancing the SOI beyond 310 °bTDC indicates piston impingement. Higher fuel pressure decreased the PN emissions regardless of the injection timing, but the magnitude of improvement was dependent on the injection timing.

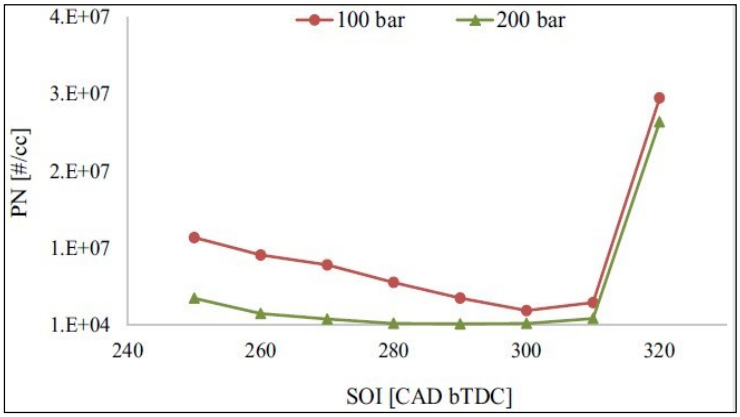

Fig. 2.33 Increase in fuel pressure typically reduces particle formation. Very early SOI timings lead to spray impingement on the piston and lead to a sharp increase in PN, whereas very late injection timing reduces the available time for mixture formation and also affect PN negatively [161-162].

2.4.9.3. Number of Injection Events

The higher particle number emissions associated with operating the engine at higher loads pose additional challenges for meeting future stringent emissions regulations. In the following study [163], the potential of using multiple injection strategies (double injection and triple injection strategy during the intake stroke in homogeneous combustion mode) to reduce particle number emissions in a 2.0 liter boosted SIDI gasoline engine at 1000 rpm, 11 bar BMEP condition was investigated using Horiba Mexa SPCS1000 PN measurement instrument. Measurement indicate that the double injection strategy causes a 60% reduction in particle number concentration and up to 80% reduction when implementing triple injection strategy as compared to baseline single injection strategy, demonstrating the potential of multiple injections as a promising strategy for lower particle emissions at high load operating conditions. Fuel spray penetration increases with increasing fuel mass, so breaking the injection into multiple events decreases the penetration, minimizing wetting of the piston or other surfaces. One of the primary advantages of multi-injection is to begin the spray event at an earlier timing without wetting the piston than would be possible for single injection. The tip wetting of injector can increase or decrease depending on injector design and engine operating conditions.

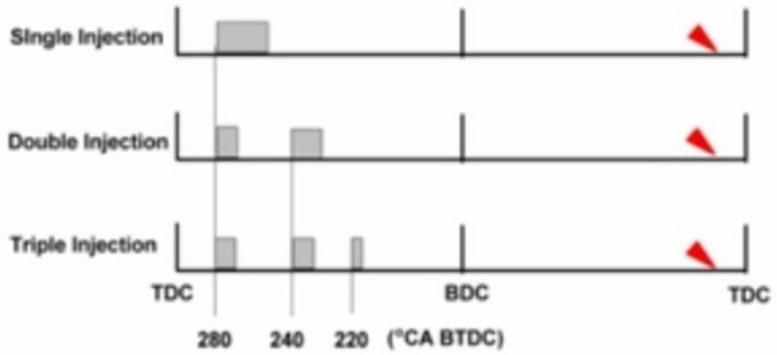

Fig. 2.34 Schematic Diagram of injection timing for single and multiple injection strategies. Split ratio is 4:6 for double injection, and 4:4:2 for triple injection [163].

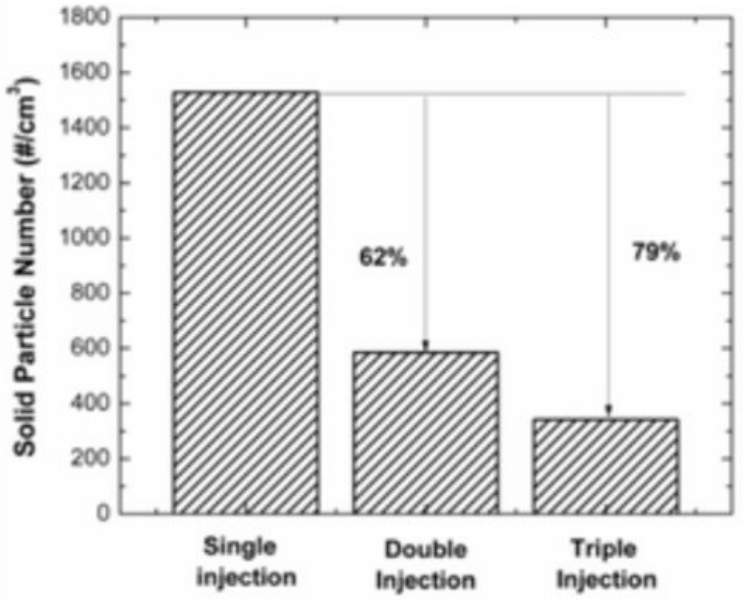

Fig. 2.35 Particle Number emissions comparison for single injection, double injection and triple injection strategies at 1000 rpm, 11 bar BMEP [163].

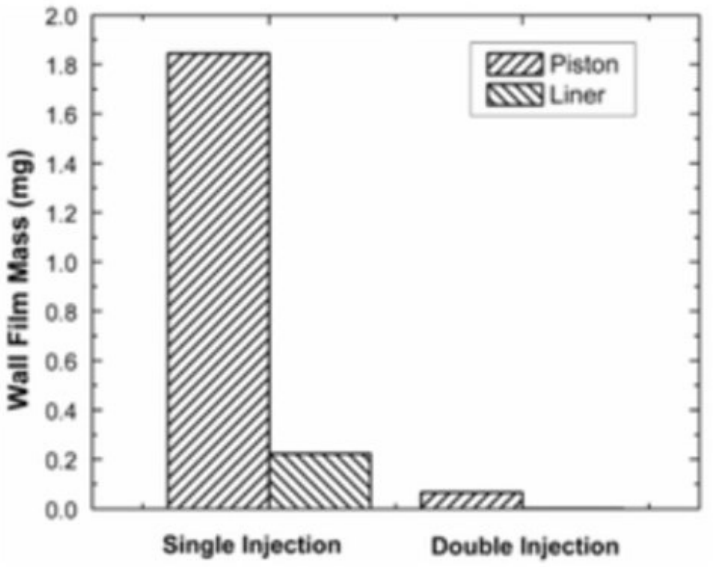

Fig. 2.36 Wall film mass comparison between single injection and double injection at 1000 rpm, 11 bar BMEP. Injection settings are shown in Figure 2.34 [163].

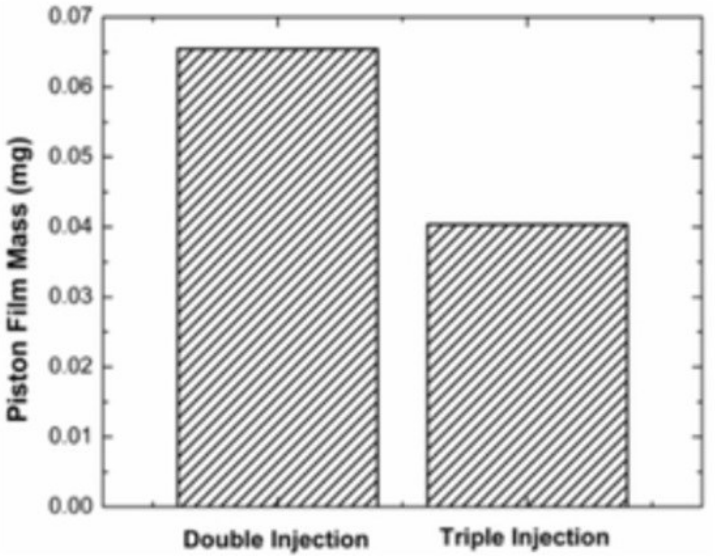

Fig. 2.37 Wall film mass comparison (piston film mass) between single injection and double injection at 1000 rpm, 11 bar BMEP. Injection settings are shown in Figure 2.34 [163].

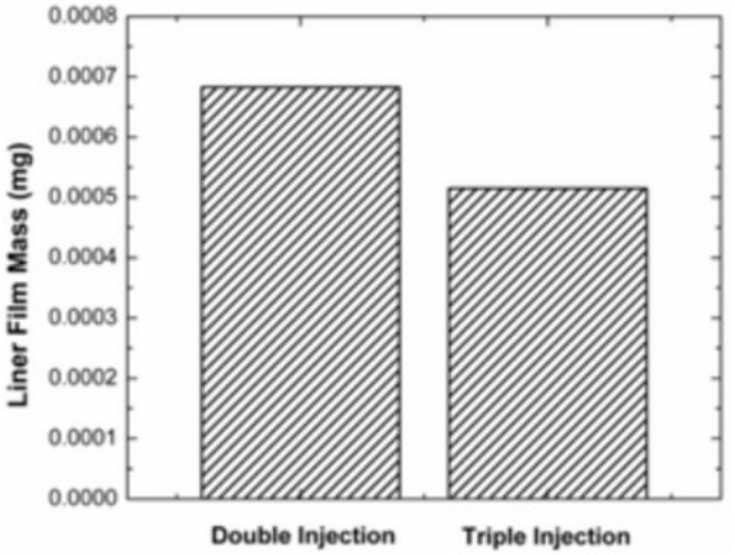

Fig. 2.38 Wall film mass comparison (liner film mass) between single injection and double injection at 1000 rpm, 11 bar BMEP. Injection settings are shown in Figure 2.34 [163].

The 3D CFD simulation reveals that the dominant reasons for the observed particle number reduction with double injection are the significant reduction in fuel-piston and fuel-liner impingement, and the improvement in mixture preparation at the end of compression. For triple injection strategy, the fuel impingement is further reduced and a better air-fuel mixture is obtained, resulting in further reduction in particle number emissions.

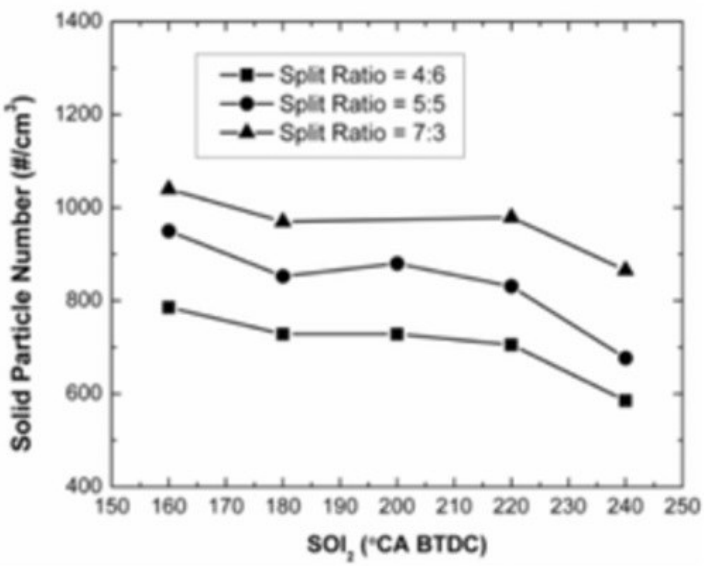

Fig. 2.39 Effects of the second injection (SOI2) and split ratio in mass on particle number emissions at 1000 rpm, 11 bar BMEP [163].

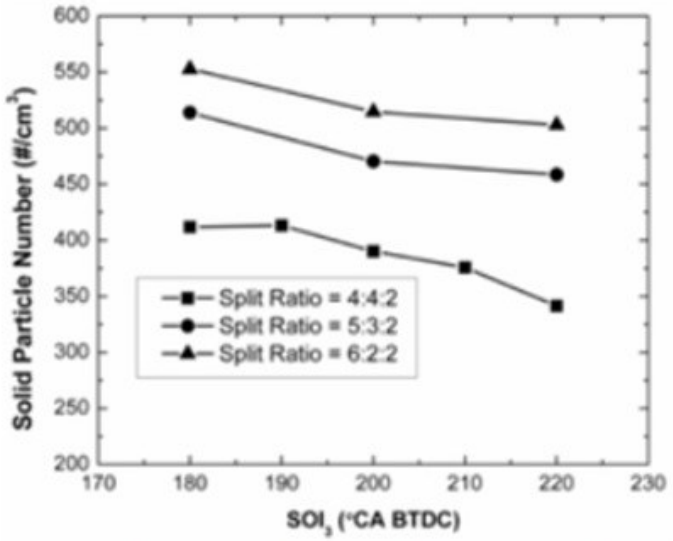

Fig. 2.40 Effects of the third injection (SOI3) and split ratio in mass on particle number emissions at 1000 rpm, 11 bar BMEP [163].

Regardless of double injection and triple injection strategy, the particle number emissions tend to increase when retarding the final injection timing. This trend is attributed to the deteriorated mixture preparation due to the limited time of spray evaporation and mixing. Reducing the first injection mass is beneficial for lower particle number emissions both for double injection and triple injection strategies during the intake stroke. The reduction in fuel impingement on cylinder liner and piston top is believed to be the dominant reason.

In addition to the previous study, the studies [161-162] show that an incorrect management of the SOI and of the split factor could lead to an unwanted PN increase. The effect of multiple injection at mid-load operation is shown in Figure 2.41. The fuel rail pressure was held constant at 200 bar. Finding the optimum injection timing, number of injections, and split of fuel masses is often a matter of experimental trial and error.

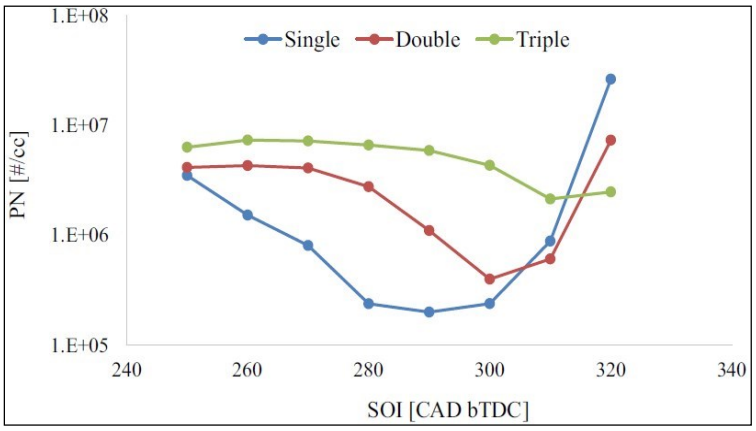

Fig. 2.41 Multiple injection strategies have the potential to reduce PN emission due to piston impingement when used in the right context [161-162].

2.4.10. Fuel Impact on Particle Formation

Gasoline direct injection (GDI) engines are becoming the standard for gasoline light duty vehicles in both the United States and Europe, replacing the traditional port fuel injection (PFI) engines, due to their improved thermal efficiency and lower carbon dioxide (CO_2) emissions [164, 165]. Especially in the United States, GDI platforms have been introduced by automakers as a pathway to reduce net greenhouse gas (GHG) emissions from the transportation sector and meet the federal Corporate Average Fuel Economy (CAFE) standard. However, GDI engines produce higher particulate matter (PM) emissions compared to their PFI counterparts. GDI involves the direct spray of fuel into the combustion chamber.

Late evaporation of this fuel can lead to localized poor air-fuel mixing or diffusion-governed combustion that favors PM formation, especially during cold-start conditions [166, 167].

The use of biofuels in the United States and Europe has also been promoted for the past decades in an effort to reduce GHG emissions from the transportation sector due to environmental protection concerns. Biomass-derived ethanol is the most popular biofuel in the United States, where all the gasoline sold contains up to 10% ethanol by volume (E10). The ethanol utilization is on the rise in the United States, with the U.S. Environmental Protection Agency (EPA) allowing 15% of ethanol by volume (E15) to be sold in the market [168].

The positive environment for ethanol growth was also favored by mandates put in place by the Energy Independence and Security Act of 2007 (EISA) and the Renewable Fuel Standard. In addition to lower concentrations of gasoline-ethanol blends, gasoline is allowed to contain as much as 83% of ethanol by volume and as little as 51% of ethanol by volume [169]. Higher levels of ethanol can be used in flexible fuel vehicles (FFVs), which are designed for this purpose and are certified for emissions compliance by testing with E0 and E85 [170, 171]. Analogous to ethanol, higher alcohols have been the subject of increased interest as potential fuels in spark ignition (SI) engines [172, 173, 174]. Particular emphasis has been given to butanol isomers, which combines the advantages of an energy density, closer to that of gasoline, with the oxygen content and renewability of ethanol [175, 176]. PM formation in SI direct injection engines is well documented [177, 178, 179, 180]. Polycyclic aromatic hydrocarbons (PAHs) are known species to play a major role in the process of soot formation in GDI combustion [181, 182]. The formation process of PAH is dominated by acetylene (C_2H_2), which is present in a larger amount in fuel rich flames. By reactions with CH and CH_2, C_3H_3 is formed, which tends to form a benzene ring (aromatic ring) by recombination and rearrangement. By abstraction of hydrogen and acetylene addition (HACA mechanism), these PAH molecules grow planar. Spatial structures with a graphite-like structure are formed from the plain PAH molecules and grow further by the HACA mechanism. These built-up three dimensional structures are known as primary soot particles. Due to surface growth and coagulation, the soot formation continues and grows. This process is followed by the agglomeration of colliding particles, building up loosely structured agglomerates. Soot oxidation can occur at the precursor, nuclei, and particle stages of the soot formation process. There are many species in or near the flame that could oxidize soot, such as O_2, O, OH, CO_2, and H_2O.

For the premixed, stoichiometric combustion in gasoline engines, the soot oxidation process is assumed to be dominated by OH, as the concentration of O and O_2 is on a low level [183, 184, 185, 186]. Fuel composition is critical to the formation of PM in GDI engines [187, 188, 189]. It should be expected that different fuels have different concentrations of PM emissions [190, 191]. So when comparisons are made between tests using different fuels, it would be useful to have a particulate matter index (PMI) that enables a correction to be made based on the key fuel properties. Aikawa et al. [192] developed a model to correlate PM emissions with the vapor pressure and the double bond equivalent (DBE) of the fuel components. The DBE is a measure of how unsaturated a hydrocarbon is and can be defined from:

$$DBE = \frac{2C - H + 2}{2} \quad .(12)$$

where C, H, and N are the number of carbon, hydrogen, and nitrogen atoms, respectively, in an organic compound.
The PMI links the PM emissions with the vapor pressure and the DBE of the components in the fuel weighted by mass fraction (*Wt*) as follows:

$$PM\ Index = \sum_{i=1}^{n} I_{(443\,k)} = \sum_{i=1}^{n} \frac{DBE_i + 1}{V \times P_{(443k)}} \times Wt_i \quad .(13)$$

As above mentioned, the DBE is a measure of the number of double bonds and rings in the fuel. Particulate emissions can correlate with DBE values and higher boiling points for different chemical species in the fuel. Differences in molecular structure and DBE between paraffins and aromatic hydrocarbons contribute to greater particulate emissions for aromatics [193, 194]. For example, the DBE values of paraffins is 0, whereas the DBE values of aromatic hydrocarbons, depending on the molecular structure, are approximately 4 to 7. In addition, components with higher boiling points and lower corresponding vapor pressures evaporate more slowly, resulting in a greater tendency for diffusion combustion instead of premixed combustion. This results in more imperfect fuel mixing and diffusion-controlled burning of thin films of liquid fuel on the piston, leading to higher particulate emissions [195]. The work undertaken by Aikawa et al. [192] used a PFI engine and had no independent control of the fuel vapor pressure or DBE, as commercial gasolines were used, along with a base fuel, to which different components were added. Indolene was used as a base fuel, to which were added 10% by mass of components such as 2,2,4-trimethylpentane, dodecane, ethylbenzene, and 1,2,4-trimethylbenzene. The PMI range of the fuels tested was 1.01–3.86. The index range of over 1,400 worldwide fuels available was calculated with a mean PMI of 2.12. Furthermore, Aikawa et al. [192] evaluated the vapor pressure at a range of temperatures and found the best correlation between PMI and particle emissions for the vapor pressure at a temperature of 443 K. Leach at al. [196] further investigated the model of Aikawa et al. [192] using a spray-guided GDI engine with designed fuels where the DBE and the vapor pressure were varied independently.

In contrast to Aikawa et al. [192], who calculated the PMI by volume fractions, Leach et al. [196] calculated a particle number index (PNI), using mass fractions. However, they stated that in the majority of cases the relative difference in calculation of PMI and PNI is less than 15%. It should also be noted that in their work, the engine was operated at low engine speed (1500 rpm), low load (0.18 MPa IMEP), and with a rich mixture (λ = 0.9). Dageförde et al. [197] investigated different fuels and fuel blends at catalyst heating operation, and their results supported the findings of Aikawa et al. [192] and Leach et al. [196], as the particle number emissions could be reduced by operating the engine with oxygenated fuel blends as well as with alkylate fuel. The ethanol and n-butanol blends (E40 and B40) have a reduced amount of aromatic compounds and thus a lower DBE. However, using toluene as an aromatic compound and thus increasing DBE did not increase the PN emissions. A study by Khalek et al. [198] indicated that reductions in high boiling point aromatics and the DBE value played important roles in reducing both the PM mass and PN emissions. Karavalakis et al. [195] showed that reducing the aromatic content could effectively decrease PM mass, PN, and black carbon emissions from a fleet of PFI and GDI vehicles. The same study showed a tight correlation between the PMI and particulate emissions, as well as a strong contribution of aromatic species with high boiling points to PM formation [195]. Similar results were observed in a study conducted by Kim et al. [199] when they tested a GDI vehicle using three fuels with different aromatic contents over the New European Driving Cycle (NEDC) and the Federal Test Procedure (FTP) test cycles. The authors found that higher aromatic contents and less volatile fuel led to increases in PN emissions. Zhu et al. [200] tested two identical GDI vehicles over the WLTC test cycle using seven fuels with varying levels of aromatics and olefins contents, as well as T50 (50% vol distillation temperature) and T90 distillation parameters. The results of this study showed decreases in PM and PN emissions when the aromatic content and T90 decreased. Chan et al. [201] evaluated the particulate emissions from two vehicles when operating on two fuels with different PM indices over the FTP and the US06 Supplemental Federal Test Procedure (US06) driving cycles. They found that replacing naphthylenic aromatic hydrocarbons in the fuel (i.e., high PMI fuel) with monoaromatics and naphthenes (i.e., low PMI fuel) reduced PN and black carbon emissions. They also found that the low PMI fuel led to formation of smaller particles with diameters of about 50 nm. Jiao et al. [202] predicted the soot emissions of GDI engines using a computational fluid dynamics (CFD) model. The study confirmed that the light components of gasoline can be more easily evaporated, which affects the ignition and combustion, whereas the heavy components have a large impact on the engine emissions, especially in the presence of the fuel film. Fushimi et al. [203] tested four GDI vehicles and concluded that the high boiling point components may cause the increase in PM emissions. A major study conducted by the U.S. EPA has shown that PM emissions are greatly influenced by aromatic content and T90, followed by ethanol, T50, and RVP (Reid vapor pressure) [204]. This study, the EPAct/V2/E-89 (hereafter “EPAct”) program, was the first large parametric study of gasoline fuel effects to include PM measurements for all tests and was conducted on a fleet of 15 PFI vehicles. The results of this study showed positive coefficients for total aromatics, T90, and ethanol in PM fuel effect models, meaning that relative increases in these fuel properties were associated with higher emissions. Further analysis was conducted on the EPAct data, which replaced total aromatics and T90 fuel parameters in the original design with the PMI parameter [205]. The results showed a large coefficient for PMI, confirming its high correlation with PM emissions.

This study also showed that ethanol exacerbates the propensity of low-volatility fuel components to form PM [205]. This phenomenon was further confirmed by a follow-up study from the same group of authors where they showed that the presence of ethanol was found to have a reinforcing interaction with PMI resulting in augmented PM emissions. The authors suggested that ethanol's high heat of vaporization hinders evaporation of the higher molecular weight components of the fuels [206]. Karavalakis et al. [207] conducted a comprehensive literature review and statistical analysis for the identification of possible correlations between fuel properties, such as the distillation parameters, aromatics, and octane indices, and PM mass and total and solid PN emissions. In their review, the authors included some of the major fuel studies available in the literature such as the EPAct study, the European "Particulates" project, the Coordinating Research Council (CRC) E-94 study (phases 1 and 2), studies conducted by the California Air Resources Board (CARB), and others. The authors reported that for GDI vehicles, aromatics and distillation temperatures had the strongest positive correlations with PM mass and total PN emissions. Distillation end point was statistically significant for both PM mass and PN emissions, while T70 and T90 showed a consistent positive correlation only for total PN emissions. Other properties, such as octane indices AKI, research octane number (RON), and motor octane number (MON), and T10, generally showed more negative correlation with PM and PN emissions for GDI vehicles. The authors also presented cases where statistically significant interactions showed trends in the data related to particular combinations of engine types/model years, number of engine cylinders, and drive cycles. For example, they showed that T10 had a more significant impact on PM mass emissions (positive correlation) for larger engines for GDI vehicles, whereas end point had stronger statistically significant effects on PM mass emissions (positive correlation) for vehicles equipped with wall-guided GDI naturally aspirated engines. It is still not conclusive as to whether the use of ethanol causes an increase or decrease in particulate emissions from current SI engines. Storch et al. [208] reported measurements of two-dimensional soot volume fraction in GDI ethanol-blended spray flames ignited by a spark plug inside a spray injection chamber. They found reduced evaporation for pure ethanol and E85 blends compared to isooctane and E20, which they were ascribed to the high enthalpy of evaporation of ethanol delaying the evaporation process. They also showed higher sooting tendency of isooctane-E20 compared to pure isooctane, as well as that ethanol addition to a toluene-isooctane mixture and gasoline can increase the frequency of soot volume fractions. The authors claim that is due to the fact that ethanol changes the evaporation characteristics of the mixture due to non-ideal mixing behavior and high enthalpy of evaporation, which leads to an increased soot formation tendency. Chen et al. [209] investigated the effects of gasoline/ethanol blends in different blending proportions for PN and particle mass emissions using a single-cylinder optical access direct injection engine under cold and warm conditions at a stoichiometric condition (1500 rpm, 0.5 bar manifold absolute pressure). They found increases in both PN and PM emissions with increasing ethanol content, with these increases being more profound under cold conditions than under warm conditions (Figure 2.42). The increases in particulate emissions were attributed to the deleterious effect of ethanol on spray break-up and the evaporation efficiency as a result of its high vaporization enthalpy and low energy density. Similar findings have been reported by the same group of authors where higher ethanol concentrations led to increased PM mass and PN emissions during engine cold-start conditions [210].

These results were explained by mixture inhomogeneities caused by poor evaporation at low temperature due to the high enthalpy of evaporation of ethanol. Di Iorio et al. [211] studied the PM emissions of ethanol/gasoline blends (E0, E50, E85, and E100) in homogeneous and stratified conditions in a supercharged GDI engine. They found that the accumulation mode particles increased in the stratified mode. When the fuel was injected at the early stage of the intake stroke, there was sufficient time for evaporation and mixing with the fresh air, and improved the air/fuel mixture homogeneity. When the fuel was injected at a later stage of the intake stroke, the evaporation and mixing time was short even though the in-cylinder higher temperature was not enough to promote the fuel evaporation, and this resulted to a certain extent in stratification and uneven mixing. Once the flame front arrived at the wet surface, the diffusion combustion that occurred on the oil film contributed highly to PM formation. Similar trends have been seen by Catapano et al. [212] when they studied the effects of engine speed on PM emissions of ethanol blends. They observed a decrease in particle size distribution and PN emissions as the ethanol content in the blend increased for the cases with no significant fuel impingement at 2000 rpm. But as the engine speed was increased to 4000 rpm, the longer injection durations for ethanol blends resulted in more impingement with the piston, and the time available for vaporization was decreased, which increased the PN and sizes for the ethanol blends, as shown in Figure 2.43. Analogous increases in PN emissions were observed in a study by He et al. [213] using certification gasoline and an E20 blend at four steady-state engine operating conditions when testing a wall-guided GDI engine. It was found that fuel injection timing was the dominant factor impacting PN emissions.

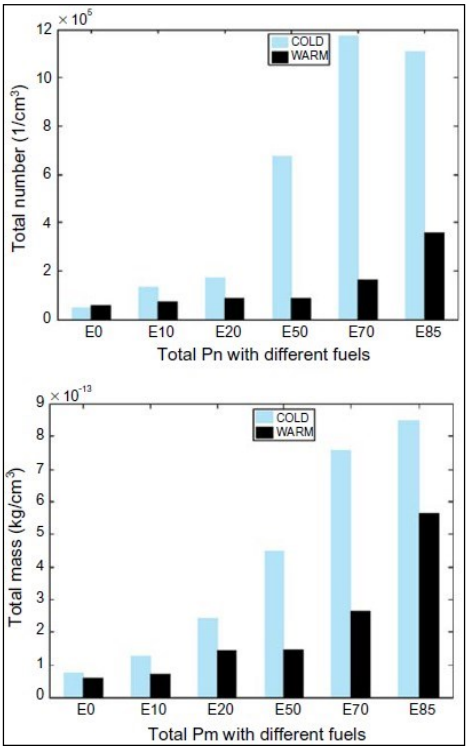

Fig. 2.42 Total particulate number (top) and total particulate mass (bottom) emission for different gasoline/ethanol blends in a cold (20°C) and a warm (80°C) engine. Chen et al. [209].

Chan et al. [214] showed that the use of E10 fuel reduced the particle emissions from a PFI vehicle and showed moderate particle reductions over the FTP cycle at standard ambient test temperature (22°C), but significantly increased particle emissions compared to neat gasoline at other ambient test temperatures (−7°C and −18°C).
The majority of the published literature have shown the beneficial effects of ethanol fueling on PM formation from GDI engines and vehicles. Esarte et al. [215] found that the presence of alcohols reduced the formation of soot and that a higher oxygen/ carbon (O/C) ratio in the reacting mixture resulted in a higher soot reduction due to the enhancement of oxidation reactions by the presence of oxygen in the mixture. Thus, the reaction rate of the particle surface growth by large hydrocarbons for the formation of the accumulation mode particles decreases. Maricq et al. [216] examined the impact ethanol/gasoline blends from a turbocharged GDI vehicle with two engine calibrations over the FTP cycle. They showed statistically significant reduction in PM mass and PN emissions when the ratio of ethanol was higher than 30% by volume for both engine calibrations. However, as the ethanol level ranged from 0% to 20%, a small benefit in PM mass and PN emissions was observed, which was within the test variability.

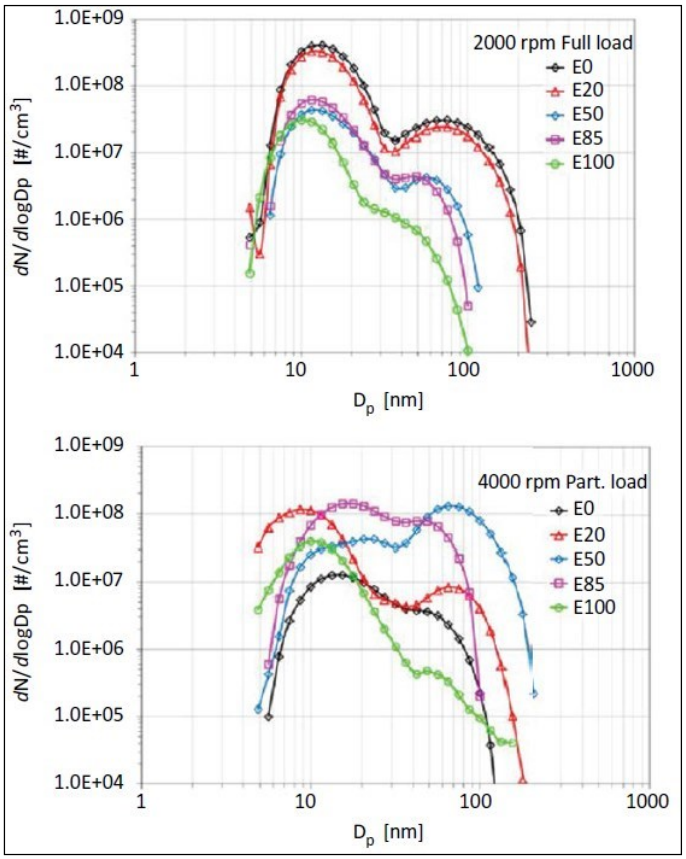

Fig. 2.43 Particle size distributions for the gasoline fuel (E0) and the ethanol blends at 2000 rpm (top) and 4000 rpm (bottom) partial load.
Catapano et al. [212].

The same study showed that the PM composition was determined to PN emissions of pure gasoline, E10, and E20 fuels under the FTP and US06 driving cycle on a GDI vehicle.
They found that the addition of ethanol could simultaneously reduce the PM mass and PN emissions in the transient phase and transition phase, which was mainly due to the PM reduction under the fuel-rich condition, whereas the PM emissions in the rich-fuel conditions were much higher than those in the stoichiometric conditions. Under steady-state conditions, the PN concentrations decreased with an increase in ethanol level. Similar to Maricq et al. [216], this work showed that most of the organic carbon (OC) in PM was effectively removed by the three-way catalyst (TWC) leaving a larger fraction of EC. In a study by Fatouraie et al. [217], they conducted experiments in a single-cylinder GDI engine at the same load conditions and at a fixed engine speed (1500 rpm) using E0/indolene and E100. They found over an order of magnitude less soot with ethanol under all operating conditions compared to indolene. Sakai and Rothamer [218] studied different ethanol blends (E10, E20, E30, E40, and E50) on a single-cylinder GDI engine to evaluate the relative sooting propensity of ethanol fueling under completely premixed and prevaporized operation. By operating the engine in this mode, the presence of liquid fuel in-cylinder was eliminated, allowing the examination of soot production from gas phase sources. The results showed that higher ethanol concentrations decreased particulate emissions. As ethanol levels increased, the particle size distribution changed from agglomeration to nucleation mode dominated profiles. At higher equivalence ratios, this shift also corresponds to the change from an accumulation mode dominated distribution for low-level ethanol blends to a nucleation mode dominated distribution at higher blends. Karavalakis et al. [219] studied the particulate emissions of a GDI FFV with a wall-guided injection system fueled with E10, E51, E83, and an isobutanol blend at a proportion of 55% by volume over the FTP and LA92 driving cycles. They found that the addition of higher ethanol blends and the isobutanol blend resulted in large reductions in PM mass, black carbon, and total and solid particle emissions, with specific fuel properties having an obvious effect on particulate emissions, such as the oxygen content and aromatic compounds. Mamakos et al. [220] also showed important reductions in total and solid PN emissions when they tested GDI FFVs on high ethanol volumetric fractions (75–85%) over the NEDC and the motorway portion of the Artemis cycle. Jin et al. [221] examined the impact of different low-, mid-, and high-ethanol blends (E0, E10, E30, E50, and E85) on a GDI vehicle over the FTP cycle. Their results showed strong PN and PM mass reductions for the high-ethanol blends relative to E0 and E10 fuels. As the ethanol content was increased, the size-resolved PN concentration showed a decrease in the accumulation mode. Finally, Zhang et al. [222] showed that with an increase in the ethanol ratio, the accumulation mode particles were significantly reduced, with the nucleation mode particles being the majority of the total particle concentration. This finding was attributed to the lower combustion temperature with the increase of the ethanol ratio, whereas fewer primary carbon particles were generated by the pyrolysis of fuel vapor and dehydrogenation reaction decreased due to the lower aromatic content and the higher oxygen content in the fuel. According to the above statements, the main cause of the gasoline engine particles is the non-premixed combustion of the incompletely evaporated and mixed fuel.
Thus, if the fuel molecules contain oxygen to improve the combustion of the local zone, then it will help to inhibit the generation of soot particles.

Based on this hypothesis, Oh et al. [223] studied the effects of oxygen content on the PM emissions of a GDI engine equipped with a centrally mounted injector, a GDI engine equipped with a side-mounted injector, and a PFI engine. They found that increasing the oxygen content in gasoline helped reduce the PM emissions of the GDI engine, especially during the start-up phase. Wang et al. [224] compared the PM emissions of gasoline and ethanol in a single-cylinder spray-guided GDI engine under the conditions of 3.5 bar to 8.5 bar IMEP and stoichiometric air/fuel ratio. It was found that the ethanol would produce less PM emissions but more PN emissions. Vuk and Vander Griend [225] researched the particulate emissions from a GDI vehicle that was fueled with various ethanol/gasoline blends and operated over the FTP and US06 driving cycles. They found major reductions in both PM mass and PN emissions with ethanol concentrations as low as 10%, suggesting that ethanol promoted faster evaporation of wetted walls in situations of fuel impingement, while also providing additional oxygen in fuel-rich diffusion flames. On a different study conducted on a spray-guided GDI engine, it was found that the accumulation mode particles and the average diameter decreased with an increase in the oxygen concentration in the rich air/fuel mixture [226]. For the stoichiometric mixture, the particle concentration of E85 was significantly lower than that of the other fuels, whereas the particle concentrations of E30, M30 (30% by volume of methanol), and gasoline were equivalent. The effect of air/fuel ratio on the PM of the E85 was less pronounced compared to gasoline and E30, and the accumulation mode particles were very low, especially under the rich mixture condition. From these results, it can be inferred that the oxygen content of the fuel molecules can reduce the concentration of the intermediate substance of the soot formation precursor. Another possible biofuel that is receiving widespread attention for SI engine applications is butanol [227, 228], whose isomers have research octane numbers ranging from 96 for straight n-butanol to 105 for the branched tert-butanol [229]. A study by Li et al. [230] conducted in a 1.8L turbocharged GDI engine fueled with gasoline and n-butanol, isobutanol, sec-butanol, and tert-butanol blends at ratios from 10% to 50% by volume showed that sec-butanol/gasoline yielded the lowest PN emissions, closely followed by n-butanol/gasoline, isobutanol/gasoline, and tert-butanol/gasoline. The mean particle diameter decreased with the addition of butanol due to the reduction in the fraction of larger particles. Sec-butanol blends shifted to smaller particle sizes, while tert-butanol blends to larger particle sizes. Storey et al. [231] found that the addition of 48% butanol (equivalent oxygen content as E30) in a GDI engine at 2600 rpm and 8 bar BMEP under rich conditions with advanced injection reduced smaller particles, while an important peak in accumulation mode particles could be observed compared to pure gasoline. The distributions showed a unimodal shape, and the butanol blend shifted the distribution to greater diameters, although butanol emitted fewer total particles than gasoline. Hergueta et al. [232] studied the effect of 33% butanol by volume in commercial gasoline containing 5% of ethanol and gasoline in a GDI engine. With the use of a transmission electron microscope (TEM), they showed that the butanol blend did not increase the primary particle diameters, due to the oxygen content of butanol that could limit the rate of soot formation and at the same time promote soot oxidation. Chan [233] tested a GDI vehicle fueled with iB16 (16% isobutanol) over the FTP and US06 driving cycles at standard and cold ambient temperatures.

For the standard and cold ambient temperature FTP testing, the iB16 blend resulted in lower solid PN and black carbon emissions compared to gasoline.

Lattimore et al. [234] carried out experiments with a single-cylinder GDI engine at an engine load of 8.5 bar and various compression ratios between 10.7 and 11.5 with B20 (20% by volume of n-butanol). They found that n-butanol addition to gasoline significantly reduced the accumulation mode PN emission, due to the earlier combustion phasing and thus increased post-combustion oxidation time. They also showed that Bu20 had more nucleation mode particles than gasoline, due to the lower soot accumulation mode particles that reduced nuclei adsorption. In a study by Karavalakis et al. [219], four alcohol blends were examined (E10, E51, E83, and 55% of isobutanol or Bu55) in GDI FFV over the FTP and LA92 driving cycles. While the isobutanol blend had lower total aromatics compared to E51 and E83 blends, it exhibited higher PN emissions than these fuels, as shown in Figure 2.44. This finding was due to the lower oxygen content of the isobutanol blend and the higher content of heavier monoaromatic and naphtheno-aromatic hydrocarbons with high boiling points relative to E83. Additionally, the authors stated that branched butanols can produce intermediate higher molecular weight radicals, such as propene and butane, than ethanol, which react to produce higher molecular weight soot products. In a different study by Karavalakis et al. [235], when they tested lowand mid-level isobutanol blends in two GDI passenger cars over the FTP and LA92 driving cycles, they found PM mass, PN, and black carbon emissions reductions with increasing the alcohol level in the fuel.

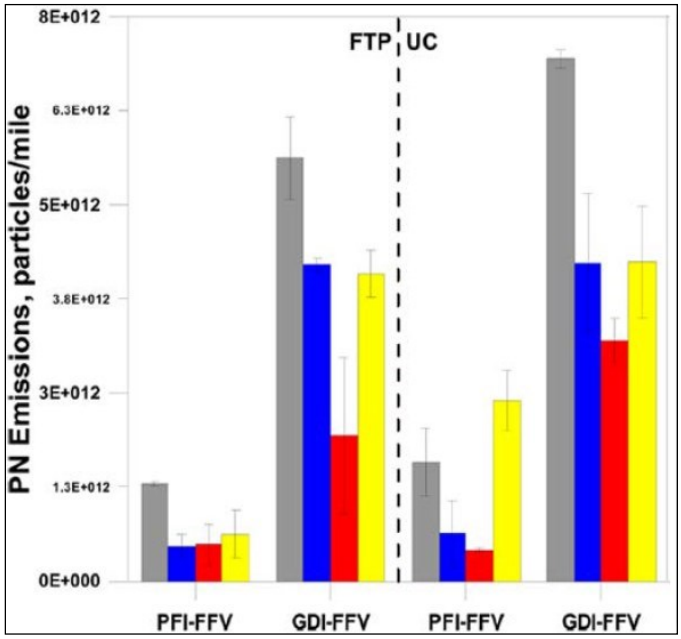

Figure 2.44 Particle number emissions for the PFI-FFV and GDI-FFV over the FTP and LA92 cycles. The colors represent: E10 (gray), E51 (blue), E83 (red), and Bu55 (yellow). Karavalakis et al. [219].

2.4.11. Review on the combustion parameters that influence the PN Emissions

In the following pictures the effects of the principal engine's parameters on the PN emissions and the principal strategies for its reduction are shown.

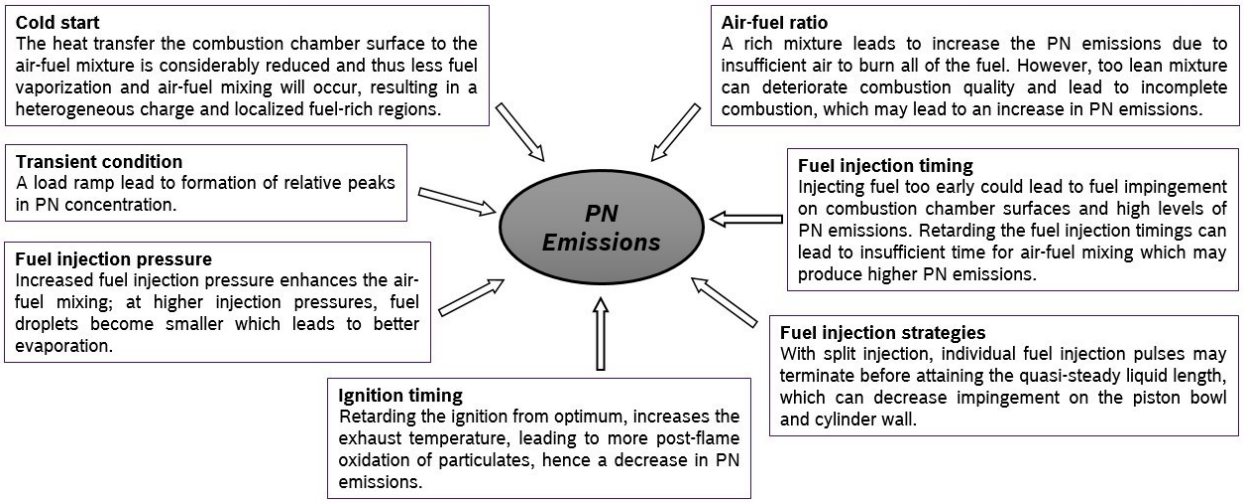

Figure 2.45 Influences on particle formation according. Adapted from Bertsch et al. [125].

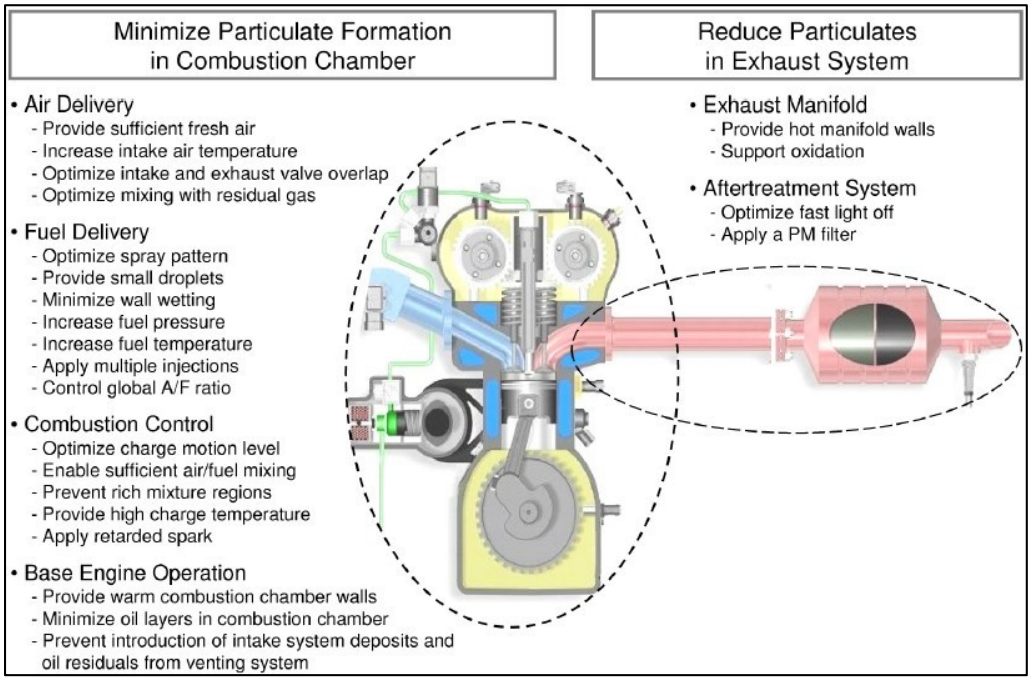

Figure 2.46 Strategies Towards Meeting Future Particulate Matter Emission Requirements in Homogeneous Gasoline Direct Injection Engines. [236]

3. Case of Study

3.1. Experimental Investigation of Impact of Injection Timing on Particulate Number Emission of a Modern Gasoline Direct Injection Engine using RON 98 and RON 95 E5 Fuels

3.1.1. Introduction

Injection timing is a key parameter for influencing PN mechanisms. For homogeneous-charge engine operation, which is the norm for most of the speed/load operating points of most production DI engines, injection happens during the intake stroke. Injection timing is often a compromise between fuel consumption and PN. Fuel consumption is generally improved as injection timing is moved earlier (presumably due to better mixing), but the likelihood of spraying fuel on the piston and causing PN due to piston wetting also increases with earlier injection timing, so injection timing should be chosen to be sufficiently late to avoid the piston. The injection timing also determines how much time is available for the charge to mix and for any liquid films to dry. Injection timing is often chosen to be as early as possible while still avoiding piston impingement, with an additional safety factor. This trade-off timing is significantly different depending on the engine geometry (e.g., side-vs. centrally mounted injectors) and the injector spray targeting. The following study focused on the effects of the injection timing on the particulate matter emissions with emphasis on the particles number that was investigated for a gasoline direct injection (GDI) engine fueled with two types of gasoline RON 95 E5 - RON 98, and under different engine operating conditions.

3.1.2. Experimental Setup

A GDI engine with turbocharger, centrally located spark plug and side-mounted injector was used for study in this work. With regard to the lube oil, it was used Selenia SAE 0W 30, in addition other detailed specifications of the engine are listed in Table 3.1.
The schematic of engine and experimental setup is shown in the Figures 3.1 – 3.2.
The test fuels were commercial gasoline, with a Research Octane Number (RON) of 95 and 98 and other chemical-physical properties like shown in Table 3.2.
The test engine was setup on an engine dynamometer with well controlled coolant, oil, fuel, ambient air and intercooler outlet temperatures.
A Horiba Motor Exhaust Gas Analyzer Mexa 7100-D was used for analyzing gaseous emissions, including Carbon Monoxide (CO), Hydrocarbon (HC) and Oxides of Nitrogen (NOx).

Particulate number emissions were measured in the engine-out exhaust flow using a Horiba Mexa-2100SPCS. The measurement method is based on the requirements described in Revision 4 of the UN/ECE Regulation No. 83, which is a uniform provision concerning the approval of new vehicles regarding the emission of the pollutants. The total dilution ratio of 2000 was set during the tests. With regard to the Measure System, in Table 3.3 the principal needed information are shown.

TABLE 3.1 - Test engine specification

ITEM	DESCRIPTION
Engine type	Four stroke, GDI, 4 cylinders
Valves/Cylinder	4
Displacement (l)	2.0
Induction system type	Turbocharger
Cylinder bore (mm)	84
Piston stroke (mm)	90
B/S ratio	0.93
Compression Ratio	9.5
Fuel Injector	HDEV5.2LS – 6 holes – 20 Mpa
Fuel Types	Gasoline (RON 95 E5 – RON 98)
Fuel Pressure	200 bar

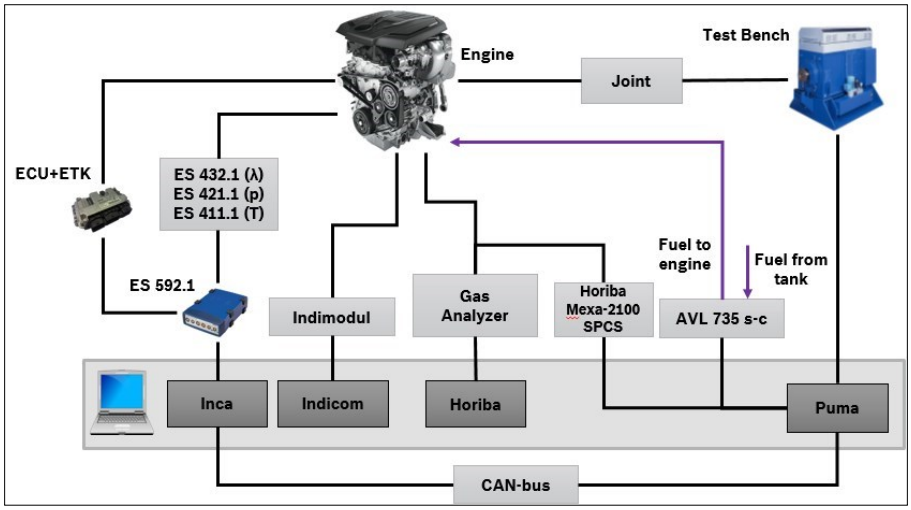

Figure 3.1 Scheme of the Experimental Setup

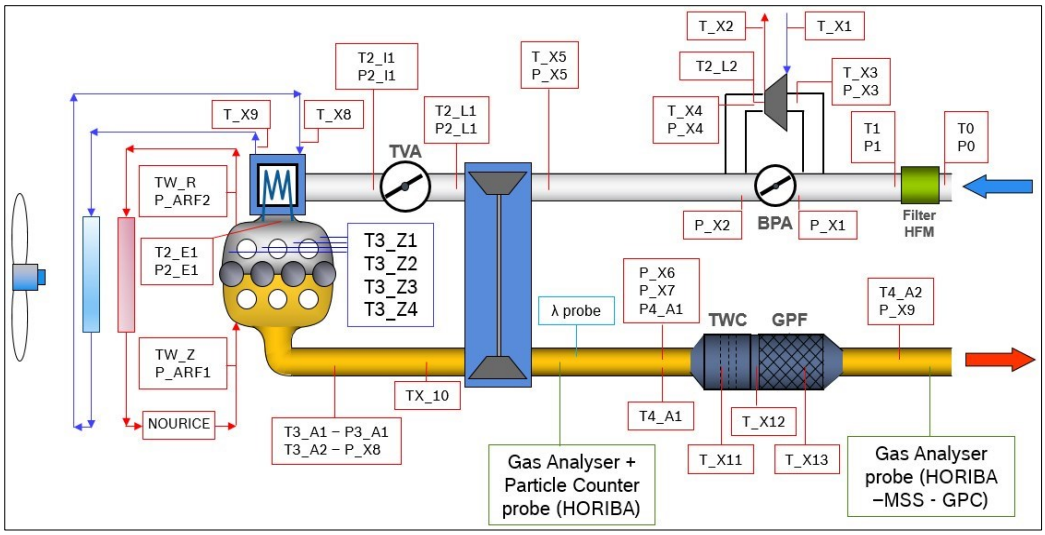

Figure 3.2 Engine Layout

TABLE 3.2 – Tested Fuels

CHARACTERISTICS	UNIT	METHOD	RON 95 E5	RON 98
Density at 15 °C	Kg/lt	EN ISO 3675	0.751	0.749
Research Octane Number (RON)	-	EN ISO 5164	96.9	98.2
Motor Octane Number (MON)	-	EN ISO 5163	86.5	87.2
Sensitivity (RON-MON)	-	Calculation	10.4	11
Antiknock Index (AKI)	-	Calculation	91.7	92.7
Vapor Pressure	kPa	EN ISO 13016-1	59.8	64.5
	PSI		8.67	9.35
Distillation				
Initial Boiling Point	°C	EN ISO 3405	33.5	33.5
10 % vol. evaporated at (T10)	°C	EN ISO 3405	44	51.1
50 % vol. evaporated at (T50)	°C	EN ISO 3405	86.4	83.2
90 % vol. evaporated at (T90)	°C	EN ISO 3405	152.9	148.2
E70	Vol %	EN ISO 3405	36.5	37.6
E100	Vol %	EN ISO 3405	58.5	61.1
E150	Vol %	EN ISO 3405	89.1	95.6
Final Boiling Point	°C	EN ISO 3405	195	180.1
Residue	Vol %	EN ISO 3405	1	1
Aromatics	Vol %	ASTM D 319	33.5	33.7
Olefins	Vol %	ASTM D 319	11.4	11.1
Saturates	Vol %	ASTM D 319	50.2	45.7
Ethanol	Vol %	EN 1601	4.9	0
Methanol	Vol %	EN 1601	0	0
Other Oxygenates Compounds	Vol %	EN 1601	0	9.5
Oxygen Content	Weight %	EN 1601	1.9	2.09
Benzene Content	Vol %	EN 12177	0.45	0.6
Lead Content	mg/lt	prEN 237	< 1	< 1
Sulphur	mg/kg	EN ISO 20846	< 10	< 10

TABLE 3.3 – Measure System

Description	Instrument
Interface module	ES 592.1
Lambda module	ES 432.1
Temperature module	ES 411.1
Pressure module	ES 421.1
Particle Counter	Horiba Mexa-2100 SPCS
Fuel Mass Flow Meter	AVL 735s
Fuel Temperature Control	AVL 735c
Engine Control Unit	ECU
ECU Interface	ETK
Combustion Analyzer	Indicom
HC, CO, NOx emissions	Horiba – Motor Exhaust Gas Analyzer Mexa-7100D

3.1.3. Results and Discussion

3.1.3.1. Impact of the Injection Timing on PN Emission using Gasoline RON 98

The four operating points OP (Speed x Load) tested are as follows:

TABLE 3.4 – Engine Operating Conditions

OP (Speed x Load)	λ [-]	Injection Strategy	Injection Pressure [MPa]	SOI Sweep [**°CA BTDC**]
OP1: 3500 rpm x 8 bar	0.98	Single in Intake Stroke	20	240° - 340°CA
OP2: 3500 rpm x 20 bar	0.91	Single in Intake Stroke	20	240° - 340°CA
OP3: 4500 rpm x 8 bar	0.98	Single in Intake Stroke	20	240° - 340°CA
OP4: 4500 rpm x 20 bar	0.77	Single in Intake Stroke	20	200° - 340°CA

Figures 3.3 – 3.4 – 3.5 – 3.6 show the PN emissions indicator for every operating condition. It can be seen that for each operating condition an appropriate SOI, at which the engine generated the lowest PN emission, could be found, and these SOIs advanced as speed or load increased. From figure 3.3, at 3500 rpm x 8 bar operating point there was an increase in PN soot emissions from left to right for the most advanced SOI. This behavior can be due to the increase of the fuel film on the piston surface that provides the SOI advance and consequently an increase in the pool fire intensity.

Another possible hypothesis can be related to the injector diffusion flame according to Berndorfer et al [24] where it was found that a detailed optimization of the relevant injector tip parameters controlling the atomization as well as the fuel injector tip interaction is necessary to lower the particulate number emissions in SI engines. At a fixed engine speed, an higher load means more fuel quantity, i.e. longer injection duration at constant injection pressure, which works as the primarily factor that enhance the spray penetration depth (Preussner et al., 1998 [25]), and may cause a less effective mixture preparation. In consequence, an early injection timing, together with the retarded spark timing, aids to improve the mixture preparation. According to what has just been said, from the same figure 3.3, it's possible to see that for a higher engine load, in this case at 3500 rpm x 20 bar operating point, we have a drastic increase in PN emissions but in opposite direction compared to the previous operating point (3500 rpm x 8 bar). This last result demonstrates that the fuel film does not influence the soot emissions and that the time reduction for the Air-Fuel mixture preparation led to less time to mix and evaporate the fuel droplets, generating locally fuel rich-zones and incomplete combustion, principal factor that directly affects soot PN emissions.

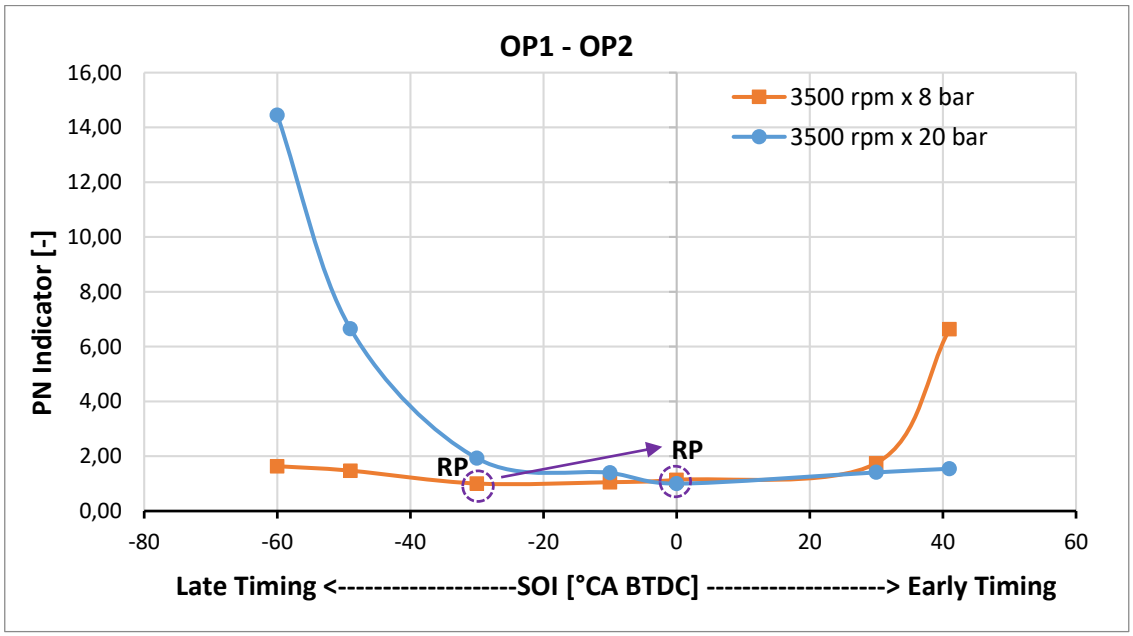

Fig. 3.3 Effects of the SOI on PN at 3500 rpm and variable load

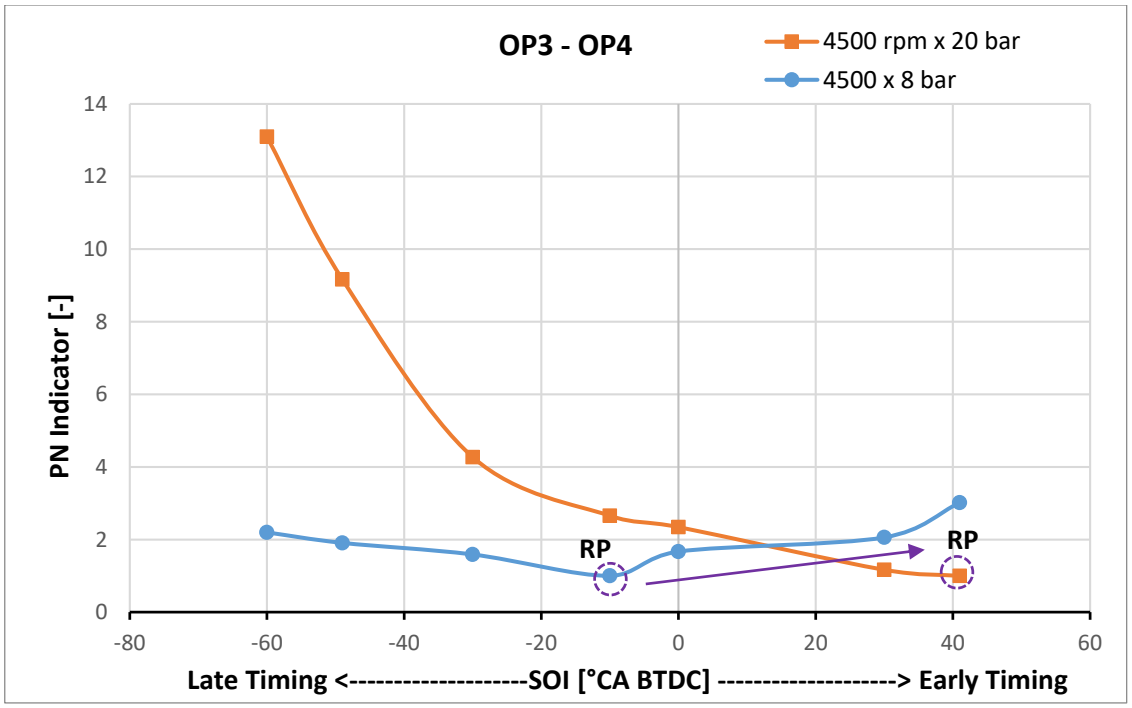

Fig. 3.4 Effects of the SOI on PN at 4500 rpm and variable load

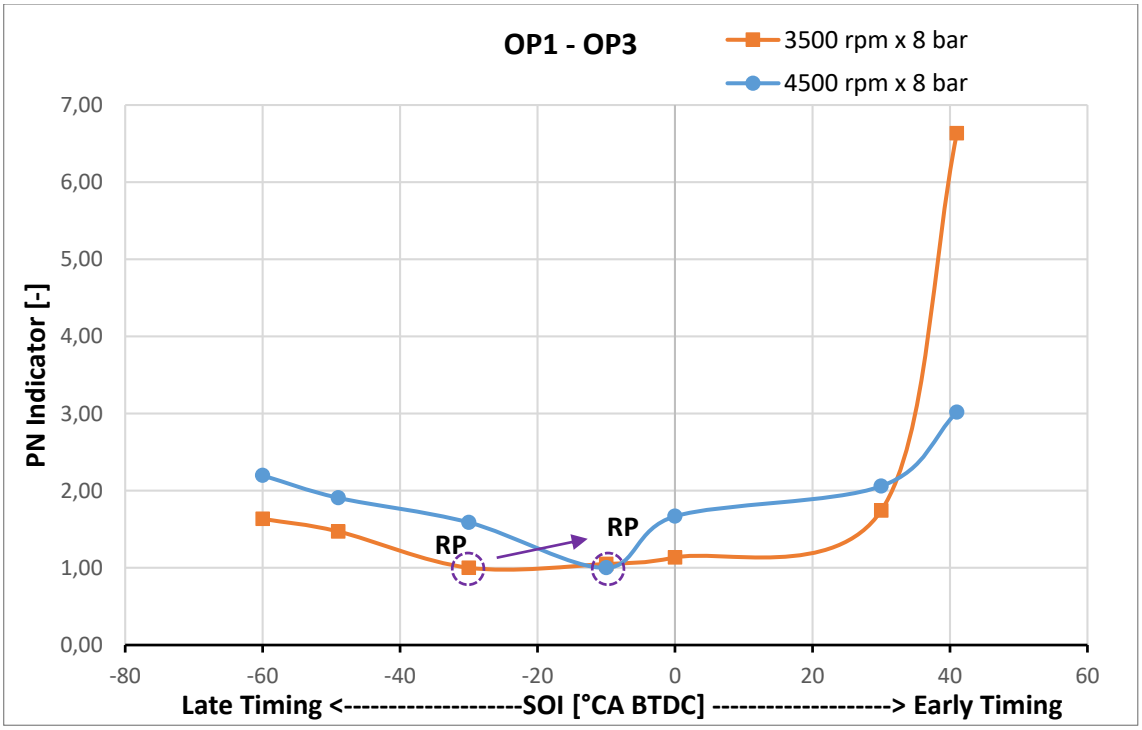

Fig. 3.5 Effects of the SOI on PN at 8 bar and variable speed

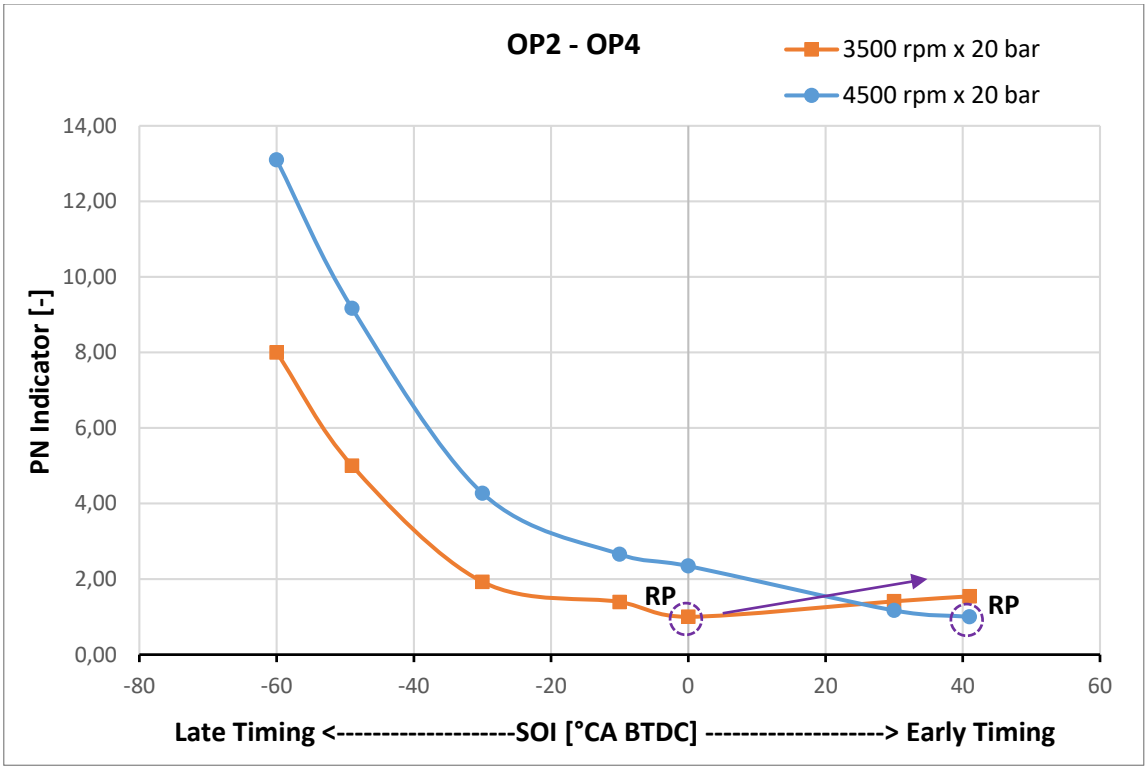

Fig. 3.6 Effects of the SOI on PN at 20 bar and variable speed

Engine speed affects fundamental properties that influence the charge induction, fuel spray development, combustion, and engine-out emissions. Higher engine speeds reduce the time available for mixing and evaporation, which can have a negative effect on charge homogeneity. However, turbulence and mean air velocity increase as the engine speed increases, which improves mixing and enhances the charge homogeneity, thus mitigating the locally rich zones in the gas phase and reducing the particulate production. The resulting effect on mixing is engine and condition specific. Regarding the fuel impingement on the piston, because piston speed increases at higher rpm, the piston moves away from the spray more quickly and reduces the piston impingement for a given SOI. As can be seen from the Figure 3.7, increased engine speed and engine load led to higher component temperatures due to more friction and a shorter time for heat transfer. Higher temperatures accelerate the evaporation of the liquid films on the components like piston, valves or walls thus reducing the negative effects of the fuel impingement but at the same time can also promote low temperature soot formation reactions. With regard to the last effects, from the Figure 3.5 it's possible to detect that for a fixed and low engine load, the increased engine speed and the higher component temperatures due to the higher exhaust temperatures reduced the impingement effects on the piston, thus leading to a good PN reduction. In addition, it was found that this last advantage is more pronounced for low engine loads by means of a comparison between the Figures 3.5 – 3.6. However, from the same figures it's also possible to see that an increased engine speed led to a higher PN emissions for later SOIs, essentially due to the less time available for the mixing and evaporation of the mixture. Similar results were observed by Zhang et al. [237].

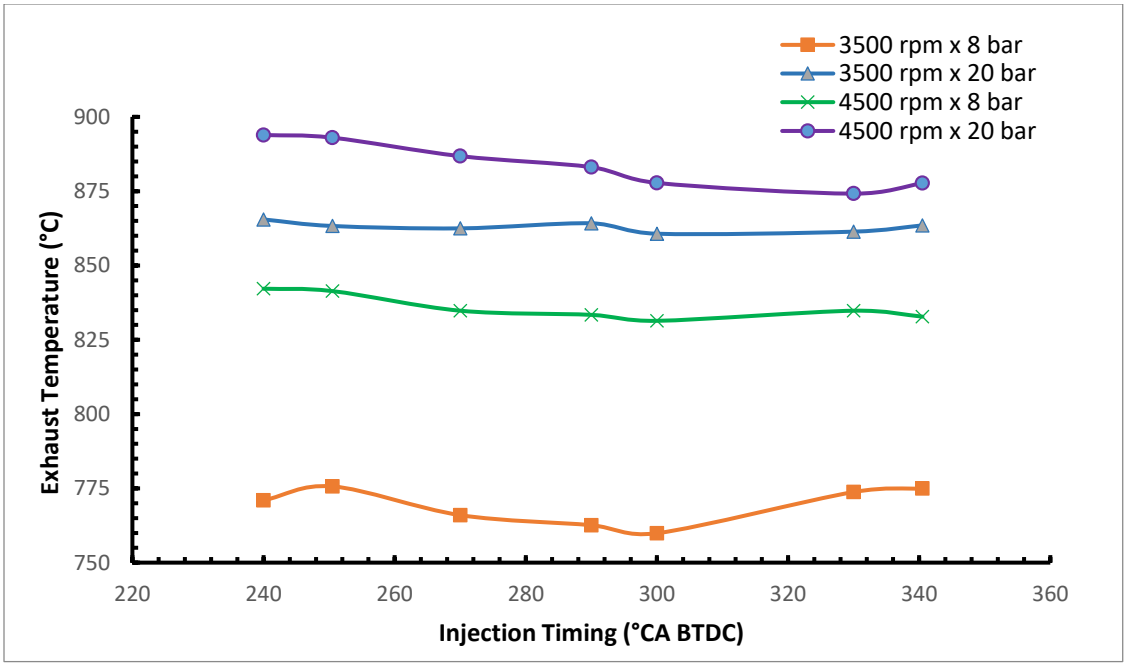

Fig. 3.7 Effects of the SOI on Exhaust Temperature

3.1.3.2. Impact of the Injection Timing on PN Emission using Gasoline RON 95 E5

The four operating points OP (Speed x Load) tested are as follows:

TABLE 3.5 – Engine Operating Conditions

OP (Speed x Load)	λ [-]	Injection Strategy	Injection Pressure [MPa]	SOI Sweep [**°CA BTDC**]
OP1: 3500 rpm x 8 bar	0.99	Single in Intake Stroke	20	265° - 340°CA
OP2: 4500 rpm x 8 bar	0.99	Single in Intake Stroke	20	265° - 340°CA
OP3: 3500 rpm x 20 bar	0.89	Single in Intake Stroke	20	265° - 340°CA
OP4: 4500 rpm x 20 bar	0.77	Single in Intake Stroke	20	265° - 340°CA

Figures 3.8 – 3.9 – 3.10 – 3.11 show the total PN emissions for every operating condition. It can be seen that for each operating condition, an appropriate SOI, at which the engine generated the lowest PN emission, could be found and these SOIs advanced as load increased otherwise remained unchanged as the engine speed increased.

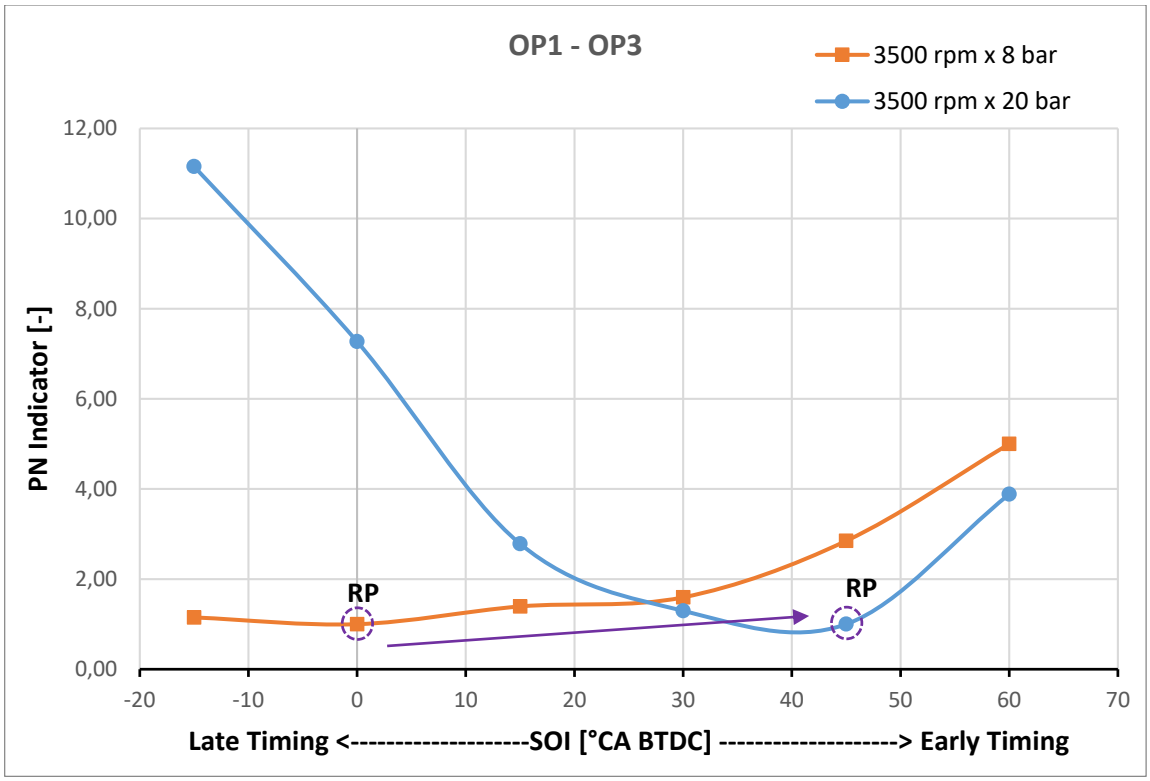

Fig. 3.8 Effects of the SOI on PN at 3500 rpm and variable load

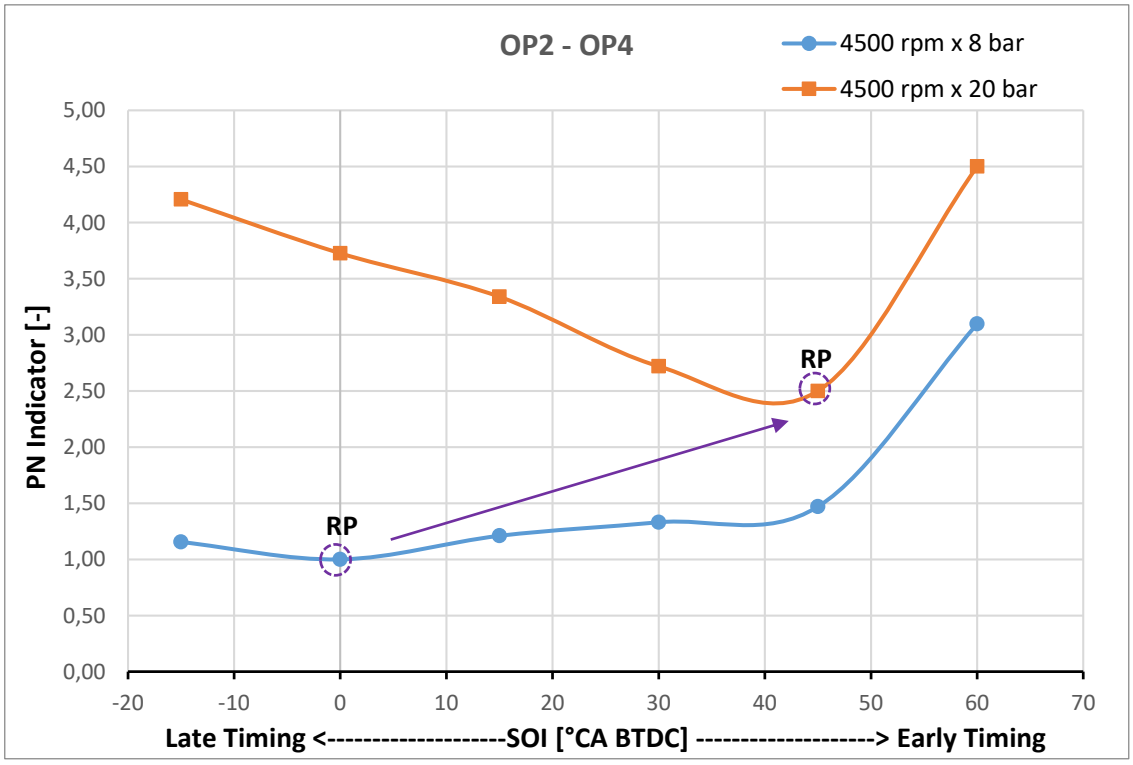

Fig. 3.9 Effects of the SOI on PN at 4500 rpm and variable load

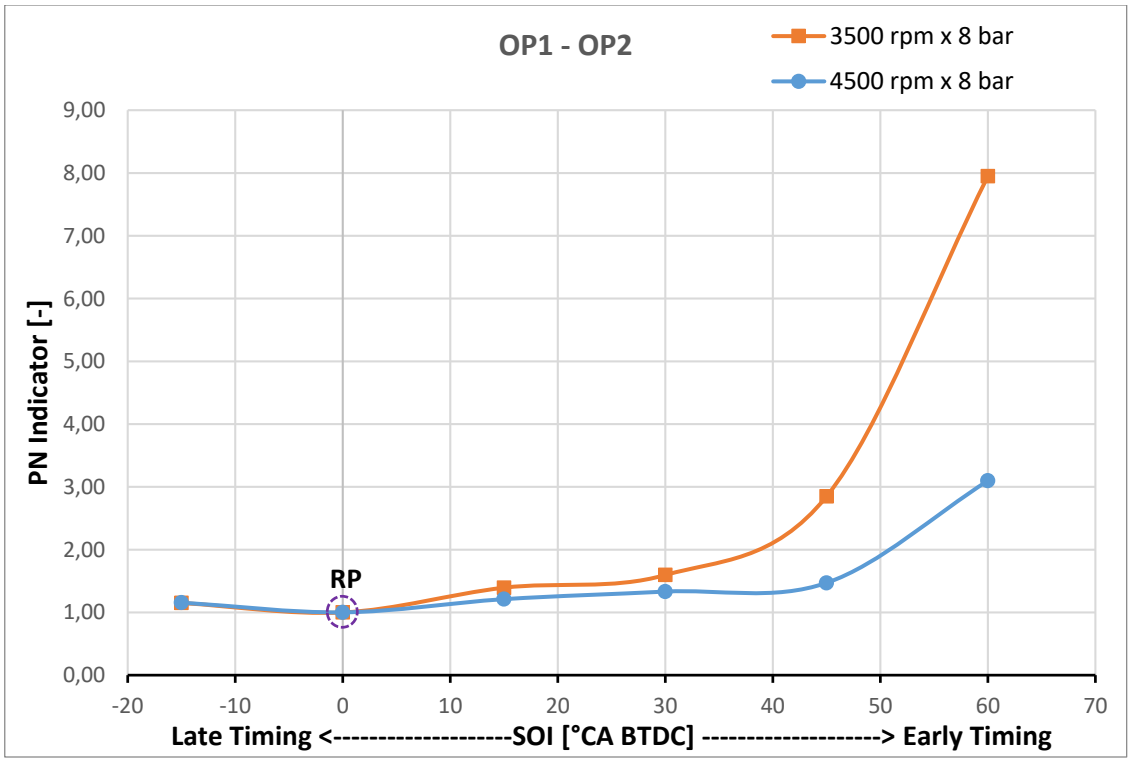

Fig. 3.10 Effects of the SOI on PN at 8 bar and variable speed

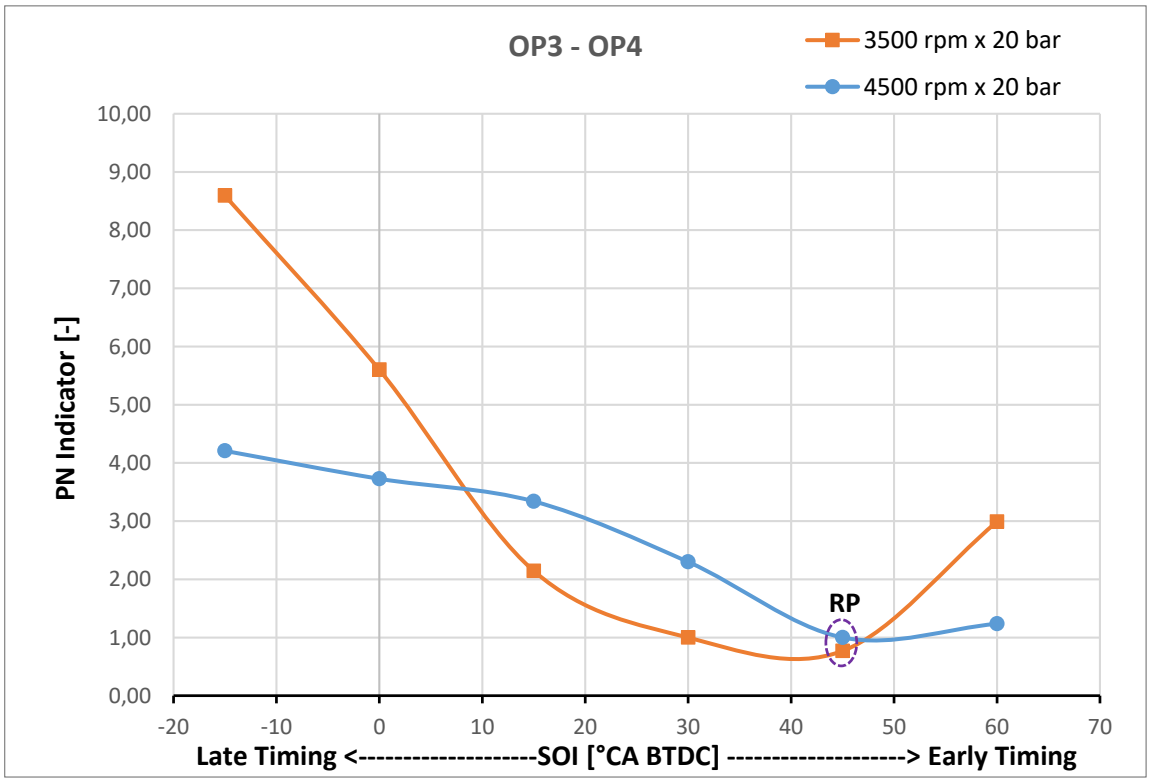

Fig. 3.11 Effects of the SOI on PN at 20 bar and variable speed

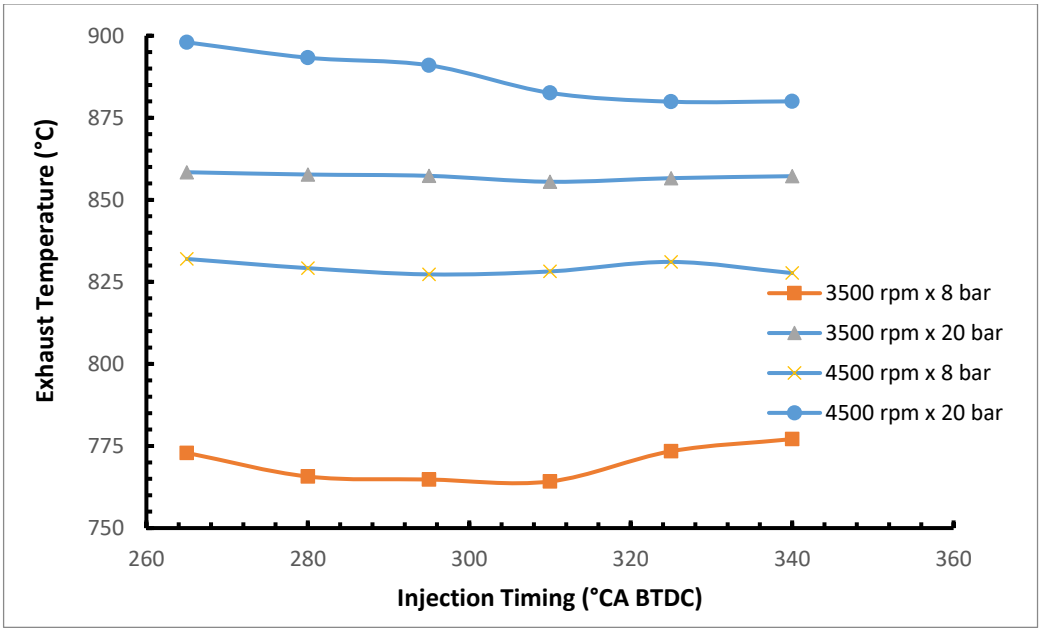

Fig. 3.12 Effects of the SOI on Exhaust Temperature

From the same Figure 3.8, at 3500 rpm x 8 bar there was an increase in PN soot emissions from left to right for the most advanced SOI. In addition from the same figure it's possible to see that for a higher engine load, in this case at 3500 rpm x 20 bar operating point, we have an increase in PN emissions from the most advanced SOI to the most retarded SOI, but in opposite direction compared to the previous operating point (3500 rpm x 8 bar). It's also possible to detect that the increased engine load led to a small reduction in PN emissions for the earlier SOIs, instead for the later SOIs became crucial in terms of emissions. The Figure 3.9 shows that for a fixed engine speed of 4500 rpm, an increased engine load has worsened the impingement effects however leading to a drastic emissions increase especially for later SOIs. The Figure 3.10 shows that for a fixed and light engine load of 8 bar, an increased engine speed led to a good PN reduction for the earlier SOIs due to the mitigation of the impingement effects.

3.1.3.3. Study on the comparison between the two fuel types

In this section are shown the results that were obtained using the two fuel types for all the operating points analyzed in this paper. From the following Figures 3.13 – 3.14 – 3.15 – 3.16, it's possible to detect the gap in PN emissions between the two different gasoline types RON 95 E5 – RON 98, underlining that this last fuel has given better results in terms of PN emissions reduction.

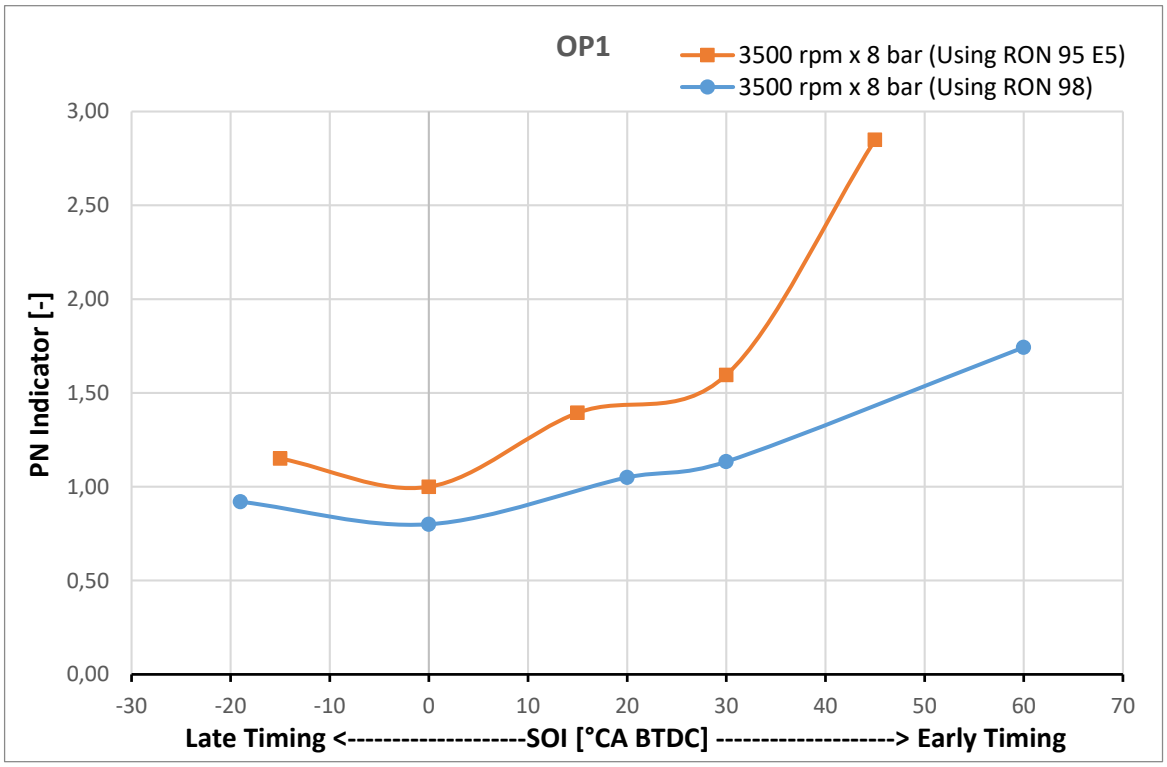

Fig. 3.13 Effects of the SOI and Gasoline Type on PN

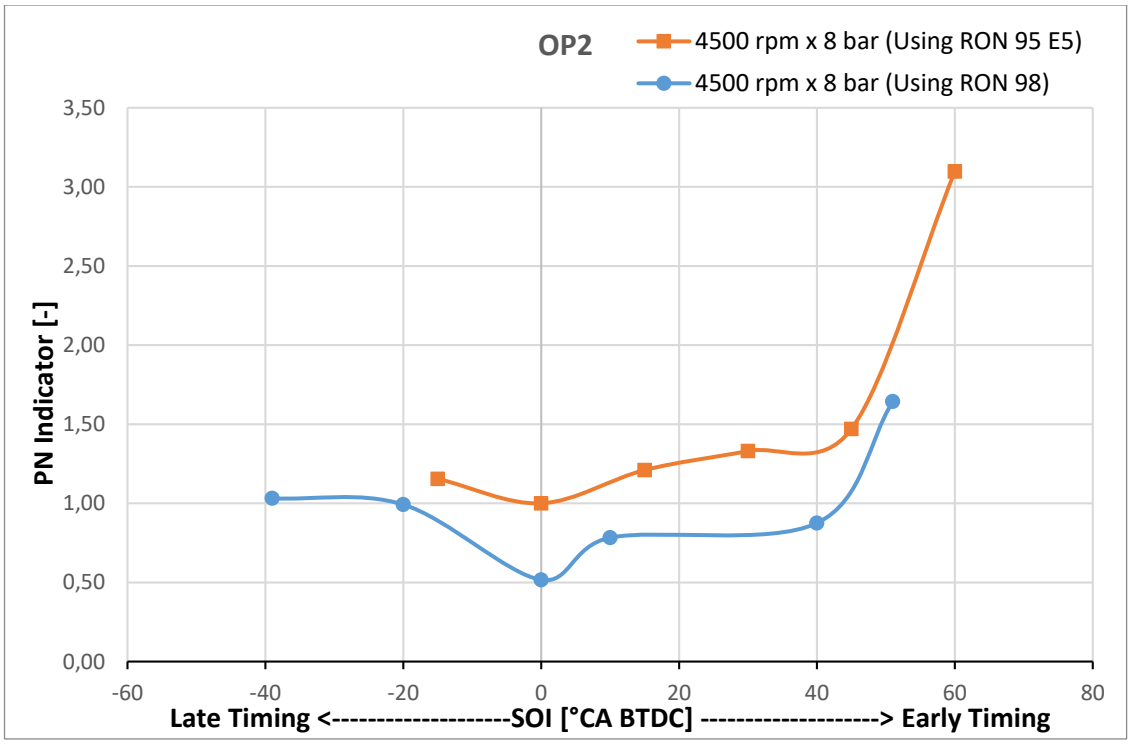

Fig. 3.14 Effects of the SOI and Gasoline Type on PN

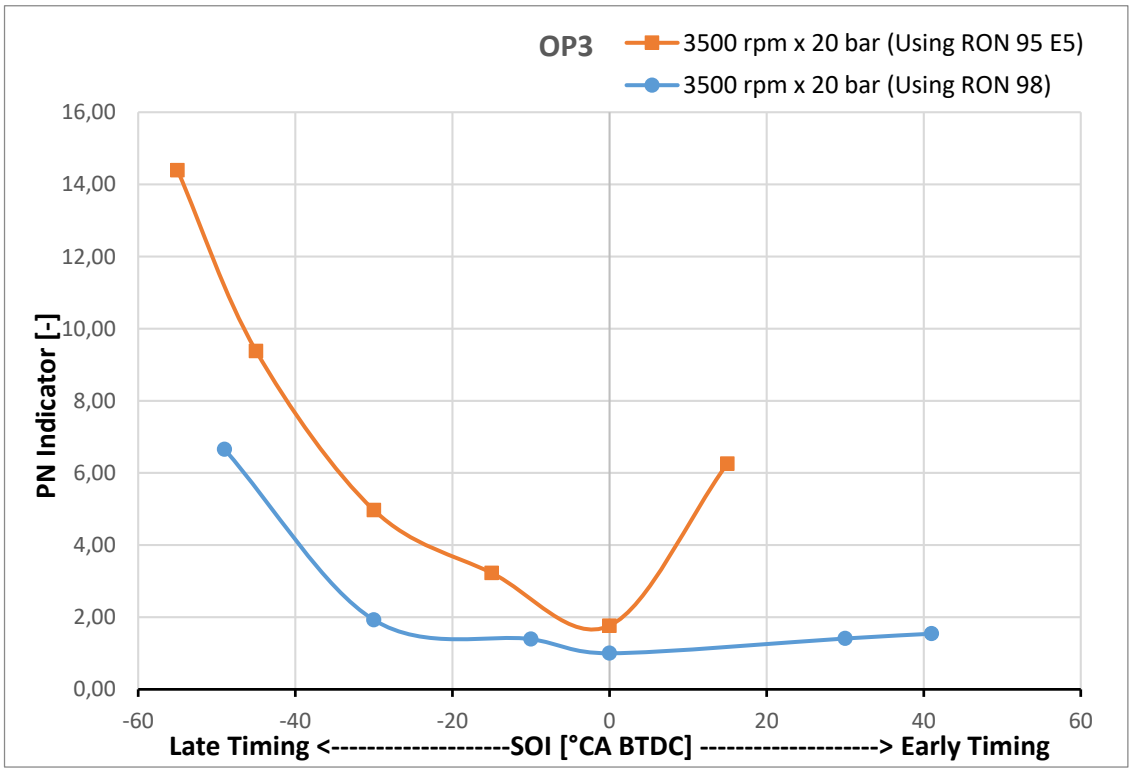

Fig. 3.15 Effects of the SOI and Gasoline Type on PN

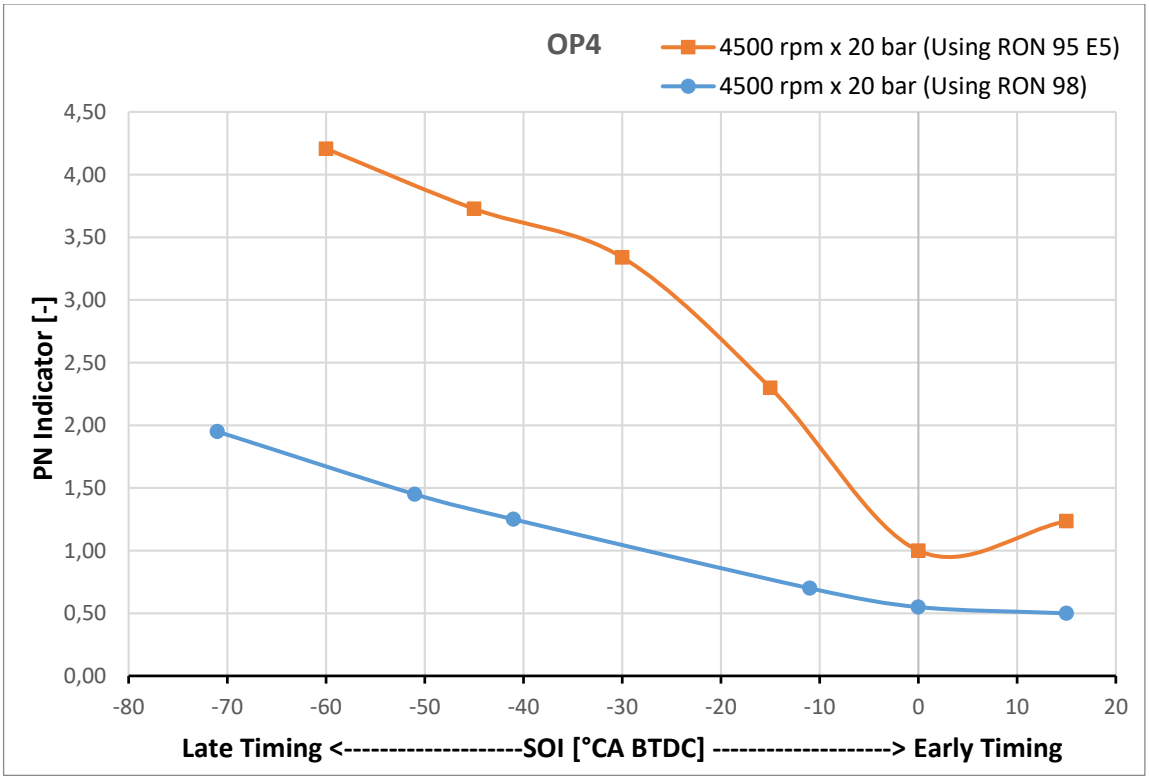

Fig. 3.16 Effects of the SOI and Gasoline Type on PN

From the previous Figures, it's possible to notice that the RON 95 E5 fuel blend has given higher PN emissions than RON 98 for all the operating points tested. In particular when liquid fuel impingement occurs (more probably due to the challenges ethanol can pose to spray formation), then a higher increase in PN emissions compared to fuel RON 98 is reported. In addition, it's interesting to note that while the engine fueled with gasoline RON 98 showed a low sensitivity to SOI in terms of PN emissions, for the engine fueled with gasoline RON 95 E5 a significant sensitivity to SOI is observed.
However, from these last results, it's very important to point out that there's a strong link between PM – PN emissions from GDI engines and the composition and properties of the gasoline. The gap in PN production between the two fuel types tested is essentially due to the key factors listed below in Table 3.6:

TABLE 3.6 – Effects of the gasoline properties on PN emissions

EMISSIONS	RON	MON	AKI	T10	T50	T90	FBP	VP	OOC	OC	EC	SAT
PN	↓	↓	↓	↓	↑	↑	↑	↓	↓	↓	↑	↑

Note: ↓ Negative correlation and ↑Positive correlation

These last effects are in general dominated by the aromatic content of the fuel, but other fuel components and properties notably olefin content, oxygenate content, Sulphur content, fuel volatility, enthalpy of vaporization and boiling points of individual components have significant effect on PM emissions [238]. Some studies have reported that higher octane number (RON) in gasoline reduces PM emission from GDI engines, [239] however care should be taken with this as often octane number is increased by adding aromatic components, which would serve to increase PM emissions. In a recent study of Karavalakis et al. [240], it was found that for GDI engines, Anti-Knock Index (AKI), research octane number (RON), motor octane number (MON) and T10 (the temperature when 10% of a fuel by volume boils away during a distillation test) were negatively correlated with PM mass and PN emissions, indicating that PM and PN emissions decreased as the value of these variables increased. In the same study it was reported that T90 (the temperature when 90% of a fuel by volume boils away during a distillation test), Saturates Concentration and Final Boiling Point (FBP) showed a positive correlation with PM and PN emissions, and that T50 (the temperature when 50% of a fuel by volume boils away during a distillation test) didn't affect the emissions. In addition to this last study, the results of this work show that even T50 could affect the PN emissions with a positive correlation. From the Table 3.6 it's possible to detect that the Oxygen content and the content of other Oxygenates Compounds are negative correlated with PM and PN emissions, in fact it's well known that oxygenated fuels are seen as a potential pathway to reducing well-to-wheel CO_2 emissions from vehicles. Typically oxygenated fuels have higher vapour pressure, significantly higher ΔHvap (kJ/kg stoichiometric mixture), and significantly lower LHVs compared to gasoline. However at high levels of oxygenates, the PN emissions are reduced to almost zero, showing perhaps the dominance of the chemically bonded oxygen.

Fuel volatility has a noticeable impact on PM emissions, [241-242, 243] as a fuel with a lower vapour pressure will be slower to evaporate on injection, and produce a less well prepared mixture leading to higher PN emissions. Fuel with very low volatility impacts on the piston or walls and burns as a pool fire, leading to a significant increase in PN emissions.

On the contrary fuels with very high volatility can flash evaporate on injection, giving a poorly prepared mixture with locally rich zones, again leading to high levels of PN emissions.

With regard to the impact of Ethanol Fuel Blends, it's still not conclusive as to whether the use of Ethanol causes an increase or decrease in particulate emissions from current SI engines.

In fact for GDI engines results show both increases and decreases demonstrating that the details of the combustion system design and engine operating points are very important [244-245-246-247-248-249-250-251-252-253]. It's necessary to highlight that Ethanol has a higher heat of vaporisation and smaller vapour pressure as compared to gasoline which reduces the evaporation of ethanol blended fuel and enhances heterogeneous air-fuel mixture, consequently producing higher PM emissions [254-255].

Similar results were observed by Wang et al. [256] by means of experiments carried out at varying engine load from 3.5-8.5 bar BMEP and 1500 rpm without using a catalyst. They found that an addition of ethanol into gasoline led to higher PN emissions from GDI engine.

Luo et al. [255] studied the impact of ethanol fuel blends in a GDI engine without using a catalyst. They found that ethanol fuel blends increased particle number (PN) concentration at low load engine conditions. However, at high load engine conditions PN concentration decreased.

3.1.3.4. Conclusions

A meticulous and comprehensive investigation of the effect of the injection timing on the particulate number (PN) emissions of a gasoline direct injection engine was realized. The impact of this injection parameter on the test engine was investigated and compared under different engine speeds and load conditions.
From this study, the following conclusions may be drawn:

- Particulates can form due to multiple mechanisms. For a given operating condition, appropriate calibration settings must be chosen to mitigate PN, where one the most dominant control parameter is the injection timing. Injection timing has a strong link with the particulate number emissions due to the impingement effects on the piston and for the little time for mixture mixing, so in all cases it's possible to identify an optimum SOI in terms of PN emissions. In this case, for all engine operating points that were tested, with retarding the injection timing, particulate number (PN) emission decreased to the lowest and then increased. In particular, it was found that the injection timing corresponding to the lowest PN advanced as the engine speed and load were increased.

- Using RON 98 Fuel, it was found that at a fixed engine speed and for advanced SOIs, a higher engine load showed a positive effect on the reduction of PN production regarding the impingement effects on the piston, and that this last gain is less pronounced for higher engine speed. Furthermore, for higher engine load, the rapid increase of the particulate number linked to later SOIs and due to the insufficient time for the mixture mixing became very drastic compared to the lower loads.

- Using RON 98 Fuel, it was found that at a fixed engine load and for advanced SOIs, a higher engine speed showed a positive effect on the reduction of PN production regarding the impingement effects on the piston, and that this last gain is more pronounced for lower engine loads. However, for higher engine speed, the rapid increase of the particulate number linked to later SOIs and due to the insufficient time for the mixture mixing became very pronounced especially if associated with a high engine load.

- From the comparison between the two fuel blends, the gasoline RON 98 has given better results in terms of PN emission reduction. In particular, it was found that while the engine fueled with gasoline RON 98 showed a low sensitivity to SOI in terms of PN emissions, for the engine fueled with gasoline RON 95 E5 a significant sensitivity to SOI is observed. It's also possible to notice that the impingement effects for RON 95 E5 were more marked than RON 98, so leading to higher PN emissions for earlier SOIs. This suggests that for advanced SOIs, the fuel spray impinges on the piston and subsequently burns as a pool fire, leading to higher levels of PN.

In addition and as noted above in Table 3.2, the fuel RON 98 has a higher vapour pressure than fuel RON 95 E5, suggesting that even at the earliest injection timing it could evaporate more quickly before it has chance to impinge on the combustion chamber surfaces. With regard to the fuel RON 95 E5, it was found that the PN emissions linked to the latest SOIs were by far the worst, for the reasons above mentioned.

- The PN emission levels of the GDI engine tested are strongly associated with the fuel physical and chemical properties as well as reported in Table 3.6. In this case and for all the operating points that were tested, the results suggest that the ethanol presence with its low vapour pressure could lead to higher PN emissions when the impingement isn't avoided, so particular attention must be reserved to the calibration of the injection timing.

3.2. Numerical Study on Emissions Reduction using Multiple Injection Strategies

3.2.1. Introduction

GDI technology is now widely used due to its basic advantages in CO2 potential reduction both in homogeneous and stratified operation [257]. The fuel evaporation during intake and compression strokes reduces the cylinder charge temperature, allowing increased compression ratio and higher thermodynamic efficiency. Besides, coupled with other technologies like downsizing and lean-burn operation, additional advantages can be obtained both in terms of performance and fuel consumption. Nevertheless, this technology shows some aspects that can reveal critical for the operation of the engine, in particular dealing with soot emission. In fact, the direct injection strongly reduces the time allowed for the injection phase and the delay between the end of the injection and the spark, so that some droplets of the injected fuel can survive till to the combustion phase, especially considering stratified operation. Another important consequence of direct injection is that the fuel wall film is formed directly in combustion chamber. The mean result of these facts is a higher risk, in respect with PFI engines, of the presence of fuel in liquid phase during combustion. When the flame front surrounds the liquid fuel, inhomogeneous diffusive combustion, with a very low local air-fuel ratio, leads to a significant emission of soot [111]. The control of the amount of liquid portion of fuel in combustion chamber in the combustion phase is a key factor for the good operation of the engine, in particular approaching Euro 6 legislation which imposes a limit in particle emission both in terms of mass and particle number for direct injection spark ignition engines. As a consequence, the engine and the injection systems are even more correlated and the design of the injection system becomes one of the main challenges in GDI engines development. Different configurations for the position and the typology of the injector are possible, and every one of them shows basic pros and cons. Once the injection system design is set, another way to control the injection process is the management of the injection parameters, which are basically the start, the duration and the pressure of the injection. Currently, multiple injections in the same stroke for GDI engines is a well-known practice for catalyst heating during cold start, but it is not so usual for operation in medium and high loads in homogeneous conditions [258]. Moving toward Euro 6d emission standards, one of the main challenges for GDI engines is the reduction of particulate emission in terms of mass and particle number. In fact, in stratified operation, the droplets injected during compression stroke may cause a significant amount of soot production, due to locally non premixed combustion. Besides, in medium and high load, the liner and piston spray impingement is another possible reason of production of soot emission.

In order to meet the required performance and emission targets, focusing on the reduction of particulate emission, a multiple injection strategy can be considered as an option to control both the mixture stratification and the wall impingement.

It's well known that for the engine cold conditions, the use of multiple injection strategies is very common in order to avoid the PN increase emissions, these last linked to the piston impingement effects. In the following work a numerical investigation is performed with the aim of understanding the potential benefits of multiple injections strategies also for engine warm conditions and for an upper middle operating point. The analysis makes use of advanced simulation tool, which allows to select particular strategies to be validated on engine bench. As first step an accurate engine model and calibration setup were realized in order to have a better prediction in terms of performance, fuel consumption and pollutants emissions with regard to the measures obtained from the test bench. As second step an accurate analysis was realized with regard to the comparison between homogeneous and stratified operations, thus leading to important final considerations.

3.2.2. Engine Model and Performance Simulation Software: Gt-Power

3.2.2.1. Gt-Power

It is an engine performance simulation software, developed by Gamma Technologies Inc. GT-Power is used to predict engine performance parameters such as power, torque, airflow, volumetric efficiency, fuel consumption, turbocharger performance and matching, and pumping losses etc. Beyond basic performance predictions, GT-Power includes physical models for extending the predictions to include cylinder and tailpipe-out emissions, intake and exhaust system acoustic characteristics (level and quality), in-cylinder and pipe/manifold structure temperature, measured cylinder pressure analysis, and control system modeling. Standard GT-Power engine models are easily converted to real-time capable models for SiL or HiL simulations [259]. These models may also be included in a full system level simulation within GT-SUITE to provide accurate and physically based engine boundary conditions to the rest of the vehicle.

3.2.2.2. Gt-Suite

GT-Suite can be used for modelling each system independently or for coupling several systems together to make them interact with each other, so more complex systems can be analysed. GT-Suite 17 Calibration of Gasoline Engine in GT-Power Software Environment © 2018, Ashish Kumar, M.Tech. (Power System Engineering), Indian Institute of Technology (Indian School of Mines), Dhanbad (All Rights Reserved) includes functionalities such as GT-COOL, GT-FUEL, GT-CRANK, GT-VTRAIN, GT-DRIVE, GTSUITEmp, and GT-POWER [259].

3.2.2.3. Applications of GT-Power

GT-POWER contains comprehensive and advanced set of models for engine performance analysis, providing many features required to analyse a number of engine configurations and performance characteristics, including:

- Torque and power curves, airflow, volumetric efficiency, fuel consumption, emissions.
- Steady state or full transient analysis, under any driving scenario.
- Turbocharged, supercharged, turbocompound, e-boost, pneumatic assist.
- SI, DI, HCCI and multi-mode combustion, multi-fuel, and multi-pulse injection.
- Infinitely variable valve timing and lift (VVT and VVL).
- Controls system modelling, via built-in controls library or Simulink coupling.

3.2.3. Engine Study and Experimental Setup

3.2.3.1. Engine Study and Experimental Setup

The engine model (designed in GT-Power) which was used for the study of the Gasoline Direct Injection has the specification as given in Table 3.1 and Figure 3.2. This Model (figure 3.17) shows all the components and interconnections of the engine model that was studied and experimented on. The assembly is divided into two parts: main assembly and controller assembly. The controller assembly contains waste gate, ignition control, injector control and CAM template, and the main engine assembly which contains the intake port, air cleaner, turbocharger, intercooler, throttle, actuator, sensor, intake manifold, intake connections, injector, cylinders, engine crank case, exhaust manifold, waste gate, turbine, exhaust port and feedback connections.

The engine model used in this project is a one-dimensional representation of the physical engine taking into account the anomalies and complexities of the operation and operation modes of the engine as stated in section 3.1.2. and subsequent subsections. Object of this study is a depth investigation with regard to the CO, NO_x and PN Emissions for an upper middle operating point (n x PME) 2500 rpm x 21,5 bar. In this case the tables 3.7 – 3.8, the Figures 3.17 – 3.18 – 3.19 show the engine model realized, multiple injection strategies that have been tested and the principal calibration parameters.

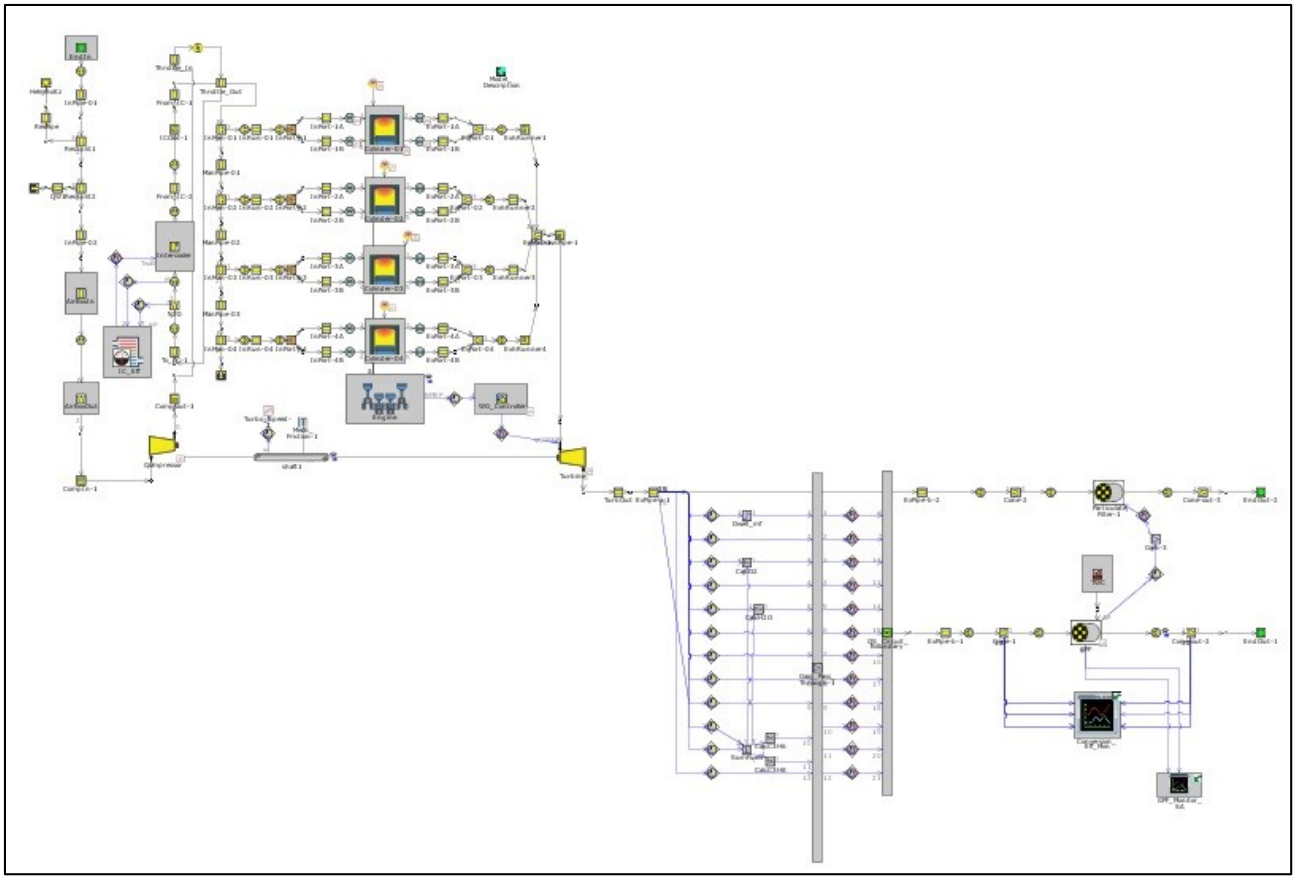

Fig. 3.17 GDI Engine Model in GT-Power

TABLE 3.7 – Multiple Injection Strategies Object of Study

Injected Fuel Mass (mg)	Fuel Injection Pressure (bar)	Injection Strategy Nomenclature	Split Factor %	Spark Timing (ºCA BTDC FIRING)	Intake Valve Opening (ºCA ATDC FIRING)	Exhaust Valve Opening (ºCA ATDC FIRING)
73,3	200	HO1	100	0	310	153
73,3	200	HO2	40 - 60	0	310	153
73,3	200	HO3	40 – 40 - 20	0	310	153
73,3	200	HP2_1	68 - 32	0	310	153
73,3	200	HP2_2	68 - 32	0	310	153
73,3	200	HP2_3	68 - 32	0	310	153

TABLE 3.8 – Main Engine Parameters

Operating Point (Speed x Load)	2500 rpm x 21,5 bar
Air-Fuel Ratio (-)	14,73
Injection Pressure	200 bar
Throttle	99,9 %
Spark Timing	0 °CA BTDC
Inlet Valve Opening	50 °CA BTDC
Inlet Valve Closing	205 °CA ATDC
Exhaust Valve Opening	27 °CA BBDC
Exhaust Valve Closing	10 °CA ATDC
Engine Conditions	Warm
Emission Sampling	Engine Out

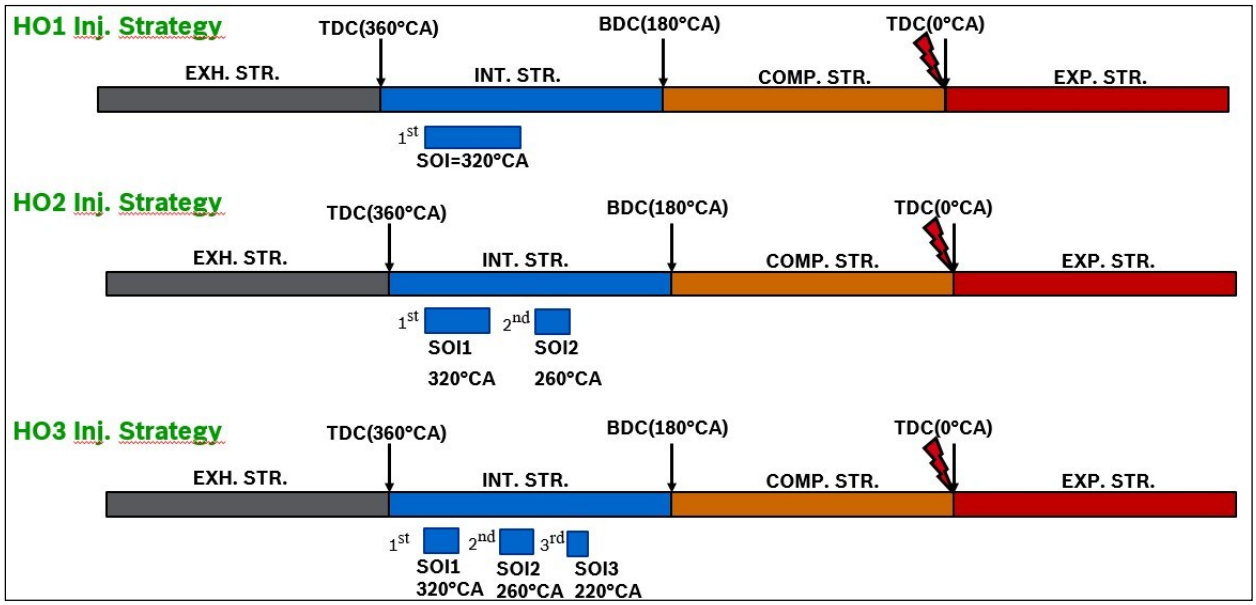

Fig. 3.18 Multiple Injection Strategies in Homogeneous Mode

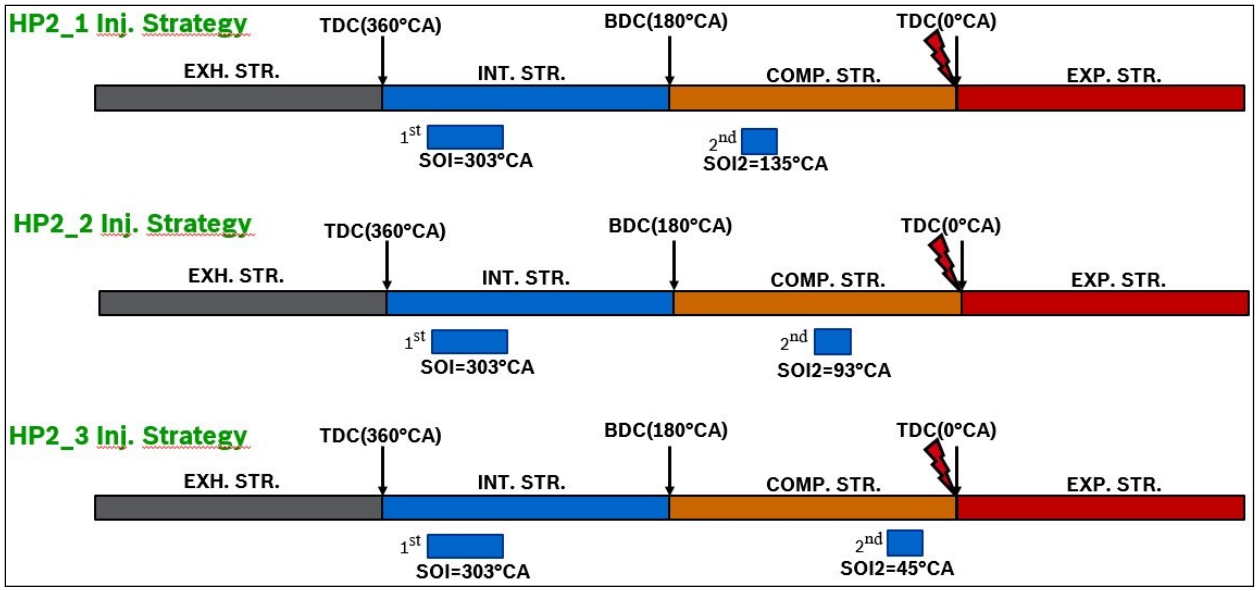

Fig. 3.19 Multiple Injection Strategies in Stratified Mode

3.2.3.2. Results and Analysis for CO and NO_x Emissions

The following figures 3.20 – 3.21, by way of example, show the prediction in terms of NO_x and CO emissions respectively for the HP2_1 and HP2_2 Injection Strategies, and that these values are very aligned with the relative measures from the test bench like follow.

NO_x Emissions from Test Bench: 3168 [ppm]

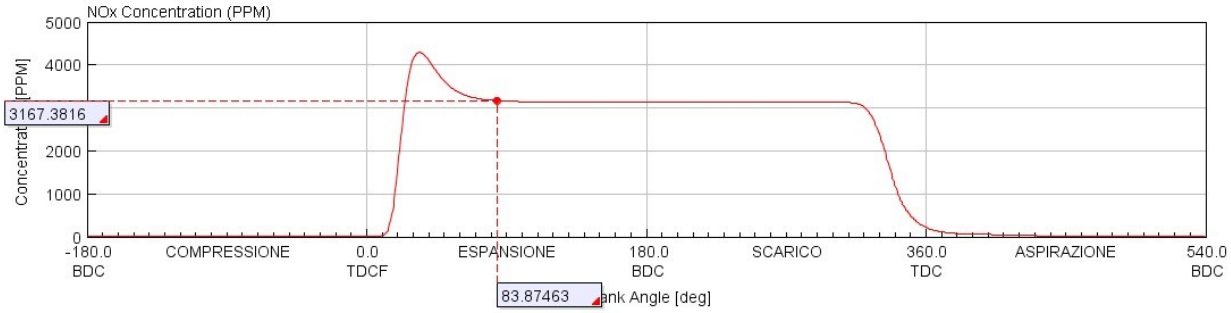

Fig. 3.20 NO_x Emissions from GT-Power using HP2_1 Injection Strategy

CO Emissions from Test Bench: 8300 [ppm]

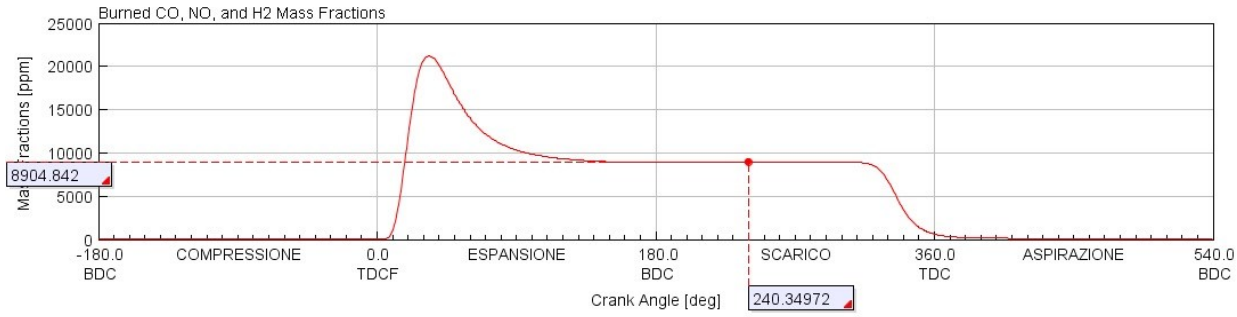

Fig. 3.21 CO Emissions from GT-Power using HP2_2 Injection Strategy

In the following figure (Fig. 3.22) it's possible to evaluate the effects of the Injection Mode on the CO and NO_x Emissions. From the same figure it's possible to detect that the HO3 injection strategy has given the best results in terms of CO emissions, conversely the HP2_3 injection strategy has given the best results in terms of NO_x emissions.

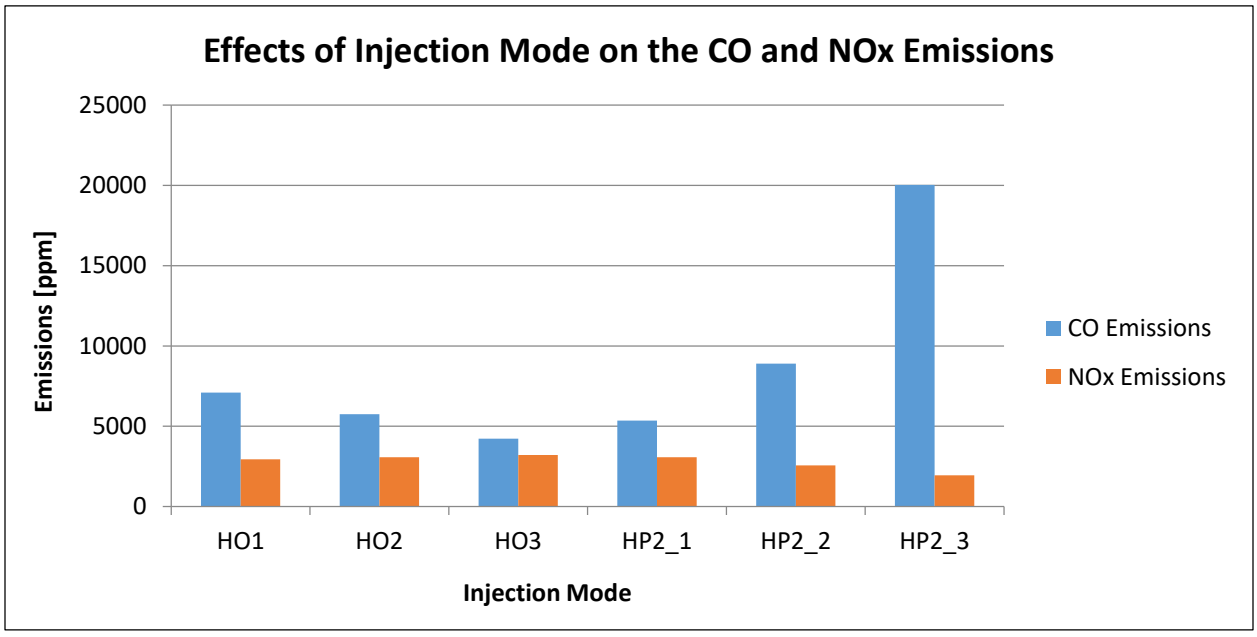

Fig. 3.22 Effects of the Injection Mode for CO and NO_x Emissions

3.2.3.3. Results and Analysis for PN Emissions

The following figure 3.23, by way of example, show the prediction in terms of PN emissions for the HP2_2 Injection Strategy, and that this value is very aligned with the relative measure from the test bench like follow.

PN Emissions from Test Bench: 5,60 E+06 [1/cm^3]

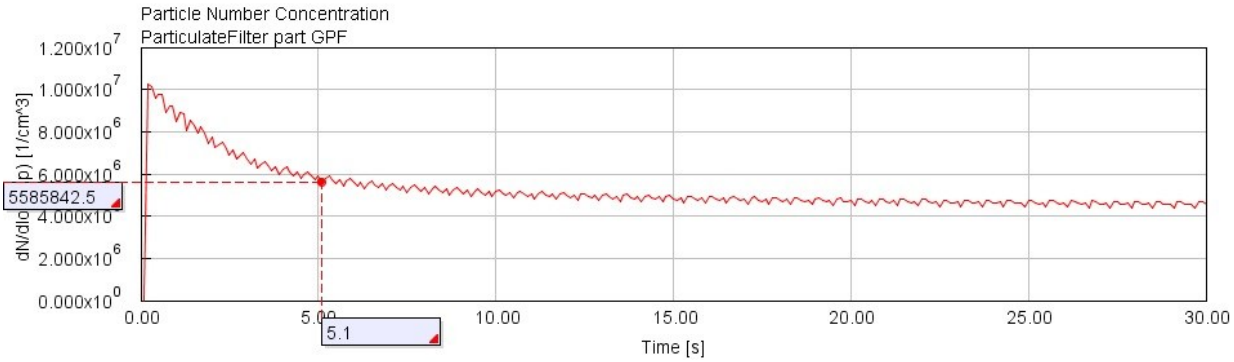

Fig. 3.23 PN Emissions from GT-Power using HP2_2 Injection Strategy

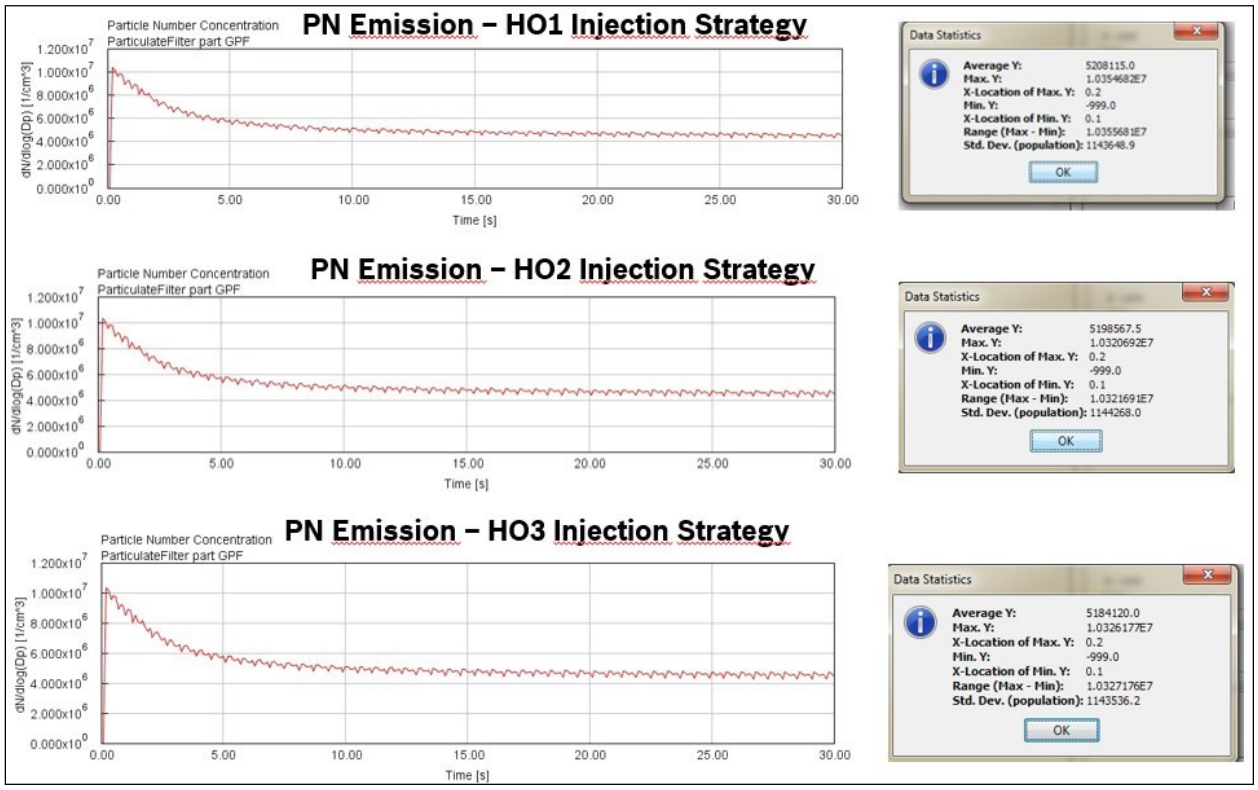

Fig. 3.24 PN Emissions from GT-Power for Homogeneous Mode

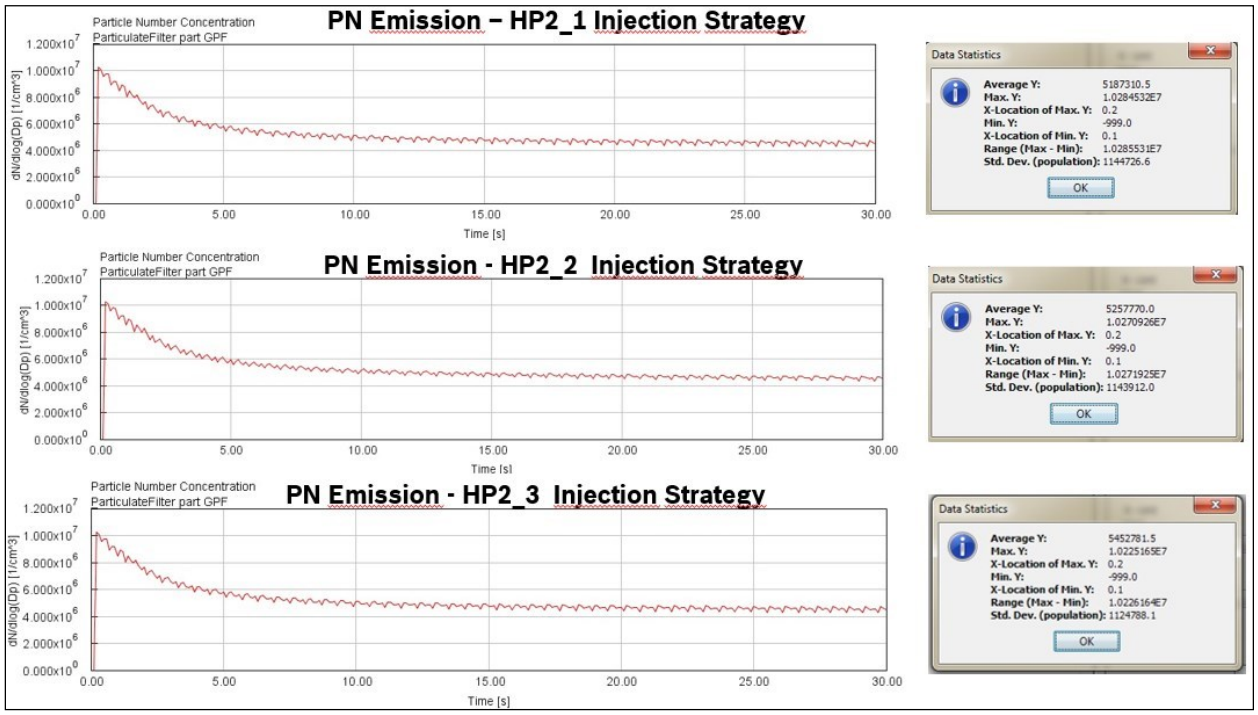

Fig. 3.25 PN Emissions from GT-Power for Stratified Mode

In the following figure (Fig. 3.26) it's possible to evaluate the effects of the Injection Mode on the PN Emissions. From the same figure it's possible to detect that the HO3 injection strategy has given the best results, conversely the HP2_3 injection strategy has given the worst results.

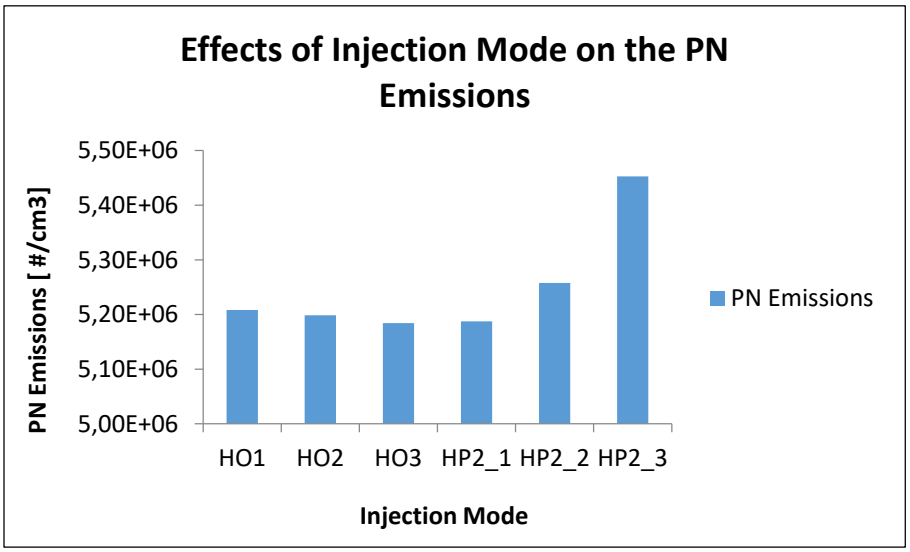

Fig. 3.26 Effects of the Injection Mode on PN Emissions

The following figure shows the effects of the injection mode on the particle number distribution with a particular focus on the particles in Nucleation and Accumulation modes. From the following figure it's possible to detect that the PN in accumulation mode shows low sensitivity with the injection mode. From the same figure it's also possible to observe that the multiple injections strategies in homogeneous mode led a good reduction with regard to the PN in nucleation mode.

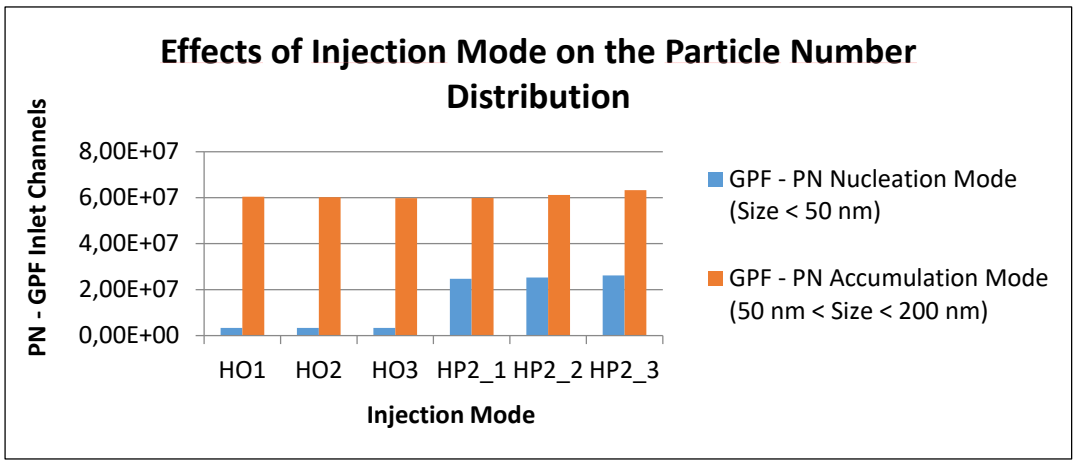

Fig. 3.27 Effects of the Injection Mode on the Particle Number Distribution

3.2.4. Conclusions

In this work a numerical comparison of different multiple injection strategies has been presented and the results of simulation have been analyzed oriented to evaluate the potential advantages of the multiple injection strategies on the soot production.
From this study, the following conclusions may be drawn:

- Multiple Injections in homogeneous mode are better than stratified mode in terms of PN emissions reduction.

- Multiple Injections in homogeneous mode during inlet stroke show a slight decrease of PN emissions compared with the single injection with advantages in terms of wall impingement reduction and mixture preparation respect of a single injection strategy for a medium-high engine load.

- A multiple injection strategy in stratified operation shows that the second injection should be avoided during the middle-late part of the compression stroke to avoid a PN increase.

- The multiple injection strategies in homogeneous mode show a smaller production of the particles in nucleation mode. In this case HO3 injection strategy has given the best results.

- The work allows to assess the effectiveness of a multiple injection strategy in DISI engines also for warm homogeneous operating conditions: the parameters introduced in injection strategy with multiple injection can be considered functional to a more effective control of the soot emission, a reduction of fuel consumption and a more efficient mixture preparation in DISI engines.

- Better CO Emission Reduction using HO3 injection strategy.

- Better NOX Emission Reduction with injections in stratified mode, in particular using HP2_3 Injection Strategy.

- A CFD Analysis would be necessary for quantitative predictions on the HC Emissions.

3.3. Research and Development of Calibration Strategies for Catalyst Heating

3.3.1. Introduction

One of the objectives of emission optimization is to heat the catalyst in the best possible way to its operating temperature so that a good emission conversion can be achieved. This can be achieved through catalyst heating. Normal operation of the engine already involves conflicting objectives from different requirements such as low fuel consumption, emissions (all components simultaneously), smooth running, comfort, available torque, so that every parameterization requires a certain compromise to balance the individual objectives. During catalyst heating, the compromise shifts temporarily such that, for instance, the mass flow and temperature of the exhaust gases are increased at the cost of fuel consumption. This can, for example, be achieved through an intentional worsening of combustion efficiency by retarding the ignition angle. In this way, the gaseous emissions can subsequently be reduced considerably as the catalyst temperature increases. The following figure shows the connection to increased fuel consumption during catalyst heating:

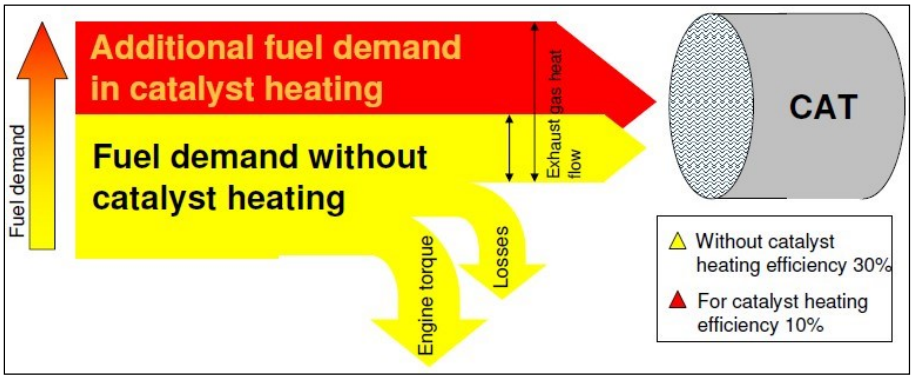

Fig. 3.28 Illustration of the catalyst heating principle

The catalyst temperature can be increased both by hot exhaust gas and by the production of heat inside the catalyst by the conversion of emissions. This requires, however, that the catalyst already is sufficient heated to support conversion and that sufficient incompletely burned components and oxygen are contained in the exhaust gas.
The effectiveness of catalyst heating and the output of emissions can be influenced by many measures. Some of them are always applicable, while some of them only if the engine is equipped with certain actuators.

The following figure gives an overview of the complex relationships.

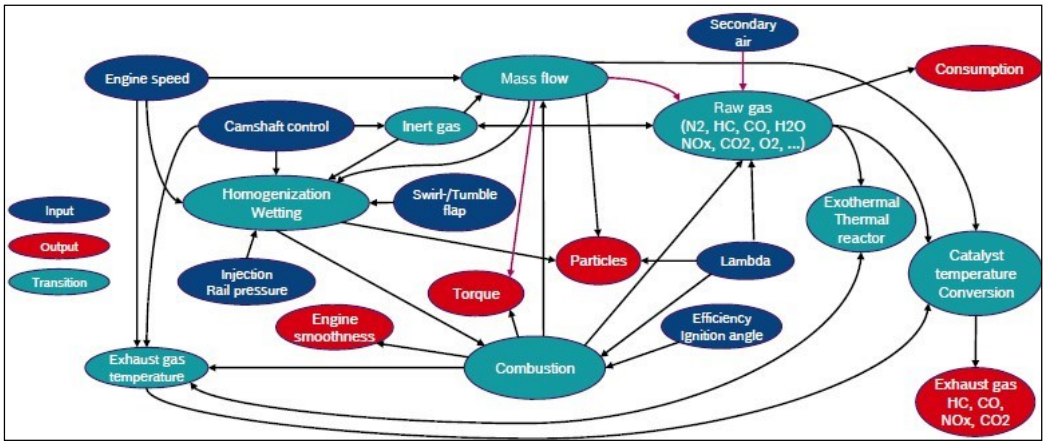

Fig. 3.29 Relationships between control factors and effects during catalyst heating

The principal strategies for the catalyst heating, are the following:

- **Engine Speed Increase:**

  To increase engine speed, the setpoint for the idle speed is increased during catalyst heating. The exhaust gas temperature and the mass flow increase at a higher engine speed. By increasing the engine speed, a larger amount of exhaust gas, which provides the catalyst heating, become available.
  At the same time, fuel consumption increases. The time available for mixture preparation decreases and homogenization can worsen along with smooth running of the engine.

- **Ignition Retarding / Combustion Efficiency:**

  Readjusting the ignition angle decreases the efficiency, which increases the exhaust gas temperature and mass flow, both of which contribute to heating of the catalyst. Fuel consumption increases, engine smoothness decreases.

- **Lambda Target Values:**

  At a slightly lean air-fuel ratio (approx. $\lambda = 1.05$), HC and CO in particular are reduced, and to some degree also NO_x.

- **Camshaft Adjustment:**

  By means of camshaft adjustment, a systematic back flow of hot exhaust gas is achieved (internal exhaust gas recirculation).
  Adjustment of the intake camshaft enhances fuel efficiency and engine smoothness, whereas adjustment of the exhaust camshaft leads to a reduction in raw emissions.

- **Swirl Control Valve:**

  The swirl control valve provides better mixture preparation, which usually allows use of more retarded ignition angles.

- **Start of Initial Injection:**

  Adjustment of the start of initial injection affects mixture preparation and reduces wetting of the cylinder wall or piston face. At the same time, there is a change in engine smoothness and raw emissions.

- **Multiple Injection (Homogeneous Split):**

  With the use of the gasoline direct injection, the amount injected is sometimes distributed over two (or more) injections. During what is called a homogeneous split an initial injection takes place during the suction cycle, the last injection during the compression cycle and, depending on the installation position of the injector, timewise either very close to injection (e.g. approx. 5° before injection in the case of central mounting) or such that a rich mixture can still reach the spark plug (e.g. 80° before TDC in the case of side mounting). This changes mixture preparation and reduces wetting of the cylinder wall or piston face. Engine smoothness is improved, permitting further retarding of the ignition angle.

  The exhaust gas mass flow and temperature can decrease. Particle emissions may decrease, because wetting is reduced, but they may also increase considerably, because the mixture in the combustion chamber is less homogeneous.

- **Rail Pressure:**

  A high rail pressure usually improves homogenization and reduces the wetting.

- **Lambda Split:**

  It’s possible to control the mixture for individual cylinders separately so that the average lambda remains neutral, however some cylinders rich , others lean. More raw emissions are produced, but are so balanced that they can react exothermically with one other in the catalytic converter if it is already converting satisfactorily. The exothermic reaction in the catalytic converter then heats it directly. Fuel consumption increases, engine smoothness decreases. If the cat is not yet warm enough or is very old, emissions increase.

- **Secondary Air Injection:**
  An effect similar to that of lambda splitting is achieved with secondary air. The mixture of all cylinders is set rich and at the same time air is blown into the exhaust system upstream of the catalyst by a pump. The exhaust gas then contains enough oxygen for the HC and CO to be oxidized in the cat exothermically. The major disadvantage is the expense for the secondary air system components, furthermore they must be monitored by diagnosis. At low temperatures, there's a risk that the secondary air system will ice over and cannot be used.

3.3.2. Experimental Setup

For the same engine described in the section 3.1, page 80, a depth study was conducted in order to find a good strategy for the catalyst heating. In this case the principal target has been the reduction of the catalyst conversion window, taking into account the following preliminary considerations:

- Mixture formation and fuel evaporation are hampered by the low temperatures conditions in the combustion chamber.
- The cold piston and cylinder walls cause fuel adsorption and flame quenching.
- Lean engine operation with late ignition and delayed combustion impede engine operation, because of in some cases very lean mixture zones in the combustion chamber deteriorate combustion and even cause flame quenching. This leads to high level of engine roughness and, at worst, misfire.
- High levels of friction losses in the cold engine due to high viscosity of the engine oil at cold temperatures.

In order to obtain a good strategy, the possible manipulable engine parameters could be the following: injection timing for up to three injection pulses, ignition Timing, mass distribution between the injection pulses, intake and exhaust valve timing, idle speed control, global air-fuel ratio, injection pressure, charge motion (tumble/swirl), fuel injection strategy (homogeneous – stratified or purely stratified).The following figure shows the principal catalyst heating strategies implemented by means of the use of multiple injection strategies.

Lean Catalyst Heating

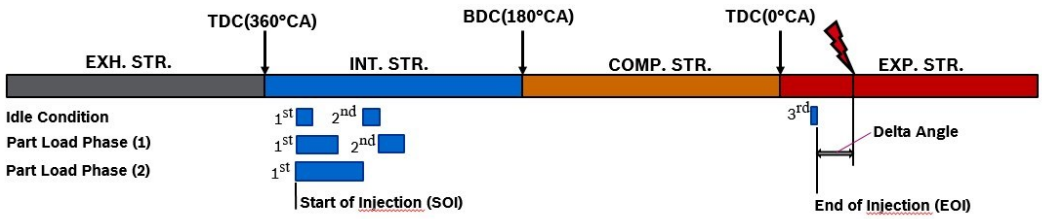

Conditions	Spark Ignition	Injection Mode	Lambda	SOIs	Injection Pressure	Splict Factor
Idle (Cold TWC)	from 10 to 30°CA ATDC	Stratified	1÷1,05	1st: 280 BTDC Firing 2nd: 2,6 ms dwell time from the 1st 3rd: 10 ATDC Firing	120 bar	42,5% 42,5% 15%
Part Load Phase (1) with rl>40% (Hot TWC)	from 5 to 30°CA ATDC	Homogeneous	1÷1,05	1st: 280 BTDC Firing 2nd: 2,6 ms dwell time from the 1st	120 bar to 200 bar	60% 40%
Part Load Phase (2) with low load and over 3000 rpm (Hot TWC)	from 5 to 30°CA ATDC	Homogeneous	1÷1,05	1st: 280 BTDC Firing	120 bar to 200 bar	100%

Fig. 3.30 Catalyst Heating Strategy

With regard to the target of this work, a good strategy has been implemented in order to allow a fast light-off of TWC, this last very useful especially in engine cold conditions. In particular, a meticolous use of the multiple injections combined with delayed ignition angles, allows to have a good PN reduction with a significant reduction of the other main emissions due to an efficient and fast catalyst heating.

3.3.3. Conclusions

Concepts:

- Multiple injections during intake stroke in order to avoid piston impingement and to enhance a good mixture preparation until TDC.

- Small Injection (e.g. 5% of entire fuel mass) after TDC shortly before ignition:
  - create rich mixture near spark plug
  - provide turbulence to the initial flame core (robust inflammation)

- Stable combustion and acceptable engine roughness with late ignition angles achieved by enriched mixture at spark plug.

- Ignition angles up to 20 ÷ 30 °CA aTDC possible → high exhaust gas heat flux to the catalyst.

- Fast Light off of the catalyst with reduced HC, CO and NO_x emissions.

4. Summary and Future Work Suggestions

First of all it's fundamental to underline that GDI engine technology has gained rapid market share since it was introduced in the year 2007 in the U.S. LDGV market. GDI engines provide, on average, 7.5% higher specific power and are, on average, 8% more fuel efficient than PFI vehicles. Manufacturers can choose to either downsize engines or provide the cars with extra horsepower by using GDI. GDI engines are more fuel efficient and powerful due to higher compression ratio and volumetric efficiency, coupled with better control of fuel and air staging. Due to the recent increase in the number of cars fitted with GDI engines in the U.S. market, it is important to study the fuel economy and emission rates of GDI vehicles, and compare them to conventional PFI vehicles. With the increasing adoption of GDI technology, particulate emissions are a focus, and both PN and PM standards are driving the rapid adoption of advanced technologies to mitigate these emissions. This justifies the ongoing research on advanced gasoline vehicle technologies, fuel blends and additives, low-temperature combustion, powertrain electrification, and advanced after-treatment systems. Particulates can form due to multiple mechanisms. An understanding of which mechanisms are present/dominant at a given condition is the first step toward mitigating those mechanisms. The dominant mechanism is a function of engine operating condition, and the operating condition is often dictated by driver input and external conditions such as road grade and ambient temperature. For a given operating condition, appropriate calibration settings must be chosen to mitigate PN, where the dominant control parameters are injection timing, fuel pressure, and multi-injection. In general, a combination of injection timing that avoids piston wetting, high fuel pressure, and the opportunity for multi-injection at certain engine conditions constitutes a good baseline for PN mitigation.

In this PhD thesis a meticulous and comprehensive investigation of the effects of the principal engine parameters on the emissions of a gasoline direct injection engine was realized. A meticulous and comprehensive investigation of the effect of the injection timing on the particulate number (PN) emissions of a gasoline direct injection engine was realized. The impact of this injection parameter on the test engine was investigated and compared under different engine speeds and load conditions. Particulates can form due to multiple mechanisms.
For a given operating condition, appropriate calibration settings must be chosen to mitigate PN, where one the most dominant control parameter is the injection timing. Injection timing has a strong link with the particulate number emissions due to the impingement effects on the piston and for the little time for mixture mixing, so in all cases it's possible to identify an optimum SOI in terms of PN emissions. In this case, for all engine operating points that were tested, with retarding the injection timing, particulate number (PN) emission decreased to the lowest and then increased. In particular, it was found that the injection timing corresponding to the lowest PN advanced as the engine speed and load were increased.
Using RON 98 Fuel, it was found that at a fixed engine speed and for advanced SOIs, a higher engine load showed a positive effect on the reduction of PN production regarding the impingement effects on the piston, and that this last gain is less pronounced for higher engine speed.

Furthermore, for higher engine load, the rapid increase of the particulate number linked to later SOIs and due to the insufficient time for the mixture mixing became very drastic compared to the lower loads. Using RON 98 Fuel, it was found that at a fixed engine load and for advanced SOIs, a higher engine speed showed a positive effect on the reduction of PN production regarding the impingement effects on the piston, and that this last gain is more pronounced for lower engine loads. However, for higher engine speed, the rapid increase of the particulate number linked to later SOIs and due to the insufficient time for the mixture mixing became very pronounced especially if associated with a high engine load. From the comparison between the two fuel blends, the gasoline RON 98 has given better results in terms of PN emission reduction. In particular, it was found that while the engine fueled with gasoline RON 98 showed a low sensitivity to SOI in terms of PN emissions, for the engine fueled with gasoline RON 95 E5 a significant sensitivity to SOI is observed. It's also possible to notice that the impingement effects for RON 95 E5 were more marked than RON 98, so leading to higher PN emissions for earlier SOIs. This suggests that for advanced SOIs, the fuel spray impinges on the piston and subsequently burns as a pool fire, leading to higher levels of PN. In addition and as noted above in Table 3.2, the fuel RON 98 has a higher vapour pressure than fuel RON 95 E5, suggesting that even at the earliest injection timing it could evaporate more quickly before it has chance to impinge on the combustion chamber surfaces. With regard to the fuel RON 95 E5, it was found that the PN emissions linked to the latest SOIs were by far the worst, for the reasons above mentioned. The PN emission levels of the GDI engine tested are strongly associated with the fuel physical and chemical properties as well as reported in Table 3.6. In this case and for all the operating points that were tested, the results suggest that the ethanol presence with its low vapour pressure could lead to higher PN emissions when the impingement isn't avoided, so particular attention must be reserved to the calibration of the injection timing.

With regard to the multiple injections strategies, the results of this work show that Multiple Injections in homogeneous mode are better than stratified mode in terms of PN emissions reduction. Multiple Injections in homogeneous mode during inlet stroke show a slight decrease of PN emissions compared with the single injection with advantages in terms of wall impingement reduction and mixture preparation respect of a single injection strategy for a medium-high engine load. A multiple injection strategy in stratified operation shows that the second injection should be avoided during the middle-late part of the compression stroke to avoid a PN increase. The multiple injection strategies in homogeneous mode show a smaller production of the particles in nucleation mode. In this case HO3 injection strategy has given the best results. The work allows to assess the effectiveness of a multiple injection strategy in DISI engines also for warm homogeneous operating conditions, the parameters introduced in injection strategy with multiple injection can be considered functional to a more effective control of the soot emission, a reduction of fuel consumption and a more efficient mixture preparation in DISI engines. With regard to the other main emissions, the results show a better CO emissions reduction using HO3 injection strategy, and a better NO_X emissions reduction with injections in stratified mode, in particular using HP2_3 Injection Strategy. Finally a CFD analysis would be necessary for quantitative predictions on the HC Emissions.

With regard to the high emissions levels during the engine cold start, an accurate catalyst heating strategy has been implemented and calibrated in order to ensure a fast light off of the TWC. The calibration has concerned the use of the multiple injection strategies, small fuel's injections after TDC shortly before ignition, delayed ignition angles.

Future studies could be useful in order to investigate the impact of the fuel's chemistry on the main emissions, experimentation of new different gasoline/Ethanol or gasoline/Methanol blends, and innovative combustion strategies as for example plasma combustion technology.

References

1. Johnson, T. and Joshi, A., “Review of Vehicle Engine Efficiency and Emissions,” SAE Technical Paper 2018-01-0329, 2018, doi:10.4271/2018-01-0329.

2. Zhao, F., Harrington, D.L., and Lai, M.C., Automotive Gasoline Direct- Injection Engines, (Warrendale: SAE International, 2002).

3. Bandel, W., Fraidl, G., Kapus, P., Sikinger, H. et al., “The Turbocharged GDI Engine: Boosted Synergies for High Fuel Economy Plus Ultra-low Emission,”SAE Technical Paper 2006-01-1266, 2006, doi:10.4271/2006-01-1266.

4. Woldring, D., Landenfeld, T., and Christie, M., “DI Boost: Application of a High Performance Gasoline Direct Injection Concept,” SAE Technical Paper 2007-01-1410, 2007, doi:10.4271/2007-01-1410.

5. Davis, R., Mandrusiak, G., and Landenfeld, T., “Development of the Combustion System for General Motors’ 3.6L DOHC 4V V6 Engine with Direct Injection,” *SAE Int. J. Engines* 1, no. 1 (2008): 85-100, doi:10.4271/2008-01-0132.

6. Davis, S.C., Williams, S.E., Boundy, R.G., and Moore, S., “2016 Vehicle Technologies Market Report,” Oak Ridge National Lab, ORNL, 2016.

7. Zhao, F, M. -C Lai, and D. L Harrington. 1999. “Automotive Spark-Ignited Direct-Injection Gasoline Engines.” Progress in Energy and Combustion Science 25 (5): 437–562. https://doi.org/10.1016/S0360-1285(99)00004-0.

8. Wyszynski, L., Stone, C., and Kalghatgi, G., "The Volumetric Efficiency of Direct and Port Injection Gasoline Engines with Different Fuels," SAE Technical Paper 2002-010839, 2002, https://doi.org/10.4271/2002-01-0839.

9. Kašpar, Jan, Paolo Fornasiero, and Neal Hickey. 2003. “Automotive Catalytic Converters: Current Status and Some Perspectives.” Catalysis Today, Fundamentals of Catalysis and Applications to Environmental Problems, 77 (4): 419–49. https://doi.org/10.1016/S0920-5861(02)00384-X.

10. Golzari, Reza, Yuanping Li, and Hua Zhao. 2016. “Impact of Port Fuel Injection and InCylinder Fuel Injection Strategies on Gasoline Engine Emissions and Fuel Economy.” SAE Technical Paper 2016-01-2174. Warrendale, PA: SAE Technical Paper. https://doi.org/10.4271/2016-01-2174.

11. Anderson, W., Yang, J., Brehob, D., Vallance, J. et al., "Understanding the Thermodynamics of Direct Injection Spark Ignition (DISI) Combustion Systems: An Analytical and Experimental Investigation," SAE Technical Paper 962018, 1996, https://doi.org/10.4271/962018.

12. Oh, Seungmook, Seokhwan Lee, Young Choi, Kern-Yong Kang, Junho Cho, and Kyoungok Cha. 2010. “Combustion and Emission Characteristics in a Direct Injection LPG/Gasoline Spark Ignition Engine.” SAE Technical Paper 2010-01-1461. Warrendale, PA: SAE Technical Paper. https://doi.org/10.4271/2010-01-1461.

13. Na Wu, Wang Xibo, Qiu Xuyun, Tao Lili and Huang Fei, "Research on optimal control for gasoline engine emissions," *World Automation Congress 2012*, Puerto Vallarta, Mexico, 2012, pp. 1-4.

14. Myung, Cha-Lee, Juwon Kim, Kwanhee Choi, In Goo Hwang, and Simsoo Park. 2012. “Comparative Study of Engine Control Strategies for Particulate Emissions from Direct Injection Light-Duty Vehicle Fueled with Gasoline and Liquid Phase Liquefied Petroleum Gas (LPG).” *Fuel* 94 (April): 348–55. https://doi.org/10.1016/j.fuel.2011.10.041.

15. Confer, K., Kirwan, J., and Engineer, N., "Development and Vehicle Demonstration of a Systems-Level Approach to Fuel Economy Improvement Technologies," SAE Technical Paper 2013-01-0280, 2013, https://doi.org/10.4271/2013-01-0280.

16. Su, Jianye, Min Xu, Peng Yin, Yi Gao, and David Hung. 2014. “Particle Number Emissions Reduction Using Multiple Injection Strategies in a Boosted Spark-Ignition Direct-Injection (SIDI) Gasoline Engine.” *SAE International Journal of Engines* 8 (1): 20–29. https://doi.org/10.4271/2014-01-2845.

17. Golzari, Reza, Yuanping Li, and Hua Zhao. 2016. “Impact of Port Fuel Injection and In-Cylinder Fuel Injection Strategies on Gasoline Engine Emissions and Fuel Economy.” SAE Technical Paper 2016-01-2174. Warrendale, PA: SAE Technical Paper. https://doi.org/10.4271/2016-01-2174.

18. Ferguson, Colin R., and Allan Kirkpatrick. 2015. *Internal Combustion Engines: Applied Thermosciences*. Chichester, West Sussex, United Kingdom: Wiley, 2015. *eBook Collection (EBSCOhost)*, EBSCO*host* (accessed April 15, 2018).

19. Kolwich, Greg. 2013. Light-Duty Technology Cost Analysis, Report on Additional Case Studies. EPA-420-R-13-008. Prepared by FEV, Inc. for U.S. Environmental Protection Agency, Ann Arbor, MI.

20. Chen, Longfei, Richard Stone, and Dave Richardson. 2012. “A Study of Mixture Preparation and PM Emissions Using a Direct Injection Engine Fuelled with Stoichiometric Gasoline/Ethanol Blends.” *Fuel* 96 (June): 120–30. https://doi.org/10.1016/j.fuel.2011.12.070.

21. Zimmerman, Naomi, Jonathan M. Wang, Cheol-Heon Jeong, Manuel Ramos, Nathan Hilker, Robert M. Healy, Kelly Sabaliauskas, James S. Wallace, and Greg J. Evans. 2016. “Field Measurements of Gasoline Direct Injection Emission Factors: Spatial and Seasonal Variability.” *Environmental Science & Technology* 50 (4): 2035–43. https://doi.org/10.1021/acs.est.5b04444.

22. Zheng, X., S. Zhang, Y. Wu, K. M. Zhang, X. Wu, Z. Li, and J. Hao. 2017. Characteristics of Black Carbon Emissions from In-Use Light-Duty Passenger Vehicles. *Environ. Pollut.* 231 (December): 348–356. doi:10.1016/j.envpol.2017.08.002.

23. Na Wu, Wang Xibo, Qiu Xuyun, Tao Lili and Huang Fei, "Research on optimal control for gasoline engine emissions," *World Automation Congress 2012*, Puerto Vallarta, Mexico, 2012, pp. 1-4.

24. Graham, Lisa. 2005. “Chemical Characterization of Emissions from Advanced Technology Light-Duty Vehicles.”*Atmospheric Environment* 39 (13): 2385–98. https://doi.org/10.1016/j.atmosenv.2004.10.049.

25. Bonatesta, F., E. Chiappetta, and A. La Rocca. 2014. “Part-Load Particulate Matter from a GDI Engine and the Connection with Combustion Characteristics.” *Applied Energy* 124 (July): 366–76. https://doi.org/10.1016/j.apenergy.2014.03.030.

26. Saliba, Georges, Rawad Saleh, Yunliang Zhao, Albert A. Presto, Andrew T. Lambe, Bruce Frodin, Satya Sardar, et al. 2017. “Comparison of Gasoline Direct-Injection (GDI) and Port Fuel Injection (PFI) Vehicle Emissions: Emission Certification Standards, Cold-Start, Secondary Organic Aerosol Formation Potential, and Potential Climate Impacts.” *Environmental Science & Technology* 51 (11): 6542–52. https://doi.org/10.1021/acs.est.6b06509.

27. Cole, R., Poola, R., and Sekar, R., "Exhaust Emissions of a Vehicle with a Gasoline Direct-Injection Engine," SAE Technical Paper 982605, 1998, https://doi.org/10.4271/982605.

28. Maricq, M. Matti, Diane H. Podsiadlik, and Richard E. Chase. 1999. “Examination of the Size-Resolved and Transient Nature of Motor Vehicle Particle Emissions.” *Environmental Science & Technology* 33 (10): 1618–26. https://doi.org/10.1021/es9808806.

29. Graham, Lisa. 2005. “Chemical Characterization of Emissions from Advanced Technology Light-Duty Vehicles.” *Atmospheric Environment* 39 (13): 2385–98. https://doi.org/10.1016/j.atmosenv.2004.10.049.

30. Price, P., Stone, R., Collier, T., and Davies, M., "Particulate Matter and Hydrocarbon Emissions Measurements: Comparing First and Second Generation DISI with PFI in Single Cylinder Optical Engines," SAE Technical Paper 2006-01-1263, 2006, https://doi.org/10.4271/2006-01-1263.

31. Braisher, M., Stone, R., and Price, P., "Particle Number Emissions from a Range of European Vehicles," SAE Technical Paper 2010-01-0786, 2010, https://doi.org/10.4271/2010-01-0786.

32. Zhan, R., Eakle, S., and Weber, P., "Simultaneous Reduction of PM, HC, CO and NOx Emissions from a GDI Engine," SAE Technical Paper 2010-01-0365, 2010, https://doi.org/10.4271/2010-01-0365.

33. Chan, Tak W., Eric Meloche, Joseph Kubsh, Deborah Rosenblatt, Rasto Brezny, and Greg Rideout. 2012. “Evaluation of a Gasoline Particulate Filter to Reduce Particle Emissions from a Gasoline Direct Injection Vehicle.” *SAE International Journal of Fuels and Lubricants* 5 (3): 1277–90. https://doi.org/10.4271/2012-01-1727.

34. Spiess, Stephanie, Ka-Fai Wong, Joerg-Michael Richter, and Raoul Klingmann. 2013. “Investigations of Emission Control Systems for Gasoline Direct Injection Engines with a Focus on Removal of Particulate Emissions.” *Topics in Catalysis* 56 (1–8): 434–39. https://doi.org/10.1007/s11244-013-9992-6.

35. Su, Jianye, Min Xu, Peng Yin, Yi Gao, and David Hung. 2014. “Particle Number Emissions Reduction Using Multiple Injection Strategies in a Boosted Spark-Ignition Direct-Injection (SIDI) Gasoline Engine.” *SAE International Journal of Engines* 8 (1): 20–29. https://doi.org/10.4271/2014-01-2845.

36. Zhan, R., Eakle, S., and Weber, P., "Simultaneous Reduction of PM, HC, CO and NOx Emissions from a GDI Engine," SAE Technical Paper 2010-01-0365, 2010, https://doi.org/10.4271/2010-01-0365.

37. Chan, Tak W., Eric Meloche, Joseph Kubsh, Deborah Rosenblatt, Rasto Brezny, and Greg Rideout. 2012. “Evaluation of a Gasoline Particulate Filter to Reduce Particle Emissions from a Gasoline Direct Injection Vehicle.” *SAE International Journal of Fuels and Lubricants* 5 (3): 1277–90. https://doi.org/10.4271/2012-01-1727.

38. Bahreini, R., J. Xue, K. Johnson, T. Durbin, D. Quiros, S. Hu, T. Huai, A. Ayala, and H. Jung. 2015. Characterizing Emissions and Optical Properties of Particulate Matter from PFI and GDI Light-Duty Gasoline Vehicles. *J. Aerosol Sci.* 90 (December): 144–153. doi:10.1016/j.jaerosci.2015.08.011.

39. Short, D., D. Vu, V. Chen, C. Espinoza, T. Berte, G. Karavalakis, T. D. Durbin, and A. Asa-Awuku. 2017. Understanding Particles Emitted from Spray and Wall-Guided Gasoline Direct Injection and Flex Fuel Vehicles Operating on Ethanol and Iso-Butanol Gasoline Blends. *Aerosol Sci. Technol.* 51 (3): 330–341. doi:10.1080/02786826.2016.1265080.

40. Seo, J., H. Y. Kim, S. Park, S. C. James, and S. S. Yoon. 2016. Experimental and Numerical Simulations of Spray Impingement and Combustion Characteristics in Gasoline Direct Injection Engines under Variable Driving Conditions. *Flow Turbul. Combust.* 96 (2): 391–415. doi:10.1007/s10494-015-9678-1.

41. Heck, Ronald M., Robert J. Farrauto, and Suresh T. Gulati. c2009. *Catalytic Air Pollution Control: Commercial Technology*. 3rd ed. Hoboken, N.J.: John Wiley.

42. Spiess, Stephanie, Ka-Fai Wong, Joerg-Michael Richter, and Raoul Klingmann. 2013. "Investigations of Emission Control Systems for Gasoline Direct Injection Engines with a Focus on Removal of Particulate Emissions." *Topics in Catalysis* 56 (1–8): 434–39. https://doi.org/10.1007/s11244-013-9992-6.

43. Minjares, R., and F. P. Sanchez. 2011. Estimated Cost of Gasoline Particulate Filters. Working Paper 2011–8. Washington, DC: International Council on Clean Transportation.

44. Wang, J. M., Jeong, C.-H., Zimmerman, N., Healy, R. M., Wang, D. K., Ke, F., and Evans, G. J. 2015. "Plume-based analysis of vehicle fleet air pollutant emissions and the 120 contribution from high emitters." *Atmos. Meas. Tech.*, 8, 3263-3275, https://doi.org/10.5194/amt-8-3263-2015.

45. Zimmerman, Naomi, Jonathan M. Wang, Cheol-Heon Jeong, Manuel Ramos, Nathan Hilker, Robert M. Healy, Kelly Sabaliauskas, James S. Wallace, and Greg J. Evans. 2016. "Field Measurements of Gasoline Direct Injection Emission Factors: Spatial and Seasonal Variability." *Environmental Science & Technology* 50 (4): 2035–43. https://doi.org/10.1021/acs.est.5b04444.

46. Adel Ahmed Abdel-Rahman Alexandria University, 1998. "On the emission from internal combustion engines: A review."

47. Way K. Cheng, Douglas Hamrin, John B. Heywood, Simone Hochgreb, Kyoungdoug Min, Michael Norris. 1993. “An overview of Hydrocarbons Emissions Mechanisms in Spark-Ignition Engines.

48. Lozhkina O. V., Lozhkin V. N. 2016. “Estimation of nitrogen oxides emissions from petrol and diesel passenger cars by means of on-board monitoring: Effect of vehicle speed, vehicle technology, engine type on emission rates.

49. C. Vovelle. Pollutants from Combustion: Formation and Impact on Atmospheric Chemistry. Nato Science Series C:. Springer Netherlands, 2013.

50. B M Masum, H H Masjuki, M A Kalam, I M Rizwanul Fattah, S M Palash, and M J Abedin. Effect of ethanol–gasoline blend on NOx emission in SI engine. Renewable and Sustainable Energy Reviews, 24: 209–222, 2013.

51. A.Y. Watson, R.R. Bates, D. Kennedy, and H.E. Institute. Air Pollution, the Automobile, and Public Health. National Academies Press, 1988.

52. Maricq, M.M., Szente, J.J., Harwell, A.L., and Loos, M.J., “Impact of Aggressive Drive Cycles on Motor Vehicle Exhaust PM Emissions,” *Journal of Aerosol Science* 113 (2017): 1-11.

53. Xue, J., Li, Y., Wang, X., Durbin, T.D. et al., “Comparison of Vehicle Exhaust Particle Size Distributions Measured by SMPS and EEPS during Steady-State Conditions,” *Aerosol Science and Technology* 49, no. 10 (2015): 984–996, doi:10.1080/02786826.2015.1088146.

54. http://www.acea.be/publications/article/access-to-euro-6-rde-monitoringdata.

55. https://ec.europa.eu/clima/sites/clima/files/transport/vehicles/docs/2011_pems_jrc_6239_en.pdf.

56. Commission Regulation (EU) 2017/1151, June 1, 2017, http://publications.europa.eu/resource/cellar/7d1c640d-62d8-11e7-b2f2-01aa75ed71a1.0006.01/DOC_1.

57. Commission Regulation (EU) 2017/1154, June 7, 2017, http://eur-lex.europa.eu/legal-content/EN/TXT/PDF/?uri=CELEX:32017R1154&from=EN.

58. Joint Research Center, “PMP IWG Progress Report,” Informal Document GRPE-75-17, 2016, http://www.unece.org/trans/main/wp29/wp29wgs/wp29grpe/grpeinf75.html.

59. Piock, W., Hoffmann, G., Berndorfer, A., Salemi, P. et al., “Strategies Towards Meeting Future Particulate Matter Emission Requirements in Homogeneous Gasoline Direct Injection Engines,” *SAE Int. J. Engines* 4, no. 1 (2011): 1455-1468, doi:10.4271/2011-01-1212.

60. Pritchard, J. and Cheng, W., “Effects of Secondary Air on the Exhaust Oxidation of Particulate Matters,” *SAE Int. J. Engines* 8, no. 3 (2015): 1088- 1097, doi:10.4271/2015-01-0886.

61. Whitaker P., Kapus, P., Ogris, M., and Hollerer, P., “Measures to Reduce Particulate Emissions from Gasoline DI engines,” *SAE Int. J. Engines* 4, no. 1 (2011): 1498-1512, doi:10.4271/2011-01-1219.

62. McNeil, S., Adamovicz, P., and Lieder, F. “Bosch Motronic MED9.6.1 EMS Applied on a 3.6L DOHC 4V V6 Direct Injection Engine,” SAE Technical Paper 2008-01-0133, 2008, doi:10.4271/2008-01-0133.

63. Peer, J., Backes, F., Sauerland, H., Hartl, M. et al., “Development of a High Turbulence, Low Particle Number, High Injection Pressure Gasoline Direct Injection Combustion System,” *SAE Int. J. Engines* 9, no. 4 (2016): 2301-2311,doi:10.4271/2016-01-9046.

64. Smith, S. and Imoehl, W., “Measurement and Control of Fuel Injector Deposits in Direct Injection Gasoline Vehicles,” SAE Technical Paper 2013-01-2616, 2013, doi:10.4271/2013-01-2616.

65. Aradi, A., Imoehl, B., Avery, N., Wells, P. et al., “The Effect of Fuel Composition and Engine Operating Parameters on Injector Deposits in a High-Pressure Direct Injection Gasoline (DIG) Research Engine,” SAE Technical Paper 1999-01-3690, 1999, doi:10.4271/1999-01-3690.

66. Wen, Y., Wang, Y., Fu, C., Deng, W. et al., “The Impact of Injector Deposits on Spray and Particulate Emission of Advanced Gasoline Direct Injection Vehicle,” SAE Technical Paper 2016-01-2284, 2016, doi:10.4271/2016-01-2284.

67. Wang, C., Xu, H., Herreros, J.M., Wang, J. et al., “Impact of Fuel and Injection System on PM Emissions from a DISI Engine,” *Appl. Energy* 132 (2014): 178e91.

68. Prakash, A., Nelson, E., Jones, A., Macias, J. et al., “Particulate Mass Reduction and Clean-up of DISI Injector Deposits via Novel Fuels Additive Technology,”SAE Technical Paper 2014-01-2847, 2014, doi:10.4271/2014-01-2847.

69. Prakash, A., Aradi, A., Imoehl, W., and Armitage, P.,“Impact of Injector Design and Fuel Composition on Particulate Number Generation,” SAE Technical Paper 2017-01-2395, 2017, doi:10.4271/2017-01-2395.

70. Ketterer, J.E. and Cheng, W.K., “On the Nature of Particulate Emissions from DISI Engines at Cold-Fast-Idle,” *SAE Int. J. Engines* 7, no. 2 (2014): 986-994,doi:10.4271/2014-01-1368.

71. Heiduk, T., Kuhn, M., Stichlmeir, M., and Unselt, F., “The New 1.8L TFSI Engine from Audi Part 2: Mixture Formation, Combustion Method and Turbocharging,”*MTZ* 72, no. 7-8 (2011): 58-64, doi:10.1365/s38313-011-0078-1.

72. Fujimoto, Y., “Introduction of Variable Compression Turbo Engine,” *Advanced Clean Cars Symposium: The Road Ahead*, September 27-28, 2016.

73. Schenk, C. and Dekraker, P., “Potential Fuel Economy Improvements from the Implementation of cEGR and CDA on an Atkinson Cycle Engine,” SAE Technical Paper 2017-01-1016, 2017, doi:10.4271/2017-01-1016.

74. Hedge, M., Weber, P., Gingrich, J., Alger, T. et al., “Effect of EGR on Particle Emissions from a GDI Engine,” *SAE Int. J. Engines* 4, no. 1 (2011): 650-666, doi:10.4271/2011-01-0636.

75. Fischer, M., Kreutziger, P., Sun, Y., and Kotrba, A., “Clean EGR for Gasoline Engines – Innovative Approach to Efficiency Improvement and Emissions Reduction Simultaneously,” SAE Technical Paper 2017-01-0683, 2017, doi:10.4271/2017-01-0683.

76. Parks, J.E., Storey, J.M.E., Prikhodko, V.Y., Debusk, M.M. et al., “Filter-based control of particulate matter from a lean gasoline direct injection engine,” SAE Technical Paper 2016-01-0937, 2016, doi:10.4271/2016-01-0937.

77. Dempsey, A.B., Curran, S.J., and Wagner, R.M. “A Perspective on the Range of Gasoline Compression Ignition Combustion Strategies for High Engine Efficiency and Low NOx and Soot Emissions: Effects of In-Cylinder Fuel Stratification,” *Int. J. Eng. Res.* 2016: 1-21.

78. Sellnau, M., “Aftertreatment for Low-Temperature Combustion and US Tier3-Bin 30 Emissions,” presented at *the SAE 2017 Light Duty Emissions Control Symposium*, Washington DC, January 2017.

79. http://www2.mazda.com/en/publicity/release/2017/201708/170808a.html.

80. Yamada, H., Inomata, S., and Tanimoto, H., “Particle and VOC Emissions from Stoichiometric Gasoline Direct Injection Vehicles and Correlation between Particle Number and Mass Emissions,” *Emiss. Control Sci. Technol.* 3 (2017): 135–141.

81. Zinola, S., Raux, S., and Leblanc, M., “Persistent Particle Number Emissions Sources at the Tailpipe of Combustion Engines,” SAE Technical Paper 2016-01- 2283, 2016, doi:10.4271/2016-01-2283.

82. Nicholas, M., Tal, G., and Turrentine, T., *Advanced Clean Cars Symposium*, https://www.arb.ca.gov/msprog/consumer_info/advanced_clean_cars/pev_data_from_uc_davis_household_study_first_year_michael_nicholas.pdf,2016.

83. AECC, "Real-Driving Emissions Test Programme Results from a Plug-In Hybrid Electric Vehicle (PHEV),"*13th Integer Emissions Summit*, Dresden,June 2017.

84. Leach, F., Stone, R., and Richardson, D., "The Influence of Fuel Properties on Particulate Number Emissions from a Direct Injection Spark Ignition Engine,"SAE Technical Paper 2013-01-1558, 2013, doi:10.4271/2013-01-1558.

85. Khalek, I., Bougher, T., and Jetter, J., "Particle Emissions from a 2009 Gasoline Direct Injection Engine Using Different Commercially Available Fuels," *SAE Int. J. Fuels Lubr.* 3, no. 2 (2010): 623-637, doi:10.4271/2010-01-2117.

86. Butler, A., Sobotowski, R., Hoffman, G., and Machiele, P., "Influence of Fuel PM Index and Ethanol Content on Particulate Emissions from Light-Duty Gasoline Vehicles," SAE Technical Paper 2015-01-1072, 2015,doi:10.4271/2015-01-1072.

87. Qin, J., Li, X., and Pei, Y., "Effects of Combustion Parameters and Lubricating Oil on Particulate Matter Emissions from a Turbo-Charged GDI Engine Fueled with Methanol/Gasoline Blends," SAE Technical Paper 2014-01-2841,2014, doi:10.4271/2014-01-2841.

88. Tanaka, D., Uchida, R., Noda, T., Kolbeck, A. et al., "Effects of Fuel Properties Associated with In-Cylinder Behavior on Particulate Number from a Direct Injection Gasoline Engine," SAE Technical Paper 2017-01-1002, 2017,doi:10.4271/2017-01-1002.

89. Kim, Y., Kim, Y., Kang, J., Jun, S. et al., "Fuel Effect on Particle Emissions of a Direct Injection Engine," SAE Technical Paper 2013-01-1559, 2013, doi:10.4271/2013-01-1559.

90. Storey, J., Lewis, S., Szybist, J., Thomas, J. et al., "Novel Characterization of GDI Engine Exhaust for Gasoline and Mid-Level Gasoline-Alcohol Blends,"*SAE Int. J. Fuels Lubr.* 7, no. 2 (2014): 571-579, doi:10.4271/2014-01-1606.

91. Aikawa, K., Sakurai, T., and Jetter, J. J., "Development of a Predictive Model for Gasoline Vehicle Particulate Matter Emissions," SAE Technical Paper 2010-01-2115, 2010, doi:10.4271/2010-01-2115.

92. Karavalakis, G., Short, D., Vu, D., Russell, R. et al., "Evaluating the Effects of Aromatics Content in Gasoline on Gaseous and Particulate Matter Emissions from SI-PFI and SIDI Vehicles," *Environ. Sci. Technol.* 49 (2015):7021−7031.

93. Yamada, H., Inomata, S., and Tanimoto, H., "Particle and VOC Emissions from Stoichiometric Gasoline Direct Injection Vehicles and Correlation between Particle Number and Mass Emissions," *Emiss. Control Sci. Technol.* 3 (2017): 135–141.

94. Chan, T.W., Saffaripour, M., Liu, F., Hendren, J. et al., "Characterization of Real Time Particle Emissions from a Gasoline Direct Injection Vehicle Equipped with a Catalyzed Gasoline Particulate Filter during Filter Regeneration," *Emiss. Control Sci. Technol.* 2, no. 2 (2016): 75-88.

95. Zhu, R., Hu, J., Bao, X., He, L. et al., "Tailpipe Emissions from Gasoline Direct Injection (GDI) and Port Fuel Injection (PFI) Vehicles at Both Low and High Ambient Temperatures,"*Environmental Pollution* 216 (2016): 223-234.

96. Murad, S., Camm, J., Davy, M., and Stone, R., "Spray Behaviour and Particulate Matter Emissions with M15 Methanol/Gasoline Blends in a GDI Engine," SAE Technical Paper 2016-01-0991, 2016, doi:10.4271/2016-01-0991.

97. Chan, T., "The Impact of Isobutanol and Ethanol on Gasoline Fuel Properties and Black Carbon Emissions from Two Light-Duty Gasoline Vehicles," SAE Technical Paper 2015-01-1076, 2015, doi:10.4271/2015-01-1076.

98. Hergueta, C., Bogarra, M., Tsolakis, A., Essa, K. et al., "Butanol-Gasoline Blend and Exhaust Gas Recirculation, Impact on GDI Engine Emissions," *Fuel* 208 (2017): 662–672.

99. Joshi, A., "Progress and Outlook on Gasoline Vehicle Aftertreatment Systems,"*Johnson Matthey Technol. Rev.* 61, no. 4 (2017): 311.

100. B. Hamilton and Robert Falkiner. Fuels and Lubricants Handbook: Motor Fuels. 2003

101. Derek Splitter, Alexander Pawlowski, and Robert Wagner. A historical analysis of the co evolution of gasoline octane number and spark-ignition engines. Frontiers in Mechanical Engineering, 1(16), 2016.

102. Georgios Karavalakis, Daniel Short, Diep Vu, Robert Russell, Maryam Hajbabaei, Akua Asa-Awuku, and Thomas D Durbin. Evaluating the effects of aromatics content in gasoline on gaseous and particulate matter emissions from SI-PFI and SIDI vehicles. Environmental Science & Technology, 49(11):7021– 7031, 2015.

103. Smith, S. and Imoehl, W., "Measurement and Control of Fuel Injector Deposits in Direct Injection Gasoline Vehicles," SAE Technical Paper 2013-01-2616, 2013, doi:10.4271/2013-01-2616.

104. Wen, Y., Wang, Y., Fu, C., Deng, W. et al., “The Impact of Injector Deposits on Spray and Particulate Emission of Advanced Gasoline Direct Injection Vehicle,” SAE Technical Paper 2016-01-2284, 2016, doi:10.4271/2016-01-2284.

105. Wang, C., Xu, H., Herreros, J.M., Wang, J. et al., Impact of Fuel and Injection System on PM Emissions from a DISI Engine,”*Appl. Energy* 132 (2014): 178e91.

106. Maricq, M.M., Szente, J., Adams, J., Tennison, P. et al., “Influence of Mileage Accumulation on the Particle Mass and Number Emissions of Two Gasoline Direct Injection Vehicles,” *Environ. Sci. Technol.* 47 (2013): 11890−11896.

107. Samuel, S., Hassaneen, A., and Morrey, D., “Particulate Matter Emissions and the Role of Catalytic Converter during Cold Start of GDI Engine,” SAE Technical Paper 2010-01-2122, 2010, doi:10.4271/2010-01-2122.

108. Bogarra, M., Herreros, J.M., Hergueta, C., Tsolakis, A. et al., “Influence of Three-Way Catalyst on Gaseous and Particulate Matter Emissions during Gasoline Direct Injection Engine Cold-Start,” *Johnson Matthey Technol. Rev.* 61, no. 4 (2017): 329.

109. Czerwinski, J., Comte, P., Heeb, N., Mayer, A. et al., “Nanoparticle Emissions of DI Gasoline Cars with/without GPF,” SAE Technical Paper 2017-01-1004, 2017, doi:10.4271/2017-01-1004.

110. Andersson, J., Demuynck, J., and Hamje, H., “AECC/Concawe2016 GPF RDE PN Test Programme: PN Measurement above and below 23 nm,” *21st ETHConference on Combustion Generated Nanoparticles*, Zurich, 2017.

111. Eastwood, P., *Particulate Emissions from Vehicles* (Wiley-PE Publishing Series), (Warrendale/Chichester: Published on behalf of SAE International/ John Wiley, 2008), ISBN:978-0-7680-2060-1.

112. Giechaskiel, B., Manfredi, U., and Martini, G., “Engine Exhaust Solid Sub-23 nm Particles: I. Literature Survey,” *SAE Int. J. Fuels Lubr.* 7, no. 3 (2014):950–964, doi:10.4271/2014-01-2834.

113. Giechaskiel, B. and Martini, G., “Engine Exhaust Solid Sub-23 nm Particles: II. Feasibility Study for Particle Number Measurement Systems,” *SAE Int. J. Fuels Lubr.* 7, no. 3 (2014): 935–949, doi:10.4271/2014-01-2832.

114. Kittelson, D., Patwardhan, U., Zarling, D., Gladis, D. et al., “Issues Associated with Measuring Nothing or Almost Nothing: Real-Time Measurements of Metallic Ash Emissions from Engines,” *Cambridge Particle Meeting*, 2013.

115. Dageforde, H., “Untersuchung innermotorischer Einflussgro.en auf die Partikelemission eines Ottomotors mit Direkteinspritzung,” Dissertation, Karlsruhe Institute of Technology (KIT), Karlsruhe, 2015, ISBN:978-3-8325-4054-8.

116. Hinds, W.C., *Aerosol Technology: Properties, Behavior, and Measurement of Airborne Particles*, 2nd ed., (New York: Wiley, 1999), ISBN:978-0-471-19410-1.

117. Jimenez, J.L., Bahreini, R., Cocker, D.R.I., Zhuang, H. et al., “New Particle Formation from Photooxidation of Diiodomethane (CH2I2),” *Journal of Geophysical Research* 108, no. D10 (2003): 4318, doi:10.1029/2002JD002452.

118. McMurry, P.H., Wang, X., Park, K., and Ehara, K., “The Relationship between Mass and Mobility for Atmospheric Particles: A New Technique for Measuring Particle Density,”*Aerosol Science and Technology* 36, no. 2 (2002):227–238, doi:10.1080/027868202753504083.

119. Bockhorn, H., *Soot Formation in Combustion: Mechanisms and Models* (Springer Series in Chemical Physics), Vol. 59, (Berlin/New York: Springer-Verlag, 1994), ISBN:3-540-58398-X.

120. Frenklach, M. and Wang, H., “Detailed Modeling of Soot Particle Nucleation and Growth,”*Symposium (International) on Combustion* 23, no. 1 (1991):1559–1566, doi:10.1016/S0082-0784(06)80426-1.

121. Warnatz, J., Maas, U., and Dibble, R.W., *Combustion: Physical and Chemical Fundamentals, Modeling and Simulation, Experiments, Pollutant Formation*, 4th ed., (Berlin/Heidelberg [u.a.]: Springer, 2006), ISBN:3-540-25992-9.

122. Heywood, J.B., *Internal Combustion Engine Fundamentals* (McGraw-Hill Series in Mechanical Engineering), (New York: McGraw-Hill, 1988), ISBN:0-07-100499-8.

123. Kennedy, I.M., “Models of Soot Formation and Oxidation,”*Progress In Energy and Combustion Science* 23, no. 2 (1997): 95–132, doi:10.1016/S0360-1285(97)00007-5.

124. Nagle, J. and Strickland-Constable, R.F., “Oxidation of Carbon between 1000– 2000°C,” *Proceedings of the Fifth Conference on Carbon*, University Park, 1962, 154–164, doi:10.1016/B978-0-08-009707-7.50026-1.

125. Bertsch, M., “Investigations to Reduce Particle Number Emissions from GDI Engines II,” FVV-Abschlussbericht, Project Nr. 1144 and 1188, 2016.

126. Bockhorn, H., *Soot Formation in Combustion: Mechanisms and Models* (Springer Series in Chemical Physics), Vol. 59, (Berlin/New York: Springer-Verlag, 1994), ISBN:3-540-58398-X.

127. Jiao, Q. and Reitz, R.D., “Modeling Soot Emissions from Wall Films in a Direct-Injection Spark-Ignition Engine,” *International Journal of Engine Research* 16, no. 8, (2015): 994-1013, doi:10.1177/1468087414562008.

128. Kopple, F., Seboldt, D., Jochmann, P., Hettinger, A. et al., “Experimental Investigation of Fuel Impingement and Spray-Cooling on the Piston of a GDI Engine via Instantaneous Surface Temperature Measurements,” *SAE Int. J. Engines* 7, no. 3 (2014): 1178–1194, doi:10.4271/2014-01-1447.

129. Kufferath, A., Kopple, F., Bargende, M., and Jochmann, P., “Investigation of the Parameters Influencing the Spray-Wall Interaction in a GDI Engine – Prerequisite for the Prediction of Particulate Emissions by Numerical Simulation,” *SAE Int. J. Engines* 6, no. 2 (2013): 911–925, doi:10.4271/2013-01-1089.

130. Velji, A., Yeom, K., Wagner, U., Spicher, U. et al., “Investigations of the Formation and Oxidation of Soot Inside a Direct Injection Spark Ignition Engine Using Advanced Laser-Techniques,” SAE Technical Paper 2010-01-0352, 2010, doi:10.4271/2010-01-0352.

131. Kufferath, A., Berns, S., Hammer, J., Busch, R. et al., “The EU 6 Challenge at GDI – Assessment of Feasible System Solutions,” 2012, accessed November 18, 2015, http://www.ovk.at/veranstaltungen_/symposien/2012/nachlese_en.pdf.

132. Schulz, F., Schmidt, J., Kufferath, A., and Samenfink, W., “Gasoline Wall Films and Spray/Wall Interaction Analyzed by Infrared Thermography,” *SAE Int. J. Engines* 7, no. 3 (2014): 1165–1177, doi:10.4271/2014-01-1446.

133. Bertsch, M., “Experimental Investigations on Particle Number Emissions from GDI Engines,” Dissertation, Karlsruhe Institute of Technology (KIT), Karlsruhe, 2017, doi:10.5445/IR/1000063994.

134. Dageforde, H., “Untersuchung innermotorischer Einflussgro.en auf die Partikelemission eines Ottomotors mit Direkteinspritzung,” Dissertation, Karlsruhe Institute of Technology (KIT), Karlsruhe, 2015, ISBN:978-3-8325-4054-8.

135. Denis, N. and Bertsch, M., “Investigations to Reduce Particle Number Emissions from GDI-Engines III FVV-Abschlussbericht,” Project Nr. 1188 and 1193, 2017.

136. Steimle, F., Kulzer, A., Richter, H., Schwarzenthal, D. et al., “Systematic Analysis and Particle Emission Reduction of Homogeneous Direct Injection SI Engines,” SAE Technical Paper 2013-01-0248, 2013, doi:10.4271/2013-01-0248.

137. Berndorfer, A., Breuer, S., Piock, W., and Bacho, P.V., "Diffusion Combustion Phenomena in GDi Engines caused by Injection Process," SAE Technical Paper 2013-01-0261, 2013, doi:10.4271/2013-01-0261.

138. Wiese, W., Kufferath, A., Storch, A., and Rogler, P., "Requirements for Multi-Hole Injectors to Meet Future Emission Standards in Direct-Injection Gasoline Engines [in German]," *2nd International Engine Congress*, 2015,63–80, ISBN:978-3-658-08861-3.

139. Piock, W.F., Befrui, B., Berndorfer, A., and Hoffmann, G., "Fuel Pressure and Charge Motion Effects on GDi Engine Particulate Emissions," *SAE Int. J. Engines* 8, no. 2 (2015): 464–473, doi:10.4271/2015-01-0746.

140. Dageforde, H., Koch, T., and Spicher, U., "Untersuchung von Ma.nahmenzur Reduktion der Partikel-Anzahlemissionen bei Otto-DI-Motoren,"Abschlussbericht zu FVV-Projekt Nr. 1046 (in German), 2014.

141. Bertsch, M., "Investigations to Reduce Particle Number Emissions from GDIEngines II," FVV-Abschlussbericht, Project Nr. 1144 and 1188, 2016.

142. Denis, N. and Bertsch, M., "Investigations to Reduce Particle Number Emissionsfrom GDI Engines III FVV-Abschlussbericht," Project Nr. 1188 and 1193, 2017.

143. Disch, C., Kubach, H., Pfeil, J., Koch, T. et al., "Cycle-Resolved Combustion Diagnostics of a Direct Injection Gasoline Engine in Transient Operation," *11th International Symposium on Combustion Diagnostics*, Baden-Baden, July 2014.

144. Disch, C., Koch, T., Spicher, U., and Donn, C., "Engine-in-the-Loop as a Development Tool for Emissions Optimisation in the Hybrid Context," *MTZ Worldwide* 75 (2014): 40, doi:10.1007/s38313-014-0234-5.

145. Disch, C., Pfeil, J., Kubach, H., Koch, T. et al., "Experimental Investigations of a DISI Engine in Transient Operation with Regard to Particle and Gaseous Engine-out Emissions," *SAE Int. J. Engines* 9, no. 1 (2016): 262-278, doi:10.4271/2015-01-1990.

146. Tan, C., Xu, H., Ma, H., and Ghafourian, A., "Investigation of VVT and spark timing on combustion and particle emission from a GDI Engine during transient operation," SAE Technical Paper 2014-01-1370, 2014, doi:10.4271/2014-01-1370.

147. Sabathil, D., Koenigstein, A., Schaffner, P., Fritzsche, J. et al., "The Influence of DISI Engine Operating Parameters on Particle Number Emissions," SAE Technical Paper 2011-01-0143, 2011, doi:10.4271/2011-01-0143.

148. Whitaker, P., Kapus, P., Ogris, M., and Hollerer, P., “Measures to Reduce Particulate Emissions from Gasoline DI engines,” *SAE Int. J. Engines* 4, no. 1 (2011): 1498–1512, doi:10.4271/2011-01-1219.

149. Piock, W.F., Berndorfer, A., Hoffmann, G., Salemi, P. et al., “Strategies Towards Meeting Future Particulate Matter Emission Requirements in Homogeneous Gasoline Direct Injection Engines,” *SAE Int. J. Engines* 4, no.(1) 2011: 1455–1468, doi:10.4271/2011-01-1212.

150. Altenschmidt, F., Gildein, H., Sauter, W., and Schaupp, U., “The Spray-Guided Mercedes-Benz Combustion System - Developed not only for Stratified Mode,” *SIA International Conference and Exhibition, the Spark Ignition Engine of the Future*, Strasbourg, 2011, 1–9.

151. Dageforde, H., Koch, T., Beck, K.W., and Spicher, U., “Influence of Fuel Composition on Exhaust Emissions of a DISI Engine during Catalyst Heating Operation,” SAE Technical Paper 2013-01-2571, 2013, doi:10.4271/2013-01-2571.

152. Kazour, J., Befrui, B., Husted, H., Raney, M. et al., “Innovative Sprays and Particulate Reduction with GDi Injectors,” SAE Technical Paper 2014-01-1441, 2014, doi:10.4271/2014-01-1441.

153. Kufferath, A., Berns, S., Hammer, J., Busch, R. et al., “The EU 6 Challenge at GDI – Assessment of Feasible System Solutions,” 2012, accessed November 18, 2015, http://www.ovk.at/veranstaltungen_/symposien/2012/nachlese_en.pdf.

154. Schumann, F., “Experimentelle Grundlagenuntersuchungen zum Katalysatorheizbetrieb mit strahlgefuhrter Benzin-Direkteinspritzung und Einspritzdrucken bis 800 bar,” Dissertation, Karlsruhe Institute of Technology, Karlsruhe, 2014, http://nbn-resolving.org/urn:nbn:de:swb: 90-431354.

155. Dageforde, H., “Untersuchung innermotorischer Einflussgro.en auf die Partikelemission eines Ottomotors mit Direkteinspritzung,” Dissertation, Karlsruhe Institute of Technology (KIT), Karlsruhe, 2015, ISBN:978-3-8325-4054-8.

156. Francqueville, L.d. and Pilla, G.L., “Investigation of Particle Formation Processes in a GDI Engine in Catalyst Heating Operation,”*International Symposium on Combustion Diagnostics*, At Strasbourg, France, 2012, 129–137,ISBN:9783000326691.

157. Tree, D.R. and Svensson, K.I., “Soot Processes in Compression Ignition Engines,” *Progress in Energy and Combustion Science* 33, no. 3 (2007): 272-309, doi:10.1016/j.pecs.2006.03.002.

158. Drake, M.C., Fansler, T.D., Solomon, A.S., and Szekely, G.A., "Piston Fuel Films as a Source of Smoke and Hydrocarbon Emissions from a Wall- Controlled Spark-Ignited Direct Injection Engine," SAE Technical Paper 2003-01-0547, 2003, doi:10.4271/2003-01-0547.

159. Stevens, E. and Steeper, R., "Piston Wetting in an Optical DISI Engine: Fuel Films, Pool Fires, and Soot Generation," SAE Technical Paper 2001-01-1203,2001, doi:10.4271/2001-01-1203.

160. Xu, H., Wang, C., Ma, X., Sarangi, A.K. et al., "Fuel Injector Deposits in Direct-Injection Spark-Ignition Engines," *Progress in Energy and Combustion Science* 50:63-80, 2015, doi:10.1016/j.pecs.2015.02.002.

161. Köpple, F., Seboldt, D., Jochmann, P., Hettinger, A. et al., "Experimental Investigation of Fuel Impingement and Spray-Cooling on the Piston of a GDI Engine via Instantaneous Surface Temperature Measurements," *SAE Int. J. Engines* 7, no. 3 (2014): 1178-1194, doi:10.4271/2014-01-1447.

162. Köpple, F., Jochmann, P., Kufferath, A., and Bargende, M., "Investigation of the Parameters Influencing the Spray-Wall Interaction in a GDI Engine—Prerequisite for the Prediction of Particulate Emissions by Numerical Simulation," *SAE Int. J. Engines* 6, no. 2, (2013): 911-2925, doi:10.4271/2013-01-1089.

163. Su, J., Xu, M., Yin, P., Gao Y., Hung, D. "Particle Number Emissions Reduction Using Multiple Injection Strategies in a Boosted Spark-Ignition Direct-Injection (SIDI) Gasoline Engine," SAE Int. 2014-01-2845, doi: 10.4271/2014-01-2845.

164. Alkidas, A.C. "Combustion Advancements in Gasoline Engines," *Energy Conversion and Management* 48 (2007): 2751-2761.

165. Zhao, F., Lai, M.C., and Harrington, D., "Automotive Spark-Ignited Direct-Injection Gasoline Engines," *Prog. Energy Combust. Sci.* 25 (1999): 437–562.

166. Piock, W., Hoffmann, G., Berndorfer, A., Salemi, P. et al., "Strategies Towards Meeting Future Particulate Matter Emission Requirements in Homogeneous Gasoline Direct Injection Engines," *SAE Int. J. Engines* 4 (2011): 1455-1468,doi:10.4271/2011-01-1212.

167. Stevens, E. and Steeper, R., "Piston Wetting in an Optical DISI Engine: Fuel Films, Pool Fires, and Soot Generation," *SAE Int. J. Engines* 110 (2001): 1287-1294, doi:10.4271/2001-01 1203.

168. EPA, "Ethanol Waivers (E15 and E10)," Environmental Protection Agency, 2011.

169. Yanowitz, J. and McCormick, R.L., "Effect of E85 on Tailpipe Emissions from Light-Duty Vehicles,"*Journal of the Air & Waste Management Association* 59 (2009): 172-182.

170. Hubbard, C.P., Anderson, J.E., and Wallington, T.J., "Ethanol and Air Quality: Influence of Fuel Ethanol Content on Emissions and Fuel Economy of Flexible Fuel Vehicles,"*Environ. Sci. Technol.* 48 (2014): 861-867.

171. Yanowitz, J., Knoll, K., Kemper, J., Luecke, J. et al., "Impact of Adaptation on Flex-Fuel Vehicle Emissions When Fueled with E40," *Environ. Sci. Technol.* 47 (2013): 2990-2997.

172. Zhang, Z., Wang, T., Jia, M., Wei, Q. et al., "Combustion and Particle Number Emissions of a Direct Injection Spark Ignition Engine Operating on Ethanol/Gasoline and n-Butanol/Gasoline Blends with Exhaust Gas Recirculation,"*Fuel* 130 (2014): 177-188.

173. Karavalakis, G., Short, D., Vu, D., Russell, R.L. et al., "The Impact of Ethanol and Iso-Butanol Blends on Gaseous and Particulate Emissions from Two Passenger Cars Equipped with Spray-Guided and Wall-Guided Direct Injection S.I. Engines," *Energy* 82 (2015): 168-179.

174. Irimescu, A., "Performance and Fuel Conversion Efficiency of a Spark Ignition Engine Fueled with Iso-Butanol,"*Applied Energy* 96 (2012): 477-483.

175. Xue, C., Zhao, X.Q., Liu, C.G., Chen, L.J. et al., "Prospective and Development of Butanol as an Advanced Biofuel," *Biotechnology Advances* 31 (2013): 1575-1584.

176. Tao, L., Tan, E.C.D., McCormick, R.L., Zhang, M. et al., "Techno-Economic Analysis and Life-Cycle Assessment of Cellulosic Iso-Butanol and Comparison with Cellulosic Ethanol and n-Butanol,"*Biofuels, Bioproducts, and Biorefining* 8 (2014): 30-48.

177. Velji, A., Yeom, K., Wagner, U., Spicher, U. et al., "Investigations of the Formation and Oxidation of Soot inside a Direct Injection Spark Ignition Engine Using Advanced Laser-Techniques," SAE Technical Paper 2010-01-0352, 2010, doi:10.4271/2010-01-0352.

178. Graskow, B., Kittelson, D., Abdul-Khalek, I., Ahmadi, M. et al.,"Characterization of Exhaust Particulate Emissions from a Spark Ignition Engine," SAE Technical Paper 980528, 1998, doi:10.4271/980528.

179. Barone, T.L., Storey, J.M.E., Youngquist, A.D., and Szybist, J.P., "An Analysis of Direct-Injection Spark-Ignition (DISI) Soot Morphology," *Atmospheric Environment* 49 (2012): 268-274.

180. Sgro, L.A., Sementa, P., Vaglieco, B.M., Rusciano, G. et al., "Investigating the Origin of Nuclei Particles in GDI Engine Exhausts," *Combustion and Flame* 159 (2012): 1687-1692.

181. Richter, H. and Howard, J.B., “Formation of Polycyclic Aromatic Hydrocarbons and Their Growth to Soot - A Review of Chemical Reaction Pathways,” *Prog. Energy Combust. Sci.* 26 (2000): 565-608.

182. Bockhorn, H., *Soot Formation in Combustion: Mechanisms and Models* (Springer Series in Chemical Physics), Vol. 59, (Berlin/New York: Springer-Verlag, 1994), ISBN:3-540-58398-X.

183. Frenklach, M. and Wang, H., “Detailed Modeling of Soot Particle Nucleation and Growth,”*Twenty-Third Symposium (International) on Combustion*, The Combustion Institute, Pittsburgh, 1990, 1559-1566.

184. Heywood, J.B., *Internal Combustion Engine Fundamentals* (McGraw-Hill Series in Mechanical Engineering), (New York: McGraw-Hill, 1988), ISBN:0-07-100499-8.

185. Raj, A., Prada, I.D.C., Amer, A.A., and Chung, S.H., “A Reaction Mechanism for Gasoline Surrogate Fuels for Large Polycyclic Aromatic Hydrocarbons,”*Combustion and Flame* 159 (2012): 500-515.

186. Choi, B.S., Choi, S.K., and Chung, S.H., “Soot Formation Characteristics of Gasoline Surrogate Fuels in Counterblow Diffusion Flames,” *Proceedings of the Combustion Institute* 33 (2011): 609-616.

187. Kobayashi, Y. and Arai, M., “Characteristics of PM Exhausted from Pool Diffusion Flame with Gasoline and Surrogate Gasoline Fuels,” SAE Technical Paper 2015-01-2024, 2015, doi:10.4271/2015-01-2024.

188. Burke, S.C., Ratcliff, M., and McCormick, R., “Distillation-based Droplet Modeling of Non-Ideal Oxygenated Gasoline Blends: Investigating the Role of Droplet Evaporation on PM Emissions,” SAE Technical Paper 2017-01-0581,2017, doi:10.4271/2017-01-0581.

189. Leach, F., Stone, R., Fennell, D., Hayden, D. et al., “Predicting the Particulate Matter Emissions from Spray-Guided Gasoline Direct Injection Spark Ignition Engines, *Proceedings of the Institution of Mechanical Engineers, Part D: Journal of Automobile Engineering* 231 (2017): 717-730.

190. Chapman, E., Winston-Galant, M., Geng, P., and Konzack, A., “Global Market Gasoline Range Fuel Review using Fuel Particulate Emission Correlation Indices,” SAE Technical Paper 2016-01-2251, 2016, doi:10.4271/2016-01-2251.

191. Chapman, E., Winston-Galant, M., Geng, P., and Latigo, R., “Alternative Fuel Property Correlation to the Honda Particulate Matter Index (PMI),” SAE Technical Paper 2016-01-2250, 2016, doi:10.4271/2016-01-2250.

192. Aikawa, K., Sakurai, T., and Jetter, J.J., "Development of a Predictive Model for Gasoline Vehicle Particulate Matter Emissions," *SAE Int. J. Fuels Lubr.* 3, no. 2 (2010): 610-622, doi:10.4271/2010-01-2115.

193. Hellier, P., Ladommatos, N., Allan, R., Filip, S. et al., "The Importance of Double Bond Position and Cis-Trans Isomerisation in Diesel Combustion and Emissions," *Fuel* 105 (2013): 477-489.

194. Ogawa, T., Araga, T., Okada, M., and Fujimoto, Y., "Effects of Diesel Fuel Properties on Particulate Emissions from D.I. Diesel Engine – Part 2: Chemical Analysis and Characterization of Diesel Oil," SAE Technical Paper 9437494,1994.

195. Karavalakis, G., Short, D., Vu, D., Russell, R. et al., "Evaluating the Effects of Aromatics Content in Gasoline on Gaseous and Particulate Matter Emissions from SI-PFI and SI-DI Vehicles," *Environ. Sci. Technol.* 49 (2015): 7021-7031.

196. Leach, F., Stone, R., and Richardson, D., "The Influence of Fuel Properties on Particulate Number Emissions from a Direct Injection Spark Ignition.

197. Dageförde, H., Koch, T., Beck, K.W., and Spicher, U., "Influence of Fuel Composition on Exhaust Emissions of a DISI Engine during Catalyst Heating Operation," SAE Technical Paper 2013-01-2571, 2013, doi:10.4271/2013-01-2571.

198. Khalek, I.A., Bougher, T., and Jetter, J.J., "Particle Emissions from a 2009 Gasoline Direct Injection Engine Using Different Commercially Available Fuels," *SAE Int. J. Fuels Lubr.* 3, no. 2 (2010): 623-637, doi:10.4271/2010-01-2117.

199. Kim, Y., Kim, Y., Kang, J., Rew, S. et al., "Fuel Effect on Particle Emissions of a Direct Injection Engine," SAE Technical Paper 2013-01-1559, 2013,doi:10.4271/2013-01-1559.

200. Zhu, R., Hu, J., Bao, X., He, L. et al., "Effects of Aromatics, Olefins and Distillation Temperatures (T50 and T90) on Particle Mass and Number Emission from Gasoline Direct Injection (GDI) Vehicles," *Energy Policy* 101 (2017): 185-193.

201. Chan, T.W., Lax, D., Gunter, G.C., Hendren, J. et al., "Assessment of the Fuel Composition Impact on Black Carbon Mass, Particle Number Size Distributions, Solid Particle Number, Organic Materials, and Regulated Gaseous Emissions from a Light-Duty Gasoline Direct Injection Truck andPassenger Car,"*Energy and Fuels* 31 (2017): 10452-10466.

202. Jiao, Q. and Reitz, R.D., "The Effect of Operating Parameters on Soot Emissions in GDI Engines," SAE Technical Paper 2015-01-1071, 2015,doi:10.4271/2015-01-1071.

203. Fushimi, A., Kondo, Y., Kobayashi, S., Fujitani, Y. et al., “Chemical Composition and Source of Fine and Nanoparticles from Recent Direct Injection Gasoline Passenger Cars: Effects of Fuel and Ambient Temperature,”*Atmospheric Environment* 124 (2016): 77-84.

204. U.S. Environmental Protection Agency, “Assessing the Effect of Five Gasoline Properties on Exhaust Emissions from Light-Duty Vehicles Certified to Tier 2 Standards: Analysis of Data from EPAct Phase 3 (EPAct/V2/E-89),”Final Report, EPA-420-R-13-002, April 2013, http://www.epa.gov/otaq/models/moves/epact.htm.

205. Butler, A.D., Sobotowski, R.A., and Hoffman, G.J., “Influence of Fuel PM Index and Ethanol Content on Particulate Emissions from Light-Duty Gasoline Vehicles,” SAE Technical Paper 2015-01-1072, 2015, doi:10.4271/2015-01-1072.

206. Sobotowski, R.A., Butler, A.D., and Guerra, Z., “A Pilot Study of Fuel Impacts on PM Emissions from Light-Duty Gasoline Vehicles,” SAE Technical Paper 2015-01-9071, 2015, doi:10.4271/2015-01-9071.

207. Karavalakis, G., Durbin, T.D., Yang, J., Ventura, L. et al., “Fuel Effects on PM Emissions from Different Vehicle/Engine Configurations: A Literature Review and Statistical Analysis,” SAE Technical Paper 2018-01-0349, 2018,doi:10.4271/2018-01-0349.

208. Storch, M., Koegl, M., Altenhoff, M., Will, S. et al., “Investigation of Soot Formation of Spark-Ignited Ethanol-Blended Gasoline Sprays with Single- and Multi-Component Base Fuels,” *Applied Energy* 181 (2016): 278-287.

209. Chen, L., Stone, R., and Richardson, D., “A Study of Mixture Preparation and PM Emissions Using a Direct Injection Engine Fueled with Stoichiometric Gasoline/Ethanol Blends,” *Fuel* 96 (2012): 120-130.

210. Chen, L. and Stone, R., “Measurement of Enthalpies of Vaporization of Isooctane and Ethanol Blends and Their Effects on PM Emissions from a GDI Engine,” *Energy & Fuels* 25 (2011): 1254-1259.

211. Di Iorio, S., Lazzaro, M., Sementa, P., Vaglieco, B.M. et al., “Particle Size Distributions from a DI High Performance SI Engine Fuelled with Gasoline-Ethanol Blended Fuels,” SAE Technical Paper 2011-24-0211, 2011, doi:10.4271/2011-24-0211.

212. Catapano, F., Di Iorio, S., Lazzaro, M., Sementa, P. et al., “Characterization of Ethanol Blends Combustion Processes and Soot Formation in a GDI Optical Engine,” SAE Technical Paper 2013-01-1316, 2013, doi:10.4271/2013-01-1316.

213. He, X., Ratcliff, M.A., and Zigler, B.T., “Effects of Gasoline Direct Injection Engine Operating Parameters on Particle Number Emissions,” *Energy & Fuels* 26 (2012): 2014-2027.

214. Chan, T.W., Meloche, E., Kubsh, J., Brezny, R. et al., “Impact of Ambient Temperature on Gaseous and Particle Emissions from a Direct Injection Gasoline Vehicle and its Implications on Particle Filtration,” SAE Technical Paper 2013-01-0527, 2013, doi:10.4271/2013-01-0527.

215. Zhao, F., Lai, M.C., and Harrington, D., “Automotive Spark-Ignited Direct-Injection Gasoline Engines,” *Prog. Energy Combust. Sci.* 25 (1999): 437–562.

216. Piock, W., Hoffmann, G., Berndorfer, A., Salemi, P. et al., “Strategies Towards Meeting Future Particulate Matter Emission Requirements in Homogeneous Gasoline Direct Injection Engines,” *SAE Int. J. Engines* 4 (2011): 1455-1468,doi:10.4271/2011-01-1212.

217. Fatouraie, M., Wooldridge M.S., Petersen, B.R., and Wooldridge, S.T., “Effects of Ethanol on In-Cylinder and Exhaust Gas Particulate Emissions of a Gasoline Direct Injection Spark Ignition Engine,” *Energy and Fuels* 29 (2015):3399-3412.

218. Sakai, S. and Rothamer, D., “Effect of Ethanol Blending on Particulate Formation from Premixed Combustion in Spark-Ignition Engines,” *Fuel* 196 (2017): 154-168.

219. Karavalakis, G., Short, D., Russell, R.L., Jung, H. et al., “Assessing the Impacts of Ethanol and Iso-Butanol on Gaseous and Particulate Emissions from Flexible Fuel Vehicles,”*Environmental Science and Technology* 48 (2014):14016-14024.

220. Mamakos, A., Martini, G., Marotta, A., and Manfretti, U., “Assessment of Different Technical Options in Reducing Particle Emissions from Gasoline Direct Injection Vehicles,” *Journal of Aerosol Science* 63 (2013): 115-125.

221. Jin, D., Choi, K., Myun, C.L., Lim, Y. et al., “The Impact of Various Ethanol- Gasoline Blends on Particulates and Unregulated Gaseous Emissions Characteristics from a Spark Ignition Direct Injection (SIDI) Passenger Vehicle,” *Fuel* 209 (2017): 702-712.

222. Zhang, Z., Wang, T., Jia, M., Wei, Q. et al., “Combustion and Particle Number Emissions of a Direct Injection Spark Ignition Engine Operating on Ethanol/Gasoline and n-Butanol/Gasoline Blends with Exhaust Gas Recirculation,”*Fuel* 130 (2014): 177-188.

223. Oh, C. and Cha, G., “Influence of Oxygenate Content on Particulate Matter Emission in Gasoline Direct Injection Engine,” *International Journal of Automotive Technology* 14 (2013): 829-836.

224. Wang, C., Xu, H., Herreros, J.M., Wang, J. et al., “Impact of Fuel and Injection System on Particle Emissions from a GDI Engine,” *Applied Energy* 132 (2014):178-191.

225. Vuk, C. and Vander Griend, S.J., “Fuel Property Effects on Particulates In Spark Ignition Engines,” SAE Technical Paper 2013-01-1124, 2013,doi:10.4271/2013-01-1124.

226. Price, P., Twiney, B., Stone, R., Kar, K. et al., “Particulate and Hydrocarbon Emissions from a Spray Guided Direct Injection Spark Ignition Engine with Oxygenate Fuel Blends,” SAE Technical Paper 2007-01-0472, 2007,doi:10.4271/2007-01-0472.

227. Wallner, T. and Frazee, R., “Study of Regulated and Non-Regulated Emissions from Combustion of Gasoline, Alcohol Fuels and their Blends in a DI-SI Engine,” SAE Technical Paper 2010-01-1571, 2010, doi:10.4271/2010-01-1571.

228. Pechout, M., Dittrich, A., and Vojtisek-Lom, M., “Operation of an Ordinary PFI Engine on n-butanol and Iso-butanol and Their Blends with Gasoline,”SAE Technical Paper 2014-01-2618, 2014, doi:10.4271/2014-01-2618.

229. Rankovic, N., Bourhis, G., Loos, M., and Dauphin, R., “Understanding Octane Number Evolution for Enabling Alternative Low RON Refinery Streams andOctane Boosters as Transportations Fuels,” *Fuel* 150 (2015): 41-47.

230. Li, L., Sun, K., and Duan, J., “Effects of Butanol Isomers on the Combustion Characteristics and Particle Number Emissions of a GDI Engine,” SAE Technical Paper 2017-01-2323, 2017, doi:10.4271/2017-01-2323.

231. Storey, J., Lewis, S., Szybist, J., Thomas, J. et al., “Novel Characterization of GDI Engine Exhaust for Gasoline and Mid-Level Gasoline-Alcohol Blends,”SAE Technical Paper 2014-01-1606, 2014, doi:10.4271/2014-01-1606.

232. Hergueta, C., Bogarra, M., Tsolakis, A., Essa, K. et al., “Butanol-Gasoline Blend and Exhaust Gas Recirculation, Impact on GDI Engine Emissions,” *Fuel*, 208 (2017): 662-672.

233. Chan, T.W., “The Impact of Isobutanol and Ethanol on Gasoline Fuel Properties and Black Carbon Emissions from Two Light-Duty Gasoline Vehicles,” SAE Technical Paper 2015-01-1076, 2015, doi:10.4271/2015-01-1076.

234. Lattimore, T., Herreros, J.M., Xu, H., and Shuai, S., “Investigation of Compression Ratio and Fuel Effect on Combustion and PM Emissions in a DISI Engine,” *Fuel* 169 (2016): 68-78.

235. Karavalakis, G., Short, D., Vu, D., Villela, M. et al., “Evaluating the Regulated Emissions, Air Toxics, Ultrafine Particles, and Black Carbon from SI-PFI and SI-DI Vehicles Operating on Different Ethanol and Iso-Butanol Blends,” *Fuel* 128 (2014): 410-421.

236. *Piock, W., Hoffmann, G., Berndorfer, A., Salemi, P., Fusshoeller, B., "Strategies Towards Meeting Future Particulate Matter Emission Requirements in Homogeneous Gasoline Direct Injection Engines".*

237. Zhang, M., Hong, W., Xie, F., Su, Y., Han, L., Wu, B. (2017). Experimental investigation of impacts of injection timing and pressure on combustion and particulate matter emission in a spray-guided GDI engine. International Journal of Automotive Technology, Vol. 19, No. 3, pp. 393-404 (2018) – DOI 10.1007/s12239-018-0038-8.

238. Raza, M., Chen, L., Leach, F., Ding, S. (2018). A review of particulate number (PN) emissions from gasoline direct injection engine (GDI) engines and their control techniques. Energies 2018, 11, 1417; doi:10.3390/en11061417.

239. Di Iorio, S., Catapano, F., Sementa, P., Vaglieco, B.M., Florio, S., Rebesco, E., Terna, D. Effect of Octane Number Obtained with different oxygenated components on the engine performance and emissions of a small GDI engine; SAE Technical Paper; SAE International: Warrendale, PA, USA, 2014.

240. Karavalakis, G., Durbin, D.T., Yang, J. (2018). Fuel effects on PM Emissions from different vehicle/engine configurations: A literature review. SAE Technical Paper 2018-01-0349, doi:10.4271/2018-01-0349.

241. Aikawa, K., Sakurai, T., Jetter, J.J. Development of a predictive model for gasoline vehicle particulate matter emissions. SAE Int. J. Fuels Lubr. 2010, 3, 610-622.

242. Aikawa, K., Jetter, J.J. Impact of gasoline composition on particulate matter emissions from a direct-injection gasoline engine: Applicability of the particulate matter index. Int. J. Engine Res. 2013, 15, 298-306.

243. Kim, Y., Kim, Y., Kang, J., Jun, S., Rew, S., Lee, D., Park, S. Fuel effect on particle emissions of a direct injection engine; SAE Technical Paper; SAE International: Warrendale, PA, USA, 2013.

244. Catapano, F., Di Iorio, S., Lazzaro, M., Sementa, P., Vaglieco, B.M. Characterization of Ethanol Blends Combustion Processes and Soot formation in a GDI optical engine; SAE Technical Paper; SAE International: Warrendale, PA, USA, 2013.

245. Chen, L., Stone, R., and Richardson, D., "A Study of mixture preparation and PM emission using a direct injection engine fueled with stoichiometric gasoline/ethanol blends," Fuel 96 (2012): 120-130.

246. Karavalakis, G., Short, D., Vu, D., Russell, R.L., Asa-Awuku, A., Jung, H., Johnson, K.C., Durbin, T.D. The impact of Ethanol and iso-butanol blends on gaseous and particulate emissions for two passenger cars equipped with sprayguided and wall-guided direct injection SI (spark ignition) engine. Energy 2015, 82, 168-179.

247. Chen, L.; Stone, R.; Richardson, D. A study of mixture preparation and PM emissions using a direct injectionChen, L.; Stone, R.; Richardson, D. A study of mixture preparation and PM emissions using a direct injection engine fuelled with stoichiometric gasoline/ethanol blends. Fuel 2012, 96, 120–130.

248. Wang, C.; Xu, H.; Herreros, J.M.; Wang, J.; Cracknell, R. Impact of fuel and injection system on particle emissions from a GDI engine. Appl. Energy 2014, 132, 178–191.

249. Karavalakis, G.; Short, D.; Vu, D.; Villela, M.; Asa-Awuku, A.; Durbin, T.D. Evaluating the regulate emissions, air toxics, ultrafine particles, and black carbon from SI-PFI and SI-DI vehicles operating on different ethanol and iso-butanol blends. Fuel 2014, 128, 410–421.

250. Maricq, M.M.; Szente, J.J.; Jahr, K. The Impact of Ethanol Fuel Blends on PM Emissions from a Light-Duty GDI Vehicle. Aerosol. Sci. Technol. 2012, 46, 576– 583.

251. Zhang, Z.; Wang, T.; Jia, M.; Wei, Q.; Meng, X.; Shu, G. Combustion and particle number emissions of a direct injection spark ignition engine operating on ethanol/gasoline and n-butanol/gasoline blends with exhaust gas recirculation. Fuel 2014, 130, 177–188.

252. Storey, J.; Barone, T.; Norman, K.; Lewis, S. Ethanol Blend Effects on Direct Injection Spark-Ignition Gasoline Vehicle Particulate Matter Emissions. SAE Int. J. Fuels Lubr. 2010, 3, 650–659.

253. Chen, L.; Braisher, M.; Crossley, A.; Stone, R.; Richardson, D. The Influence of Ethanol Blends on Particulate Matter Emissions from Gasoline Direct Injection Engines; SAE Technical Paper; SAE International: Warrendale, PA, USA, 2010.

254. Sarathy, S.M.; Oßwald, P.; Hansen, N.; Kohse-Höinghaus, K. Alcohol combustion chemistry. Prog. Energy Combust. Sci. 2014, 44, 40–102.

255. Luo, Y.Q.; Zhu, L.; Fang, J.H.; Zhuang, Z.Y.; Guan, C.; Xia, C.; Xie, X.M.; Huang, Z. Size distribution, chemical composition and oxidation reactivity of particulate matter from gasoline direct injection (GDI) engine fueled with ethanol-gasoline fuel. Appl. Therm. Eng. 2015, 89, 647–655.

256. Wang, C.; Xu, H.; Herreros, J.M.; Wang, J.; Cracknell, R. Impact of fuel and injection system on particle emissions from a GDI engine. Appl. Energy 2014, 132, 178–191.

257. Van Basshuysen, R., Gasoline Engine with Direct Injection: Processes, Systems, Development, Potential, Vieweg Teubner, 2009.

258. Costa, M., Allocca, L., Montanaro, A., Sorge, U.,Reduction of Fuel Consumption of a GDI Engine by Split Injections, ILASS - Europe 2011, Estoril, Portugal, September 2011.

259. "GT-Power User Manual V2016", Gamma Technologies Inc. Reference Manual.

260. Boger, T., Cutler, W., Powertrain Series "Reducing Particulate Emissions in Gasoline Engines" SAE Handbook.